

# Functional and Prognostic Role of MicroRNAs in Cancer Associated Fibroblasts and Stroma in Oral Squamous Cell Carcinoma



Saroj Rajthala

Thesis for the degree of Philosophiae Doctor (PhD)  
University of Bergen, Norway  
2023

UNIVERSITY OF BERGEN



# Functional and Prognostic Role of MicroRNAs in Cancer Associated Fibroblasts and Stroma in Oral Squamous Cell Carcinoma

Saroj Rajthala



Thesis for the degree of Philosophiae Doctor (PhD)  
at the University of Bergen

Date of defense: 23.11.2023

© Copyright Saroj Rajthala

The material in this publication is covered by the provisions of the Copyright Act.

Year: 2023

Title: Functional and Prognostic Role of MicroRNAs in Cancer Associated Fibroblasts and Stroma in Oral Squamous Cell Carcinoma

Name: Saroj Rajthala

Print: Skipnes Kommunikasjon / University of Bergen

---

## **Scientific environment**

This project was carried out at Oral Cancer Research Group and Experimental Pathology Research Group at Center for Cancer Biomarkers CCBIO, a Norwegian Centre for Excellence, and Gade Laboratory for Pathology, Department of Clinical Medicine, Faculty of Medicine, University of Bergen, and Department of Pathology, Haukeland University Hospital, Bergen, Norway. The work was conducted under the supervision of Professor Anne Christine Johannessen, Professor Daniela Elena Costea and Professor Dipak Sapkota.

Clinical data and patients' materials were collected from the diagnostic archive at Department of Pathology, Haukeland University Hospital, Bergen, Norway. Laboratory work for all patients was undertaken at Centre for Cancer Biomarkers (CCBIO), Gade Laboratory for Pathology, University of Bergen and Department of Pathology, Haukeland University Hospital.

This work was supported by The Research Council of Norway through its Centres of Excellence funding scheme, (Grant No. 22325) and Helse Vest (Grants No. 911902/2013 and 912260/2019).

## **Acknowledgements**

I am grateful to all my supervisors for all the learning opportunities and experience, and for every support I have received. I would also like to thank to Center for Cancer Biomarkers CCBIO, Research Council of Norway, Institute of Clinical Medicine, Faculty of Medicine, University of Bergen and Helse-Vest for allowing me to pursue a PhD degree. I wish to extend my thanks to my colleagues and friends at the Gade Laboratory for Pathology, my co-authors and the academic and administrative staff at Center for Cancer Biomarkers CCBIO and Institute of Clinical Medicine for their help. Finally, I am thankful to everyone, including my near and dear ones for having immense patience with me.

---

## Abstract in English

Recent studies have shown that in addition to the transformation of epithelial cells, dysfunction of stroma is crucial in oral carcinogenesis, and cancer-associated stroma can regulate the phenotype of cancer cells and influence the clinical outcome. The aim of this study was to investigate the role of micro RNAs (miRNAs) dysregulation in cancer-associated fibroblasts (CAF) in oral squamous cell carcinoma (OSCC). CAF and normal oral fibroblasts (NOF) were isolated from biopsies of OSCC patients and healthy individuals after informed consent. Global miRNA expression was first profiled using Illumina version 2 panels. Unsupervised clustering of global miRNA expression showed two separate clusters for CAF and NOF, and SAM analysis revealed significant differential expression of 12 miRNAs between CAF and NOF. Functional impact of two significantly Differentially expressed miRNAs between CAF and NOF, miR-204 and miR138, was assessed in 2D and 3D-organotypic co-cultures using miRNA mimic and inhibitors. Modulation of miR-204 expression in CAF resulted in alteration of their motility with effect on suprajacent OSCC cell invasion in 3D-organotypic co-culture models. Furthermore, 3'UTR miRNA target reporter assay showed ITGA11 as a direct target of miR-204 in CAF. In conclusion, these results showed that miR-204 has a tumor suppressive function through inhibition of fibroblast migration by modulating the expression of several different molecules and by directly targeting ITGA11. Moreover, stromal miR-204 was identified as an independent prognostic biomarker for OSCC patient survival. On the other hand, expression of miR-138 showed marked heterogeneity both in OSCC tissues and cultured fibroblasts. Ectopic miR-138 expression altered fibroblasts' morphology, reduced their motility and collagen contraction ability, and suppressed invasion of suprajacent OSCC cells in 3D models. Inhibition of miR-138 resulted in the opposite outcome. Transcript and protein examination showed that the anti-tumour effect of miR-138 in CAFs was associated to changes in CAF phenotype-specific molecules, focal adhesion kinase axis, and TGF $\beta$ 1 signaling pathway. Taken together, results of this thesis demonstrate significant alteration of miRNAs in the stromal compartment of OSCC and identify miR-204 and miR-138 with a tumour suppressive function when expressed in CAF.

## Abstract in Norwegian

Nyere studier har vist at forandringer i bindevevscellene som omgir kreftsvulsten er viktige for utviklingen av munnhulekreft. Kreftstroma kan regulere fenotypen av kreftcellene, og på den måten kan påvirke klinisk forløpet av kreftsykdommen. Målet med denne studien var å undersøke dereguleringen av mikro-RNA (miRNAs) i kreft assosierte fibroblaster (KAF) i oralt plateepitelkarsinom (OPK). KAF og normale orale fibroblaster (NOF) ble isolert fra biopsier av pasienter med OPK og friske individer etter informert samtykke. Globalt miR-uttrykk ble profilert ved bruk av Illumina versjon 2-paneler. Uovervåket gruppering av KAF og NOF etter globalt miR-uttrykk viste separate klynger for KAF og NOF, og SAM analysen påviste 12 miRNAs som uttrykkes ulikt i KAF og NOF. Den funksjonelle rollen av to ulikt uttrykte miRNA-er, miR-204 og miR-138, ble vurdert i 2D- og 3D-organotypiske ko-kulturer ved bruk av miRNA-mimik og hemmere. Ved å modulere miR-204-ekspressjon i KAF ble deres morfologi og motilitet endret, og dette påvirket invasjonen av kreftcellene i 3D-organotypiske ko-kulturmodeller. Videre, viste 3'UTR miRNA-målreporteranalyse at ITGA11 var et direkte mål for miR-204. Disse funnene påviste at miR-204 har en tumorundertrykkende funksjon ved å hemme migrasjonen av fibroblaster gjennom modulering av uttrykket av flere forskjellige molekyler og ved direkte målretting av ITGA11. I tillegg, ble miR-204 i bindevevet identifisert som en uavhengig prognostisk biomarkør for OPK. Uttrykk av miR-138 viste markert heterogenitet både i OPK vev fra pasienter og i dyrkede fibroblaster. Ektopisk uttrykk av miR-138 reduserte fibroblastenes motilitet og sine evner til å kontrahere kollagen, og undertrykket invasjonen av nærliggende OPK celler. Hemming av miR-138 resulterte i motsatt resultat. Transkripsjon og proteinundersøkelsene viste at antitumor effekten av miR-138 i KAF var assosiert med endringer av KAF-fenotypespesifikke molekyler, fokal adhesjonskinaseakse og TGF $\beta$ 1-signalveien. Samlet, viser resultatene av denne avhandlingen betydelige endringer av miRNA uttrykk i bindevevet av OPK sammenlignet med fibroblaster fra normal munnslimhinne og identifiserer miR-204 og miR-138 som har tumorundertrykkende funksjon ved å endre KAF sin fenotype og motilitet.

---

## List of Publications

- I. Profiling and Functional Analysis of microRNA Deregulation in Cancer-Associated Fibroblasts in Oral Squamous Cell Carcinoma Depicts an Anti-Invasive Role of microRNA-204 via Regulation of Their Motility. **Rajthala S**, Min A, Parajuli H, Debnath KC, Ljøkjel B, Hoven KM, Kvalheim A, Lybak S, Neppelberg E, Vintermyr OK, Johannessen AC, Sapkota D, Costea DE. **Int J Mol Sci**. 2021 Nov 4;22(21):11960. doi: 10.3390/ijms222111960.
  
- II. Combined In Situ Hybridization and Immunohistochemistry on Archival Tissues Reveals Stromal microRNA-204 as Prognostic Biomarker for Oral Squamous Cell Carcinoma. **Rajthala S**, Dongre H, Parajuli H, Min A, Nginamau ES, Kvalheim A, Lybak S, Sapkota D, Johannessen AC, Costea DE. **Cancers** (Basel). 2021 Mar 15;13(6):1307. doi: 10.3390/cancers13061307.
  
- III. MicroRNA-138 Abates Fibroblast Motility with Effect on Invasion of Adjacent Cancer Cells. **Rajthala S**, Parajuli H, Dongre HN, Ljøkjel B, Hoven KM, Kvalheim A, Lybak S, Neppelberg E, Sapkota D, Johannessen AC, Costea DE. **Front Oncol**. 2022 Mar 17;12:833582. doi: 10.3389/fonc.2022.833582. eCollection 2022.

*The papers are published in full open source journals under Creative Commons Attribution Licence (Attribution-NonCommercial 3.0 Unported - CC BY-NC 3.0) that permits use, distribution and reproduction in any medium, provided the original work is properly cited.*



## Abbreviations

BCIP	5-Bromo-4-chloro-3-indolyl phosphate
CAF	Cancer associated fibroblasts
DOI	Depth of invasion
ECM	Extra cellular matrix
EGFR	Epidermal growth factor receptor
EMT	Epithelial mesenchymal transition
ENE	Extra-nodal extensions
FAP	Fibroblast associated protein
FFPE	Formalin-fixed paraffin-embedded
FOXP3	Forkhead box P3
FSP-1	Fibroblast-specific protein 1
HDI	Human development index
HGF	Hepatocyte growth factor
HNSCC	Head and neck squamous cell carcinoma
HPV	Human papilloma virus
IHC	Immunohistochemistry
ISH	In-situ hybridization
LN	Lymph node
MMP	Matrix metalloproteases

---

NBT	Nitro blue tetrazolium
NGS	Next-generation sequencing
IOD	Integrated optical density
OPMD	Oral potentially malignant disorder
OS	Overall survival
OSCC	Oral squamous cell carcinoma
PDGF	Platelet-derived growth factor
PD-L1	Programmed death-ligand 1
PDPN	Podoplanin
PPAP	Positive pixel area percentage
RFS	Recurrence-free survival
ROS	Reactive oxygen species
RT-qPCR	Quantitative reverse transcription polymerase chain reaction
TCGA	The cancer genome atlas
TF	Tumour front
TGF- $\beta$	Transforming growth factor beta
TME	Tumour microenvironment
VEGF	Vascular endothelial growth factor
WPI	Worst pattern of invasion
$\alpha$ SMA	Alpha smooth muscle actin

---

## Contents

<i>Scientific environment</i>	3
<i>Acknowledgements</i>	4
<i>Abstract in English</i>	5
<i>Abstract in Norwegian</i>	6
<i>List of Publications</i>	7
<i>Abbreviations</i>	8
<i>Contents</i>	10
<b>1. Introduction</b>	<b>13</b>
<b>1.1 Oral cancer: epidemiology and risk factors</b>	<b>13</b>
<b>1.2 Pathogenesis of OSCC</b>	<b>15</b>
<b>1.3 OSCC histology, staging, and clinicopathological characteristics</b>	<b>19</b>
<b>1.4 Prognostic indicators of OSCC</b>	<b>20</b>
<b>1.5 Tumor microenvironment in OSCC</b>	<b>25</b>
<b>1.6 Cancer-associated fibroblasts (CAFs)</b>	<b>27</b>
1.6.1 Heterogeneity of CAFs	27
<b>1.7 Introduction to microRNAs</b>	<b>30</b>
<b>1.8 miRNA biogenesis</b>	<b>32</b>
<b>1.9 miRNA alterations in OSCC</b>	<b>32</b>
<b>1.10 miRNA as therapeutics</b>	<b>34</b>
<b>2. Aims of the study</b>	<b>35</b>
<b>2.1 Rationale for the study</b>	<b>35</b>
<b>2.2 Study hypothesis</b>	<b>35</b>

---

2.3	Main aim	35
2.4	Specific aims	35
3.	<i>Methodological considerations</i>	36
3.1	Study models	36
3.2	Retrospective patient cohort	36
3.3	Primary fibroblast isolation and characterization	37
3.4	Cell culture	37
3.5	3D organotypic culture	38
3.6	miRNA modulation in fibroblasts	39
3.7	miRNA expression profiling	40
3.8	qRT-PCR	40
3.9	Western blot	41
3.10	miRNA target identification	41
3.11	miRNA dual luciferase target reporter assay	41
3.12	miRNA <i>in situ</i> hybridization and pan-cytokeratin immunohistochemistry double staining	44
3.13	miRNA quantification in OSCC tissues	46
3.14	TCGA miRNA data analysis	46
3.15	Statistical analysis	46
4.	<i>Results</i>	48
4.1	Paper I	48
4.1.1	miRNA array	48
4.1.2	Identification of <i>ITGA11</i> as a target for miR-204 in CAFs	48
4.1.3	Functional role of miR-204 in CAFs	49

---

<b>4.2 Paper II</b>	<b>50</b>
4.2.1 Combined miRNA ISH and IHC staining and quantification	50
4.2.2 miRNA-204 as a prognostic marker in OSCC	50
<b>4.3 Paper III</b>	<b>51</b>
4.3.1 Functional role of miR-138 in CAFs	51
4.3.2 Heterogenous expression of miR-138 in OSCC tissues	51
<b>5. Discussion</b>	<b>53</b>
<b>6. Conclusions</b>	<b>60</b>
<b>7. Further perspectives</b>	<b>61</b>
<b>Source of data</b>	<b>62</b>

---

# 1. Introduction

## 1.1 Oral cancer: epidemiology and risk factors

Oral cancer comprises malignancies arising in the mobile tongue, floor of the mouth, gingiva, palate, buccal mucosa, and mucosal part of the lips. Oral cavity is a relatively common site for cancer, accounting 377 713 new cases and 177 757 deaths worldwide in 2020 and is estimated to increase by 41.7% and 47% respectively by 2040 [1, 2]. There is a large geographical variation in oral cancer incidences (*Figure 1*), which has been associated to region-specific risk factors [3].

Smoking, including smokeless tobacco and excessive alcohol consumption are the major risk factors, accounting up to 90% of oral cancer [4]. Exposure to carcinogenic substances from tobacco, such as benzo-(a)-pyrene and nitrosamines [5], and from alcohol and its metabolite acetaldehyde [6] have been implicated in progressive genetic insults. Acetaldehyde can damage the genome by crosslinking opposing DNA strands [7]. In addition, alcohol association to cancer is linked to abduced or reduced activity of an enzyme acetaldehyde dehydrogenase that detoxify acetaldehyde to acetate [8]. As per global cancer observatory, of the new cases of oral cancer in 2020, 75 000 cases have been attributed to alcohol drinking (International Agency for Research on Cancer, WHO). The high incidences of oral cancer observed in Eastern Europe and Australia/New Zealand [9] have been linked to tobacco smoking and alcohol consumption.

Oral cancer is highly frequent in South Central Asia and Melanesia [9], and there it has been linked to use of betel quid and smokeless tobacco. Meanwhile, highly prevalent in Australia, North America, Europe and Oceania, the cancer of the lip has been linked to exposure to ultraviolet radiation from the Sun [10].

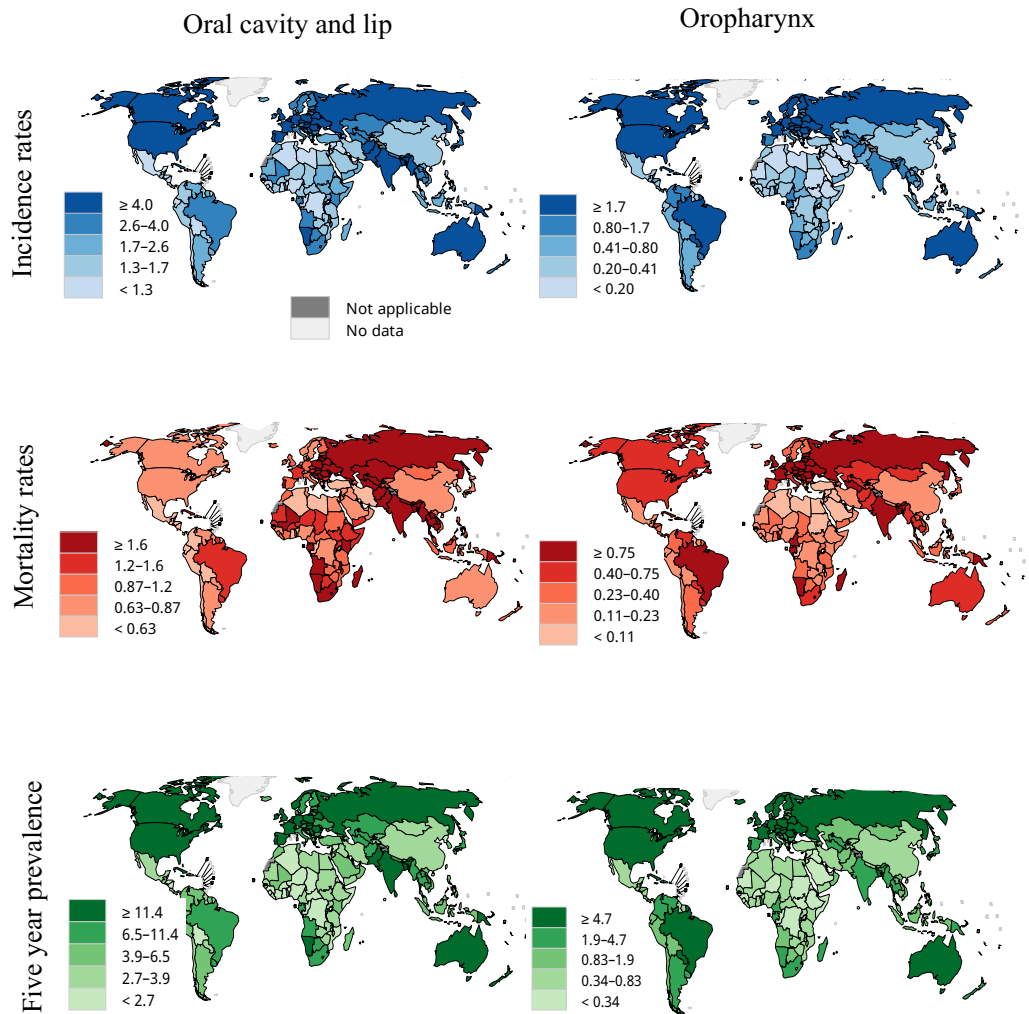


**Figure 1.** Age-standardized incidence and mortality rates, and five-year prevalence of oral and oropharynx cancer in the world in 2020 (per 100,000). Data source: GLOBOCAN 2020, IARC, World Health Organization.

---

The global distribution of oral cancers seems to be also affected by other factors such as human development index (HDI) status and gender status, with higher incidences of oral cancer in countries ranked with lower HDI (overall cancer incidence is higher with higher HDI), and in male group [9].

The human papillomavirus (HPV)-associated head and neck cancers, especially oropharyngeal tumors in developed countries are on rise [11]. Compared to oropharyngeal cancer where there is a high incidence of high-risk HPV infection (up to 87.5%) [12], the contribution of HPV to the etiology of oral cancer is much lower (up to 12.5%) [13, 14].

Among oral cancers, oral squamous cell carcinomas (OSCC) which arise from oral squamous cell epithelium are the most common type and represent 90% of oral cancer [1].

## 1.2 Pathogenesis of OSCC

It is widely accepted that tumor pathogenesis is a multistep evolutionary process [15]. During this process, the cells acquire abilities to sustain proliferation, evade growth suppression, resist cell death, replicative immortality, activate invasion and metastasis, evade immune attack, form new blood vessels, and change cellular metabolism. Underlying these acquired hallmarks is the genomic instability [16]. In cancer, genomic instability involves complex genetic alterations including copy number alterations (amplifications and deletions), chromosomal fusions, germline and somatic mutations, and epigenetic changes (DNA methylation and histone modification) resulting in oncogenic or tumor suppressive gene functions [17, 18]. A recent review investigating the evidence of the contribution of these hallmarks to OSCC has revealed that extensive research efforts are needed since some hallmarks completely lack evidence from OSCC or the evidence is very scarce [19].

Clinical observations have suggested for long that OSCC can progress from lesions such as oral leukoplakia, oral lichen planus and oral submucous fibrosis. These conditions are called oral potentially malignant disorders (OPMDs) as they can



progress to invasive carcinoma with occurrence of additional genetic alterations [20, 21].

A genetic multistep progression model of oral carcinogenesis has been proposed and demonstrated by studies showing how sequential genetic events lead to the formation of mutated 'patches' first, then extensive cancerized fields that later develop in invasive lesions [22].

This model clarifies how cases of OSCC can clinically occur after the presence of oral leukoplakia or other OPMDs. This is part of the concept of "field cancerization" which was initially proposed by Slaughter et al. in 1953 to illustrate the histological alterations (*i.e.*, dysplasia and/or hyperplasia) present throughout the entire mucosa of the upper aerodigestive tract in patients with head and neck cancer [23]. These changes arise due to persistent exposure to carcinogens, particularly tobacco, and molecular studies have corroborated the clinical and micromorphological changes first described by Slaughter to molecular alterations [24]. This concept explains occurrence of second primary tumors and the high rates of local recurrence in OSCC, which can be attributed to changes in the normal tissue adjacent to the primary tumor [25].

There is now evidence showing abnormal DNA content and molecular alterations already from the OPMD stage, the most investigated being alterations of p53 (*TP53*), Cyclin D1 (*CCND1*), and podoplanin (*PDPN*). [26]. There are also studies showing alterations of miRNA already in OPMDs compared to normal mucosa, indicating a complex biology of oral cancer progression and that miRNA play a role in oral cancer development [27, 28]. Nevertheless, OSCC can develop without formation of premalignant lesions.

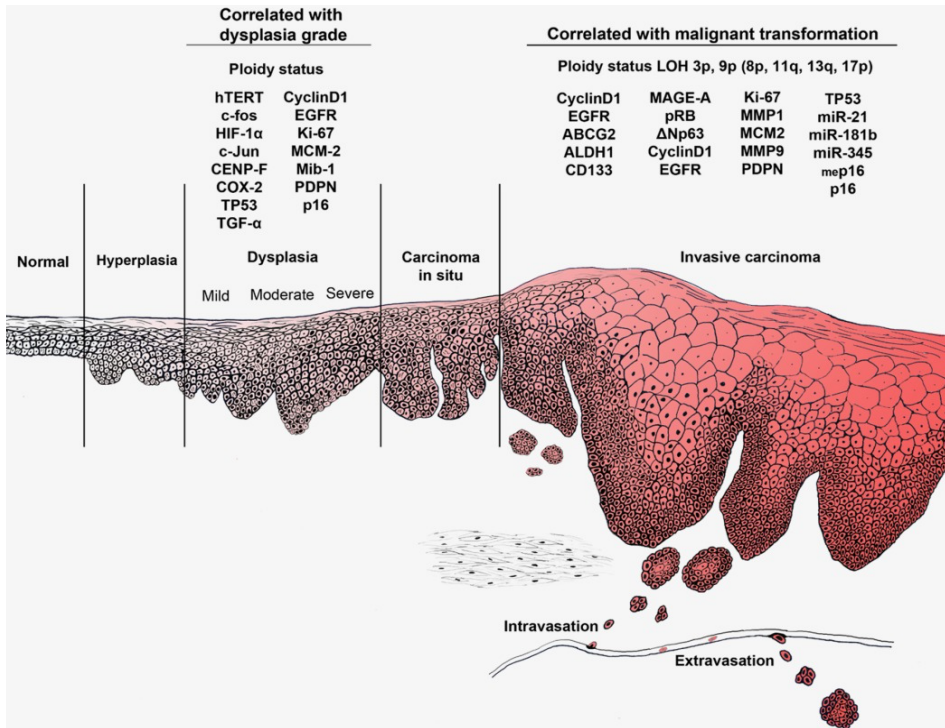


**Figure 2.** Schematic view of genetic alterations in OPMD and their association with progression to OSCC. From [26] under Creative Commons Attribution Licence CC BY-NC 3.

The genetic landscape has been characterized in head and neck squamous cell carcinoma (HNSCC), including subsets of OSCC by several studies on cohorts with different demographic characteristics [17, 29-34]. In average, HNSCC seems to be characterized by 141 copy number alterations, and 62 chromosomal fusions per tumor. A comprehensive genomic characterization of 279 head and neck squamous cell carcinoma (HNSCC, 172 oral cavity, 33 oropharynx and 72 laryngeal) showed near universal loss-of-function *TP53* mutation and *CDKN2A* inactivation in smoking related HNSCC group (86% of cases). HPV-associated tumors were dominated by activating mutation of *PIK3CA*. Among others, common somatic mutations and copy number alterations in HNSCC included *FAT1*, *CASP8*, *NOTCH1*, *AJUBA*, *KMT2D* and *NSD1* [17].

<i>GENE</i>	<i>TCGA</i>	<i>COSMIC</i>	<i>Dongre et al</i>
<i>TP53</i>	72	41	43
<i>CDKN2A</i>	22	16	19
<i>FAT1</i>	23	5	22
<i>PIK3CA</i>	21	8	
<i>NOTCH1</i>	19	10	
<i>KMT2D</i>	18	5	4
<i>NSD1</i>	10	4	6
<i>CASP8</i>	9	5	4
<i>HRAS</i>	4	8	
<i>FBXW7</i>	5	3	
<i>AJUBA</i>	6	0	
<i>NFE2L2</i>	6	5	
<i>TGFBR2</i>	4	1	
<i>CUL3</i>	4	2	
<i>FLG</i>			19
<i>FGFR3</i>			7
<i>KMT2C</i>			6
<i>SMAD4</i>			4
<i>TRAF3</i>	1	0	4
<i>NOTCH2</i>			4

**Table 1.** Most frequent somatic mutations and copy number alterations in HNSCC in % of total cases [17, 35].

### 1.3 OSCC histology, staging, and clinicopathological characteristics

The normal oral mucosa consists of the outermost layer - the epithelium, the middle layer called the lamina propria or connective tissue, and the innermost layer known as the submucosa. The epithelium of the normal oral mucosa is a stratified squamous epithelium which presents variations between different sites of the oral cavity in terms of keratinisation and extensibility (Figure 3). Irrespective of the anatomical sub-location, the oral epithelium has an extremely well-regulated structure with a basal cell layer where the stem cell resides and the cell proliferation takes place, a squamous (middle) and a superficial cell layer where the cells differentiate and desquamate respectively [36]. The homeostasis of the normal oral epithelium is maintained by a continuous cell proliferation that replaces the cells lost at the superficial cell layer by desquamation [37]. The lamina propria or connective tissue is a dense layer that provides support and nourishment to epithelium. It contains various types of cells, including fibroblasts, blood vessels, and immune cells. The submucosa is the deepest layer of the normal oral mucosa. It consists of loose connective tissue and serves as a transition between the oral mucosa and the underlying structures, such as muscle or bone.

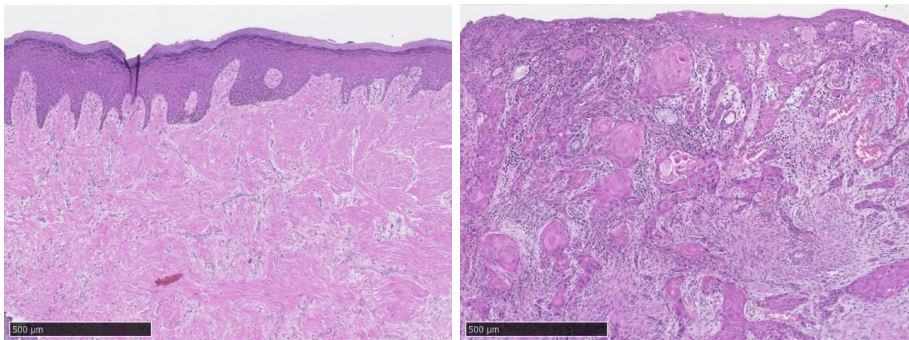


**Figure 3.** Tissue sections (hematoxylin-eosin staining, 5x magnification) of normal oral mucosa from gingiva (left panel) and OSCC (right panel). Own pictures.

OSCC is characterized by the uncontrolled growth of squamous cells within the epithelium and an altered morphology and structure in which the normal architecture of the oral mucosa is disrupted, as exemplified in Figure 3. The epithelium exhibits cytological (cellular) changes such as atypia, hyperchromatism and pleomorphism, and tissue changes which involve abnormal cell proliferation and disorganization. The essential characteristic of OSCC is, as for any other epithelial malignancy, the invasion of the abnormal epithelium deeper into the underlying connective tissue [15]. As the tumor progresses, OSCC may invade surrounding tissues, such as muscle or bone. It can also spread to nearby lymph nodes and, in advanced stages, to distant organs through a process called metastasis [38].

OSCC, which is detected via clinical examination of oral cavity and further confirmed with a histological examination of a biopsy, is often diagnosed at advanced stages leading to severely reduced patient survival. With the current diagnostic and treatment modalities (surgery, radiation and chemotherapy), the 5 years survival is less than 50% [1, 39]. Late diagnosis, regional lymph node metastasis and recurrences are the main reasons for poor prognosis and reduced survival [40]. In addition, for those who survive the disease, possible disfigurement due to surgery is a huge psychological and functional burden.

## 1.4 Prognostic indicators of OSCC

There are many factors that influence the outcome of OSCC. They can be patient, tumour or treatment related [41]. The main patient-related factors which are known to influence the disease outcome are age, overall health status, and smoking and alcohol history of the patient. Treatment-related factors (Figure 4) can also influence the prognosis.

Essential for management of OSCC is to have a classification for evaluation of prognosis and guidance to treatment decisions that is robust and feasible for the clinical settings. The classification system currently used in clinics as treatment guidance to OSCC is known as the TNM classification established in 1987 by Union

for International Cancer Control and The American Joint Committee on Cancer (AJCC). This is based on the size of the tumor (T), the presence of lymph node involvement (N), and the presence of distant metastasis (M) [42]. Several modifications have been made to the TNM staging system since it emerged. In the 8<sup>th</sup> edition of the AJCC staging system published in 2017, additional variables such as the depth of primary tumor invasion (DOI) and extranodal extensions (ENE) were recommended to be included in cancer staging [43].

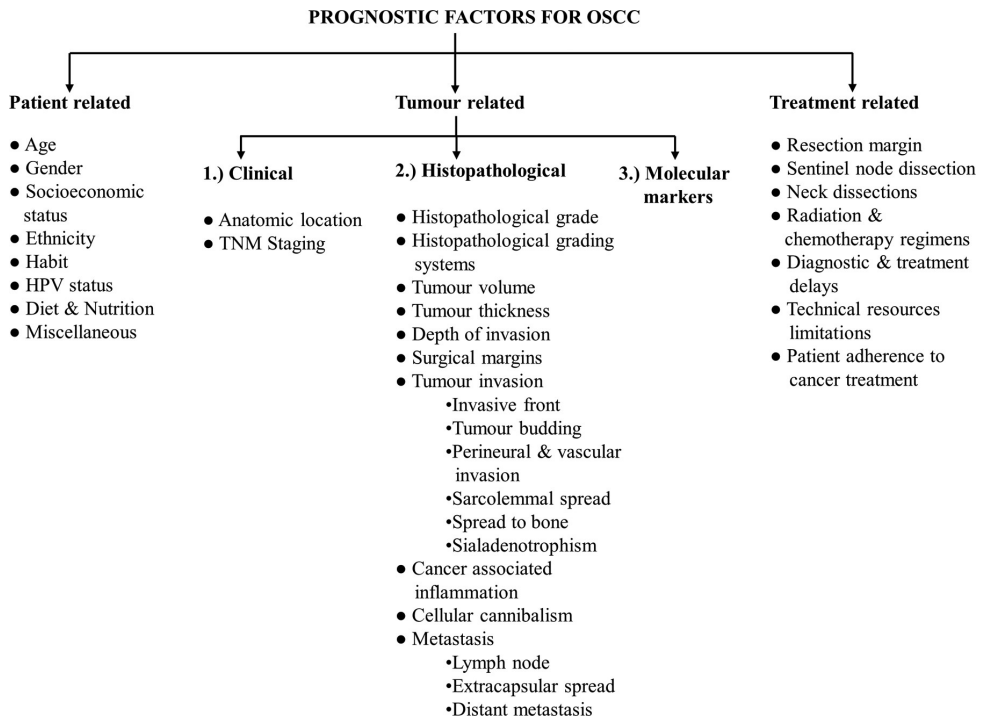


**Figure 4.** Overview on clinico-pathological prognostic determinants of OSCC. From [41] under Creative Commons Attribution Licence CC BY-NC 3.

DOI is defined as the measurement from the basement membrane of the surrounding normal mucosa to the deepest point of tumor invasion [44]. As per several studies, a depth of invasion ranging from 3 to 5 mm significantly increases the risk of nodal metastasis, thereby indicating a worse prognosis [45, 46]. According to the updated AJCC guidelines, the T category increases with every 5 mm interval of depth of invasion, significantly affecting the T stage [43, 47].

The presence of lymph node metastasis is one of the most critical prognostic factors in OSCC. ENE is defined as the "extension of metastatic carcinoma from within a lymph node through the fibrous capsule and into the surrounding connective tissue, regardless of the presence of stromal reaction. Growing body of evidence suggest that not only the presence of lymph node metastasis but also ENE, along with the number and size of metastatic lymph nodes, influence the prognosis of OSCC [47-50]. Based on this accumulating evidence in the literature that ENE is a predictor of a worse prognosis for OSCC, AJCC has incorporated ENE into pN staging [43].

Other histopathological parameters that have been reported to have prognostic value for OSCC are pattern of invasion, perineural invasion (PNI), lymphovascular invasion, tumor budding (TB), tumor-stroma ratio (TSR) and involvement of the surgical margins [51, 52]. With the recent inclusion of DOI and ENE in the current guidelines by AJCC, it is expected that more histopathological parameters will be further adopted [48]. In this respect, the invasive tumor front (ITF), TB and PNI and TSR are the most promising ones, with a clinical significance showed in metaanalysis of the existent studies in OSCC [51, 52]. However, there are controversial findings from different cohorts that raise skepticism about their universal applicability in clinical settings [53].

ITF is defined as the tumour-stromal interface including up to six tumour cell layers or isolated single tumour cells or small islands at the outmost border of a cancer lesion [54]. For several decades many studies have reported that the most active part of an OSCC lesion is located at ITF and assessment of this active area might contain prognostic information [55, 56]. The cells at ITF exhibit characteristics of epithelial-

---

mesenchymal transition (EMT), which might explain their high mobility and deep invasive properties. Histopathologically, the invasion pattern can manifest as pushing borders of cohesive cell groups, finger-like projections, small tumor islands, or tumor satellites [57]. This histopathological parameter holds predictive and prognostic value, allowing the stratification of patients into high-risk and low-risk groups [57, 58].

TB are composed of malignant cells that exhibit loss of cellular cohesion and display active invasive movement. TB is defined as the presence of a single cancer cell or a cluster of fewer than five cells within the stroma at the ITF [58]. TB has been identified as an independent prognostic marker in early-stages OSCC [59] and has been associated with a poor prognosis particularly in tongue carcinoma [58, 60, 61].

PNI refers to the invasion and dissemination of cancer cells along nerve bundles in the surrounding stroma. PNI is defined by the presence of tumor cells within any of the three layers of a nerve sheath or encirclement of at least 33% of a nerve's circumference [62]. This type of invasion can result in neuropathic pain, numbness, sensory nerve dysfunction, paralysis, disfigurement, and motor nerve dysfunction. The prevalence of PNI in OSCC ranges from 12% to 50%. Its occurrence in OSCC has been associated with higher rates of locoregional recurrence, nodal metastasis, poor prognosis, and the need for aggressive treatment approaches [63, 64].

A newer histopathological parameter is TSR that has been shown by several studies to be able to classify tumors into low- and high-risk cases. A meta-analysis showed that TSR was significantly associated with both cancer-related mortality and disease-free survival in OSCC patients [52].

The lymphocytic infiltrate and various types of inflammatory cells have been also indicated by several studies to predict the outcome of disease [54, 65]. However, the results from different studies are still controversial and a recent meta-analysis on HNSCC studies indicates great variation with tumor subsite and the need for more investigation before clinical implementation [66].



Molecular biomarkers can be used for determining cancer prognosis, predicting its recurrence, assessment of its progression and response to therapy. Numerous molecular markers have been investigated and presented as useful prognostic indicators in OSCC and tongue SCC [67]. These include *TP53* mutations, Ki-67 proliferation index, and expression status of cyclin D1, p16, EGFR (epidermal growth factor receptor) and VEGF (vascular endothelial growth factor).

In a meta-analysis on oral tongue SCC, cyclin D1 and VEGF were found to have the most promising prognostic power [68]. Due to limitations in the quality of the published studies, most being performed on small cohorts, and/or not following the REMARK criteria, no sufficient evidence was found for other molecular markers in oral tongue SCC.

Another review that analysed the studies on molecular biomarkers in OSCC concluded that the studies could not be compared and that further studies are required in order to obtain scientific evidence about a clear advantage of using molecular biomarkers for diagnostic purpose in OSCC [69]. In the new era of immunotherapy, several immune markers have been investigated in OSCC and have been suggested to be associated with a more aggressive phenotype and poor prognosis in OSCC. Nevertheless, apart from PD-L1, none of the other immune-related parameters tested have been taken into clinics for treatment decisions involving immunotherapy in metastatic/recurrent HNSCC patients [70].

## 1.5 Tumor microenvironment in OSCC

Tumor initiation and progression is dependent not only on the intrinsic properties of the cancer cells, but also controlled by the host stroma, also defined as tumor stroma, reactive tumor stroma, or tumor microenvironment (TME) [16, 71]. The “seed and soil” hypothesis, which stated the importance of tumor microenvironment (TME) for the malignant phenotype was proposed already in 1889 [72]. However, it’s only after over a century that the importance of TME in cancer initiation and progression gained momentum. Increasing evidences show that cancer progression is not merely due to intrinsic mechanisms of malignant cells that had undergone genetic alterations [73], but also a result of the cross-talk between the transformed malignant cells and the surrounding non-neoplastic cell compartment [74].

The microenvironment surrounding the transformed malignant cells is a complex and continuously evolving system, composed of activated fibroblasts generally known as cancer associated fibroblasts (CAFs), endothelial cells, pericytes, immune cells, muscle, fat and nerve cells, extracellular matrix and soluble factors [16, 38, 71, 75], as depicted in Figure 5.

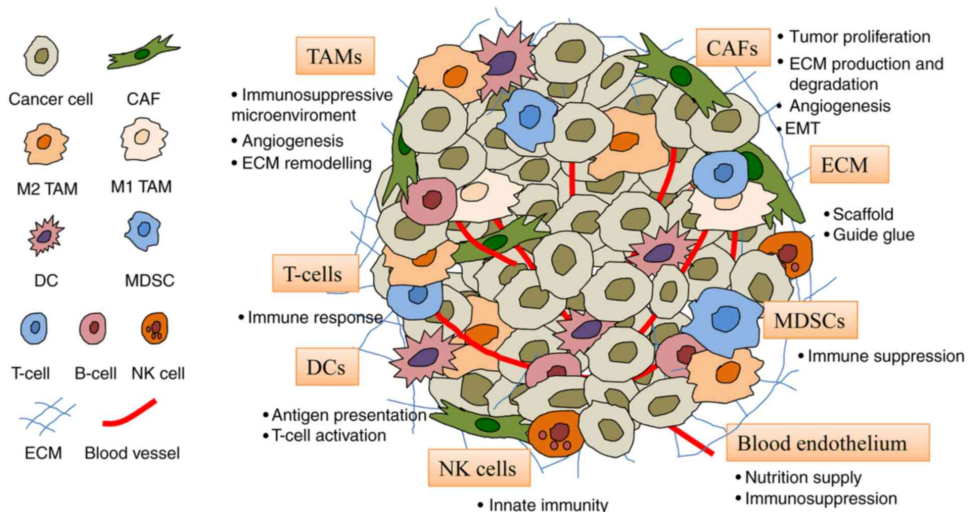


**Figure 5.** Schematic cartoon showing constituents of TME: CAFs, endothelial cells, immune cells (TAMs, DCs, T-cells, MDSCs and NK cells) and the ECM. CAF, cancer-associated fibroblast; DC, dendritic cell; ECM, extracellular matrix; MDSC, myeloid-derived suppressor cell; NK, natural killer; TAM, tumor-associated macrophage; TME, tumor

microenvironment. From [78] under the Creative Commons Attribution Licence CC BY-NC 3.

The neoplastic cells and the tumor stroma co-evolve during cancer progression. The co-evolution involves recruitment of fibroblasts, and local and bone marrow derived stromal and progenitor cells, immune cells infiltration, matrix remodeling and development of new vasculature [16, 76]. All the cell populations of the microenvironment interact and crosstalk with each other via complex communication networks and soluble factors within the surrounding non-cellular components. Nevertheless, unlike cancer cells, stromal cells are genetically stable and, therefore are attractive therapeutic targets in addition to being considered a more reliable source of tumour biomarkers [77].

HNSCC, including OSCC are among the cancers with a high stromal content [79]. Numerous studies have indicated that TME as a whole, or its components play a key role in OSCC progression and outcome, as both positive and negative regulators of HNSCC development [80].

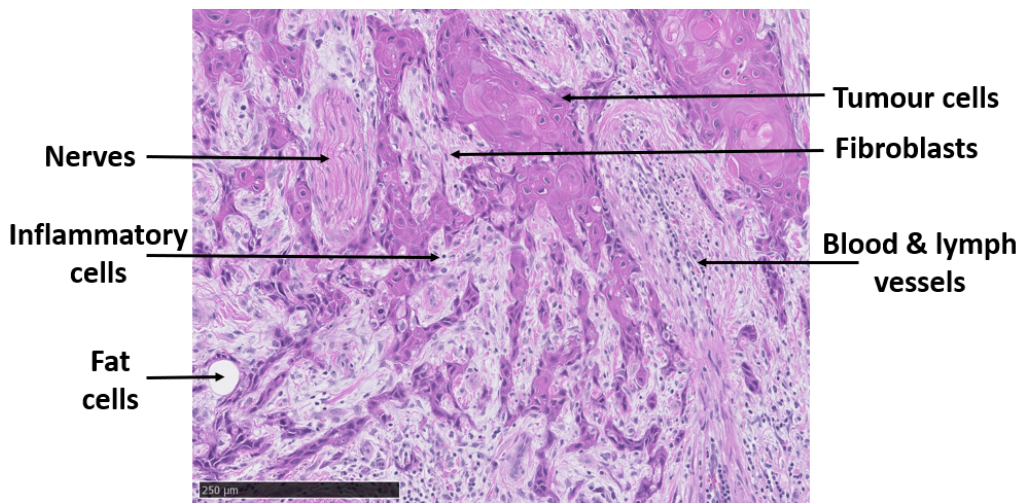


**Figure 6.** Tissues section from an OSCC lesion. Various tumor components are pointed by arrows. Own picture.

---

## 1.6 Cancer-associated fibroblasts (CAFs)

Fibroblasts are the most abundant mesenchyme-derived cell type in the stroma responsible for structural framework in the tissues. CAFs represent the most prevalent constituent cell type in TME in solid tumors, including OSCC [79]. CAFs have varying origin and therefore are heterogenous population with no single marker for identification [75].

Fibroblasts in normal tissues are activated in response to wound in the repair process [76]. Unlike the normal fibroblasts, fibroblasts in the TME (CAFs) do not regress in time and can support cancers in all stages of development, including metastasis [81]. Compared to normal fibroblasts, CAFs exhibits altered proliferation patterns, enhanced extracellular matrix production and distinct secretory profile [82, 83].

In OSCC, cancer associated fibroblasts (CAFs) have been shown to play crucial role in tumor initiation and invasion in *in vitro* cell culture studies [83-85] and *in vivo* animal studies [83]. CAFs have been also associated to lymph node metastasis [86, 87] and poor prognosis [86-90] of OSCC. However, at least some subpopulations of CAFs have also been shown to restrain tumor formation in OSCC [91, 92].

### 1.6.1 Heterogeneity of CAFs

It is widely accepted that at least one source of CAFs are the resident fibroblasts that undergo activation in response to either factors secreted by cancer cells or to environmental cues, resembling the activation process of quiescent fibroblasts in injured tissues prior to repair [93]. In the wound-healing response, quiescent fibroblasts are reversibly activated into myofibroblasts to facilitate tissue repair and regeneration, while in cancer, the regression of activated fibroblast states does not occur [94]. The activation of fibroblasts in cancer is influenced by various growth factors and cytokines, including fibroblast growth factor (FGF), transforming growth factor- $\beta$  (TGF $\beta$ ), platelet-derived growth factor (PDGF), receptor tyrosine kinase (RTK) signaling, tumor necrosis factor (TNF), and reactive oxygen species (ROS). These factors are released by cancer cells and/or infiltrating immune cells [81].

However, defining the specific cell population of CAFs remains challenging due to the lack of specific markers [93]. Most commonly used markers to characterize CAFs are fibroblast-specific protein 1 (FSP-1), vimentin, alpha-smooth muscle actin ( $\alpha$ SMA), fibroblast activating protein alpha (FAP), PDGFR $\alpha$ , PDGFR $\beta$ , and ligands belonging to the transforming growth factor  $\beta$  (TGF $\beta$ ) superfamily and bone morphogenic proteins (BMPs), epidermal growth factors (EGFs), fibroblast growth factors (FGFs), sonic hedgehog (SHH), desmin and discoidin domain-containing receptor-2 (DDR2) [93]. Of note, none of these markers is specific to CAFs. Therefore, when using these markers, consideration should be given to context, morphology, spatial distribution, and absence of lineage markers (for epithelial, endothelial, and blood-born cells) [93]. Furthermore, it is likely that many functionally activated fibroblasts do not express all these putative markers simultaneously, creating a certain degree of heterogeneity.

CAF heterogeneity could also be related to their different origins. Bone marrow-derived cells, adipocytes, smooth muscle cells, pericytes, and endothelial cells may differentiate to become CAFs, in addition to the activation of the tissue resident fibroblasts [81]. CAF heterogeneity could also be explained by their different location and the different functions of the organ/area in which they reside.

The phenotype of CAFs can as well potentially be influenced by the genetic background of the tumor. To investigate this, Lim et al. conducted a study where they isolated and compared CAFs from OSCC with intact *TP53* gene and OSCC with mutated *TP53*. The researchers observed that cancer cells derived from OSCC tumors with *TP53* mutation were capable of inducing senescence in CAFs, whereas *TP53* intact and dysplastic cells lacked this ability. *TP53 mutated* tumors showed increased expression of  $\alpha$  smooth muscle actin ( $\alpha$ SMA), and the induction of senescence led to elevated  $\alpha$ SMA levels in oral fibroblasts, resulting in a myofibroblast-like phenotype. These senescent  $\alpha$ SMA<sup>high</sup> CAFs exhibited reduced proliferation but were believed to provide greater support for tumor growth compared to non-senescent CAFs [95].

During last decade, several lines of evidence confirmed the heterogeneity and plasticity of CAFs in carcinomas, including breast and pancreatic adenocarcinoma and OSCC [79, 96] (Figure 7).

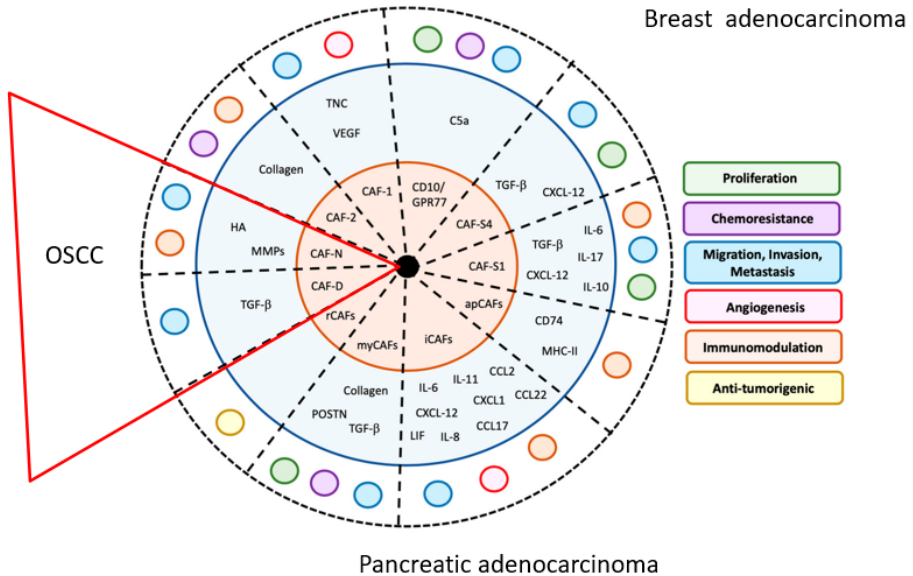


**Figure 7.** Schematic figure depicting CAF heterogeneity in breast and pancreatic adenocarcinoma and OSCC. Modified from [96] under the Creative Commons Attribution Licence CC BY-NC 3.

The presence of different subtypes of CAFs with distinct functions has been demonstrated in OSCC through functional experimental studies [83, 91, 92]. Previous study from our lab conducted a transcriptomic analysis comparing the heterogeneity of OSCC-derived CAFs with normal fibroblasts, using both 2D and 3D culture arrays [83]. The study identified two populations of CAFs. One kind was a more normal-like fibroblast population with a transcriptome and secretome more similar to that of normal fibroblasts. This group contained a higher proportion of intrinsically mobile cells, responsive to TGFβ1 and sustained high autocrine hyaluronic acid synthesis. In contrast, another type of CAFs identified comprised of CAFs with a more divergent transcriptome, had fewer motile cells, were not responsive to TGFβ1 but synthesized higher levels of TGFβ1 [83].

More recently, the advent of single-cell transcriptomic sequencing (scRNA-seq) has provided a more comprehensive understanding of the various subtypes of CAFs [97, 98]. Two main CAF subtypes and a third, minor type, were identified through scRNA-seq [98]. One subset expressed classical markers of myofibroblasts,  $\alpha$ SMA (ACTA2); the second subset expressed ECM genes, including FAP, podoplanin (PDPN), and connective tissue growth factor (CTGF); and the third, minor subset was depleted of markers for myofibroblasts and CAFs, and was interpreted as representing resting fibroblasts. Another scRNA-seq study revealed a higher degree of heterogeneity within CAFs and identified five different CAF clusters, some similar to those identified in Puram study, and a new cluster expressing CXCL8, a CAF subset associated with aggressive cancer progression [97].

Nonetheless, despite the great progress made in identifying several CAF subtypes in OSCC, the characterization of CAF heterogeneity is only at its beginning and quite incomplete, the specific functions of various CAF subsets remaining unclear.

## 1.7 Introduction to microRNAs

MicroRNAs (miRNAs) are approximately 22 nucleotides small non-coding RNAs that are post transcriptional regulators of diverse cellular function. miRNAs target mRNAs for destabilization, cleavage and translational repression [99].

Magnitude of mRNA decay and translational repression by miRNAs can vary greatly [100]. A single miRNA can bind to as many as 200 gene targets. Currently there are about 2000 predicted and experimentally verified miRNA genes. miRNAs are predicted to regulate about 60% of human genes [101].

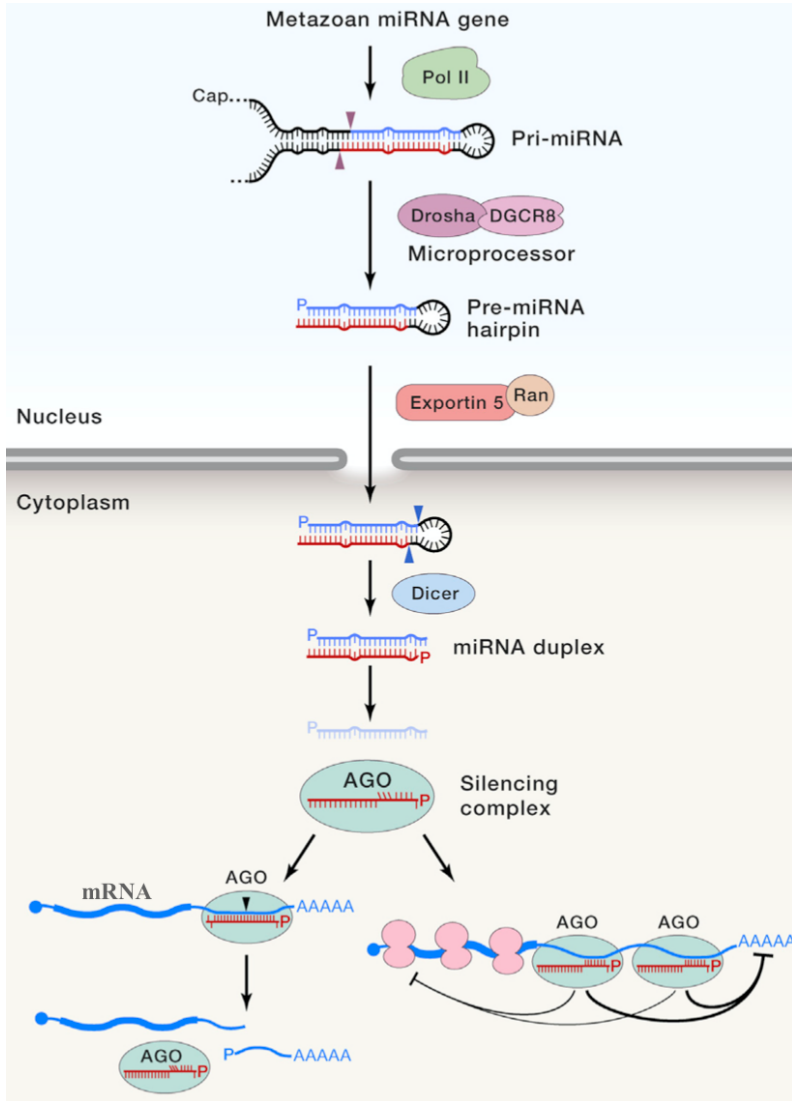


**Figure 8:** Schematic representation of the biogenesis and function of typical miRNA in animals. Modified from [99]. Used under Creative Commons Attribution Licence CC BY-NC 3.



## 1.8 miRNA biogenesis

miRNAs are initially transcribed in the nucleus by RNA polymerase II as pri-miRNAs that fold to form a hairpin structure (Figure 8). A hairpin structure is then cleaved by an endonuclease called Drosha which is a part of heterotrimeric Microprocessor complex to about 60 nucleotides stem-loop called pre-miRNA. Thereafter, the pre-miRNA is exported to the cytoplasm by the action of Exportin 5 and RAN-GTP. In the cytoplasm pre-miRNA loop is cut by another endonuclease called Dicer to generate miRNA duplex with 2 nucleotides 3' overhang on each end. The miRNA duplex is then loaded into an Argonaute protein, with concomitant expulsion of one of the strand of miRNA duplex called the passenger strand (miRNA\*) to form a mature silencing complex. The miRNA (guide strand) guides the silencing complex to pairs to its target mRNAs or other transcripts to direct posttranscriptional repression [102].

## 1.9 miRNA alterations in OSCC

Abnormal expression of microRNAs (miRNA) underlies many pathologic processes, including cancer. The idea that miRNAs could be involved in cancers, stems from the finding that over half of the investigated miRNA genes (98 of 186 known or predicted miRNA) are located in cancer-associated fragile genomic regions [103].

While tumor evolution and progression is regulated by very complex mechanisms, miRNAs are one of the major players [102]. miRNAs deregulation as a result of genetic, epigenetic and transcriptional changes have been widely recognized to be involved in all the processes of tumor development and progression in all kinds of cancer [104]. Some miRNAs act as tumor suppressors, others known as oncomiR can promote tumor initiation, growth and/or progression to metastasis.

miRNAs deregulation in OSCC and their putative use as diagnostic and prognostic biomarkers, and therapeutics agents or targets has been described in numerous previous studies (reviewed in [105-107]).

---

The largest family of miRNAs, Let-7 family was reported to be downregulated in OSCC and it was described as a “tumour suppressor miRNA” [108]. One member of this family, let-7g-5p has been reported to be a direct regulator of RAS expression. Loss of let-7g-5p was found to be associated with EMT-like phenotype of cancer cells and correlated with poor prognosis in patients with OSCC [109]. Other potentially tumour-suppressive miRNAs include miR-34c, miR-138, miR-375, and miR-204. Up-regulation of miR-196a, miR-21, miR-1237 and downregulation of miR-204, miR-144 was associated with poor prognosis of OSCC patients. The miR-196a/miR-204 expression ratio was identified as the best predictor for recurrence and survival[110].

Many other miRNAs have been proven to be differentially expressed in OSCC in several studies. Despite the growth in literature on miRNAs and their specific expression status across tissue and disease types, each new study brings up a new profile with very few common signatures. Ethnic variations in the study subjects have been suggested to be a major contributor to this difference. Most of the present literature on OSCC specific miRNAs come from European and American study subjects comprising mostly of Caucasians, Hispanics, and Blacks, whereas the major burden of the disease is on developing countries, especially the Indian Peninsula. Besides a few tissue level miRNA expression studies, the majority of the data is derived from OSCC cell lines, which is inadequate to provide a significant picture on miRNA expression status.

A recent systematic review showed that upregulation of 9 miRNAs in OSCC (miR-21, miR-455-5p, miR-155-5p, miR-372, miR-373, miR-29b, miR-1246, miR-196a, and miR-181) and downregulation of 7 miRNAs (miR-204, miR-101, miR-32, miR-20a, miR-16, miR-17, and miR-125b) was associated with poor prognosis in OSCC [111]

However, the study of the stromal aberrations of miRNAs, particularly in CAFs in OSCC, is rare. One such unique example is miR-21. miR-21 was the first miRNA to be coined as ‘oncomiR’ due to the fact that it was consistently found overexpressed in

the stroma of many different types of cancers including cancers of lung, breast, pancreas, colon, head and neck, and vulva [112-115]. In OSCC, miR-21 upregulation was associated with poor prognosis [115]. Moreover, miR-21 is known to regulate several biological functions such as cell proliferation, invasion, apoptosis and exhibit chemoresistance via targeting Ras, PDCD4, PTEN, and RECK [108, 115, 116].

## 1.10 miRNA as therapeutics

Since miRNAs target multiple genes, in complex diseases such as cancer in which entire networks are dysregulated, miRNA interventions offer chances to restore coordinated pathways. This is in complete contrast to traditional drugs with only one molecular target. Hence, miRNAs could be ideal targets for cancer therapeutics in future.

Currently, INT-1B3 (InteRNA), a miR-193a-3p mimics formulation with lipid nanoparticle, is in clinical trial phase I (NCT04675996) in patients with advanced solid tumors. MRG-106, also known as Cobomarsen, designed to inhibit miR-155 for the treatment of cutaneous T-cell lymphoma is in second phase of clinical trial (NCT03713320). Historically, other miRNA targets had been into clinical trials, unfortunately with unexpected outcomes. For an instance, Phase I trial of MRX34, a synthetic mimic of miR-34 designed to intervene advanced solid tumors had to be terminated due to immune related serious adverse events [117, 118]. While miRNAs offer flexibility in targeting multiple genes, off-target, undesired target and thereby unwanted side effects have immerged as hindrance to clinical trials. As per Ito M et al, no other miRNA drugs against malignancies [119] are under clinical study as per September 2022.

## 2. Aims of the study

### 2.1 Rationale for the study

While majority of studies focused on miRNA changes in tumor cells or tumor as a whole including in OSCC studies, our knowledge on miRNA alteration in tumor microenvironment, and in particular in cancer associated fibroblasts (CAFs) is limited.

### 2.2 Study hypothesis

Given the impact of both miRNAs, and CAFs in tumor progression, miRNA deregulation in CAFs could be a major factor in determining the behaviour and fate of tumor cells.

### 2.3 Main aim

The overall aim was to investigate miRNA deregulations in OSCC stroma and to identify the miRNAs with prognostic value and functional role on tumor progression.

### 2.4 Specific aims

1. To identify differentially expressed miRNAs in OSCC-derived CAFs as compared to normal oral fibroblasts (NOFs). (Paper I)
2. To study the role of differentially expressed miRNAs (miR-204 and miR-138) in CAFs on OSCC cell behavior modulation. (Papers I and III)
3. To establish a robust method of miRNA quantification using double staining methods (in situ hybridization for miRNA and immunohistochemistry for proteins). (Paper II)
4. To investigate if miR-204 could be used as prognostic biomarker in OSCC. (Paper II)

### 3. Methodological considerations

#### 3.1 Study models

A range of models were used in this study. Archival OSCC tissues from diagnostic archive at Department of Pathology, Haukeland University Hospital (HUS) and cell culture based *in vitro* two-dimensional (2D) and three-dimensional (3D) models were used in this study. Fresh cancer tissues and morphologically cancer free regions from OSCC patients, and fresh normal oral mucosa from healthy volunteers were collected for primary fibroblasts isolation and culture from the Department of Ear, Nose and Throat, HUS. Both archival and fresh tissue specimens were collected after the informed consent. Ethical approval was obtained from the regional ethical committee (West Norway; REKVest 3.2006.2620, REKVest 3.2006.1342). OSCC cell lines UK1 [120] and Luc4 [121] were obtained from our collaborators at Queen Mary University of London, UK.

#### 3.2 Retrospective patient cohort

Patients older than 18 years with primary diagnosis of OSCC between 1998-2012 and treated with surgery or radiotherapy or combination at HUS, Bergen, Norway were first identified. Those receiving neoadjuvant treatment, with missing tissue blocks, or missing a medical electronic journal containing clinical information at HUS were excluded from the study. The clinical information (age, gender, smoking and alcohol use, localization, TNM stage, co-morbidities, recurrence, last date of follow-up, survival) was obtained from patients' medical electronic journal (DIPS) after informed consent (N=169 patients). Formalin-fixed paraffin embedded (FFPE) tissue blocks containing the tumor front with surrounding stroma and, when available, the adjacent normal mucosa, were selected for the study. Tumor specimens were screened for HPV infection using immunohistochemistry (IHC) method with the surrogate marker p16INK4a. Nine (5.53%) HPV positive cases with strong nuclear and cytoplasmic staining in more than 70-80% of the tumor cells were excluded from the study. Finally, a total of 160 HPV-negative OSCC cases (age range: 27-93, mean =

---

65.25, median = 65) were included in the miR-204 study (Paper II). The mean follow-up time was 8.6 years, and the 5-year survival rate was 40%. An overlapping set of patients (n=38) with similar criteria were used for miR-138 study (Paper III) The use of patient samples for the biomarker study followed REMARK criteria [122].

### 3.3 Primary fibroblast isolation and characterization

NOFs were isolated from a non-cancer region of the oral mucosa or from buccal mucosa of healthy individuals after informed consent. CAFs were isolated from tumor biopsies of OSCC patients. The fibroblasts were isolated using methods involving physical and enzymatic dissociation or from tissue explant outgrowth as described in the methodology section in Paper I. After isolation, fibroblasts were characterized for lineage specific markers: ESA (epithelial specific antigen), CD31, CD45, and CD140b for epithelial cells, endothelial cells, leukocytes, and mesenchyme origin respectively [123]. The purity of each strain of primary cells, NOFs or CAFs, was confirmed by flow cytometry, which showed that 96.2% of NOFs and 99.4 %of CAFs stained positively with CD140b that recognizes the platelet derived growth factor b receptor (PDGFBR), a mesenchymal lineage marker. Expressions of ESA, CD45 and CD31 were detected neither in NOFs nor in CAFs.

### 3.4 Cell culture

Fibroblasts were propagated 2D in monolayers in cell culture dishes in Dulbecco's Modified Eagle's Medium (DMEM; D6429, SIGMA) supplemented with 10% newborn calf serum (NBCS). OSCC lines UK1 and Luc4 were propagated in DMEM/Nutrient Mixture F-12 Ham (D8437, Sigma), supplemented with 10% NBCS, 0.4 µg/mL hydrocortisone (H0888, Sigma), 1µg/mL Insulin-Transferrin-Selenium (41400-04, Thermofisher Scientific), 50µg/mL L-ascorbic acid (A7631, Sigma), and 10ng/mL epidermal growth factor (E9644, Sigma). For growing 3D organotypics, FAD medium (DMEM: Ham's F12 Nutrient mixture (31765068, Thermofisher) in ratio 1:3 with supplementation as same as growth medium for OSCC cells, except NBCS was

replaced with 0,1% Bovine Albumin Fraction V; 15260-037, Thermofisher) was used [124, 125].

### 3.5 3D organotypic culture

3D organotypic co-culture models, which resemble normal mucosa or OSCC tumor, have been well described earlier in studies by our research group [83, 124, 125], and also in Papers I and III. In 3D organotypic co-culture models, fibroblasts were embedded in rat tail collagen type I matrix (354239, BD Biosciences, NJ, USA), and then the fibroblasts populated collagen gels were layered with OSCC cells and kept submerged in growth medium for a day or two. The gels were then placed on a metal grid layered with a lens paper with OSCC cells facing the top and the gels were grown under air-nutrient interface until harvested about one week later.

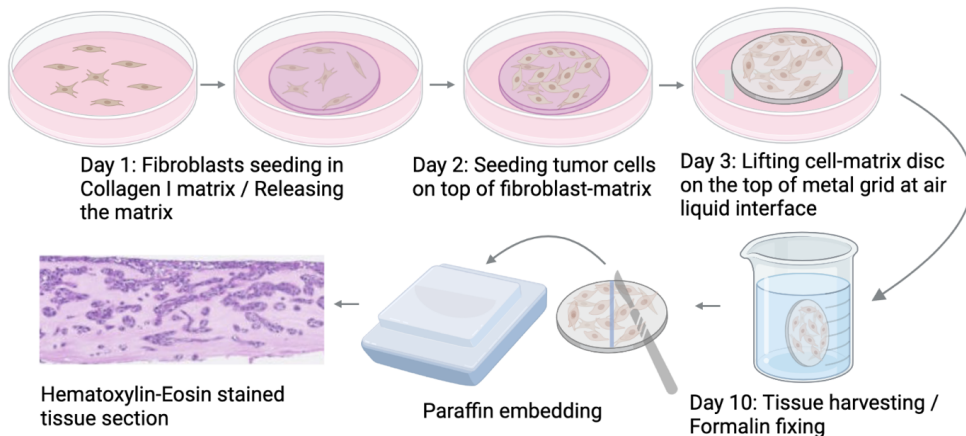


**Figure 9.** Schematic figure showing the workflow for generation of 3D organotypic cultures from primary fibroblasts and cancer cells isolated from OSCC patients, processing of the tissue and the final Hematoxylin-Eosin stained tissue section (own figure made in Biorender).

In another co-culture model, the effect of miRNA modulation in fibroblasts (motility/invasion or phenotypic changes) while maintaining fibroblasts interaction with OSCC was investigated by embedding fibroblasts in collagen on top, followed by a separating non-cell collagen layer in 24 well inserts and cancer cells embedded in (1mg/ml matrigel) on the bottom of the well for 5days. These gels were later fixed overnight in 4% buffered formalin and embedded in paraffin.

Recent studies have demonstrated differences in cell behavior or phenotype when cells are cultured in 2D and 3D environments [126, 127]. However, the *in vitro* 3-D cell culture systems better mimic the *in vivo* physiology [128]. Matrices commonly used in 3D culture are commercially available ECM proteins such as rat tail collagen I, and sarcoma ECM extract from mouse called Matrigel, which is composed of laminin, collagen, heparin sulfate and growth factors. However, the use of non-tissue specific ECM extracts is a subject of question in 3D culture studies, and still far from *in vivo* model alternatives [128].

### 3.6 miRNA modulation in fibroblasts

In order to study the effect of modulation of selected miRNAs on fibroblasts phenotype, and concomitant modulation of tumor cell phenotype, miRNAs were either inhibited with miRNA specific inhibitors or miRNA overexpression was mimicked using miRNA specific mimics in fibroblasts. miRNA mimics, inhibitors and respective controls at 50mM concentration were introduced into the cells via lipofectamine mediated reverse transfection. Forty-eight hours after transfection, fibroblasts were harvested for molecular assays or subjected to functional assays.

<i>Reagents</i>	<i>Company</i>	<i>Catalogue no</i>
miRidian miRNA mimic hsa-miR-204-5p	Dharmacon, USA	C-300563-05-0010
miRidian miRNA inhibitors hsa-miR-204-5p	Dharmacon, USA	IH-300563-07-0010
miRidian miRNA mimic hsa-miR-138-5p	Dharmacon, USA	C-300605-05-0010
miRidian miRNA inhibitors hsa-miR-138-5p	Dharmacon, USA	IH-300605-06-0010
inhibitor control	Dharmacon, USA	IN-001005-01-05
mimic control	Dharmacon, USA	CN-001000-01-05

**Table 3.** List of miRNA mimics, inhibitors and controls.



### 3.7 miRNA expression profiling

Fibroblasts were profiled for expression of 1,146 human miRNAs (>97% coverage for miRBase release 12) using 100 ng of enriched small RNAs (< 200 nucleotides) using Illumina microarray v2 panel. Data from miRNA microarray were normalized and subjected to SAM (significant analysis of microarray) analysis to identify differentially expressed miRNAs in between CAFs and NOFs. Differential regulation of the identified miRNAs was further validated by quantitative real time PCR (qRT-PCR) using Taqman assays.

### 3.8 qRT-PCR

qRT-PCR is a benchmark assay for the measurement of gene expression. Total RNA isolated from fibroblasts using miRNA isolation kit (AM1561, ThermoFisher Scientific) was used for targeted miRNA and mRNA quantification. In Papers I & II, mRNA expression was also quantified using RNA isolated using RNeasy Mini Kit (74104, Qiagen). Total RNA isolation using this kit does not capture RNAs less than 200 nucleotides in length. miRNAs expression was normalized using RNU48 while mRNA expression was normalized with GAPDH and P0.

Taqman Assays	Company	Assay ID
hsa-miR-204-5p	ThermoFisher Scientific, USA	000508
hsa-miR-21-5p	ThermoFisher Scientific, USA	001314
hsa-miR-138-5p	ThermoFisher Scientific, USA	002284
hsa-miR-155-5p	ThermoFisher Scientific, USA	002623
hsa-miR-582-5p	ThermoFisher Scientific, USA	001983
RNU48	ThermoFisher Scientific, USA	001006

**Table 2.** List of Taqman Assays (RT and qRT-PCR miRNA probes and gene probes).

---

### 3.9 Western blot

Semi-quantitative assessment of proteins was performed using Western blot technique. In brief, protein lysates of fibroblasts (48 hours post transfection in case of miRNA modulations) were resolved in 10% polyacrylamide gel and transferred to PVDF membrane. After blocking PVDF membranes with 5% dry milk or 3% BSA, the membrane was incubated with primary antibodies specifically raised against proteins of interest. It was followed by incubation with horse radish peroxidase tagged secondary antibodies, and finally visualized with Chemiluminiscent substrate. Bands of integrin  $\alpha 11$  were visualized using chemiluminescence substrate (Supersignal West Pico/Femto, Thermofisher) in an image reader (LAS 1000, Fujifilm). Protein amounts in the bands in the captured images were quantified using ImageJ Gel commands. GAPDH and Beta-actin were used as loading controls.

### 3.10 miRNA target identification

Studies from our lab have shown increased expression of integrin  $\alpha 11$  in OSCC-derived CAFs compared to NOFs, with tumor promoting role of CAFs with increased expression of *ITGA11* [83, 88]. shRNA mediated silencing of *ITGA11* in CAFs resulted in significant suppression of DOK-CAF tongue xenograft tumors in mice, and reduction of OSCC cell invasion in 3D organotypic models (Parajuli, 2017 #510).

Target conserved sites for miRNAs in 3'UTR sequences of *ITGA11* were identified using three different miRNA target prediction software TargetScan Release 7:1 [129], miRmap (Vejnar, 2012 #652) and miRDB (Wong, 2015 #651). Target identification by any two predictors led to further investigation by direct luciferase target reporter assay.

### 3.11 miRNA dual luciferase target reporter assay

Following Western blots and target recognition, miRNA target reporter assays for miR-204 and miR-138 against *ITGA11* were tested. 3'UTR sequences of *ITGA11* was retrieved from UCSC genome browser (<http://genome.ucsc.edu>) [130]. 3'UTR

sequences of two primary protein coding transcripts of ITGA11 were used for target reporter assay.

Plasmid DNA vectors (Vector Builder) with luciferase upstream of 3'UTR and renilla as a transfection control under different promoters were used for the assay. Non-complimentary mutant sequences were introduced to miR-204 and miR-138 binding sites into the control vectors. Transfection mix of plasmid vectors and miRNA mimics in lipofectamine reagent were introduced to the CAFs and 48 hours later the cells were lysed for luminometry. Reduction in luciferase signal normalized to renilla signal compared to mutant control after miR-204 and miR-138 mimics transfection into the cells indicated direct targeting of ITGA11 by the respective miRNAs. Luciferase and renilla activity were measured in luminometer using dual luciferase detection system (E1910 Promega).

**3'UTR ITGA11 sequence (NM 001004439.2) used for miR-204 target reporter assay. Highlighted in bold italic is a miR-204 binding site**

5'GGCTCCAGAGGAGACTTTGAGTTGATGGGGGCCAGGACACCAGTCCAGGTA  
GTGTTGAGACCCAGGCCTGTGGCCCCACCGAGCTGGAGCGGAGAGGAAGCC  
AGCTGGCTTTGCACTTGACCTCATCTCCCGAGCAATGGCGCCTGCTCCCTCCA  
GAATGGAAGTCAAGCTGGTTTTAAGTGGAAGTGCCCTACTGGGAGACTGGGAC  
ACCTTTAACACAG**ACCCTAGGGATTTAAAGGGACACCCCTAACACACCCAG**  
GCCCATGCCAAGGCCTCCCTCAGGCTCTGTG 3'

Predicted pairing of target region (top) and miRNA (bottom)

5' ....GACCCCUAGGGAUUU**AAAGGGAC**.... Position 236-242 of ITGA11 3'UTR  
3' UCCGUAUCCUACUGUUUCCCUU hsa-miR-204-5p

Mutant sequence: 236-242 AAAGGGA→ATTCCCT

**Part of 3'UTR ITGA11 sequence (1-1355) (NM 001004439.1) used for miR-138 target reporter assay. (Sequence in *italic* is same as NM 001004439.2, in **bold** is a miR-138 binding site)**

*5'GGCTCCAGAGGAGACTTTGAGTTGATGGGGGCCAGGACACCAGTCCAGGT  
AGTGTGAGACCCAGGCCTGTGGCCCCACCGAGCTGGAGCGGAGAGGAAG  
CCAGCTGGCTTTGCACTTGACCTCATCTCCCGAGCAATGGCGCCTGCTCC  
CTCCAGAATGGAACTCAAGCTGGTTTTAAGTGAACTGCCCTACTGGGAG  
ACTGGGACACCTTTAACACA**G**ACCCTAGGGATT**TAAAGGGACA**CCCTA  
CACACACCCAGGCCATGCCAAGGCCTCCCTCAGGCTCTGTGGAGGGCAT  
TTGCTGCCCCAGCTACTAAGGTGCTAGGAATTCGTAATCATCCCCATCCT  
CCAGAGAAACCCAGGGAGGAAGACTGTAAATACGAACCCAATCTGCACA  
CTCCAGGCCTCTAGTTCCAGAAGGATCCAAGACAAAACAGATCTGAATTC  
T GCCTTTTCTCTCACCCATCCACCCCTCCATTGGCTCCCAAGTCACACC  
CACTCCCTTCCCCATAGATAGGCCCTGGGGCTCCCGAAGAATGAACCCA  
AGAGCAAGGGCTTGATGGTGACAGCTGCAAGCCAGGGATGAAGAAAGAC  
TCTGAGATGTGGAGACTGATGGCCAGGCAAGTGGGACCAGGATACTGGA  
CGCTGTCCTGAGATGAGAGGTAGCCGGGCTCTGCACCCACGTGCATTAC  
ATTGACCGCA**ACTCACACATTCCCCACCAGCTGCAG**CCCCCTTGCTCTC  
AGCTGCCAACCCCTCCCGGGTCACTTTTGTCCAGGTACCTCATGGGAAG  
CATGTGGATGACACAATCCCTGGGGCTGTGCATTCCCACGTCTTCTTGCTG  
CAGCCTGCCCTAGACATGGACGCACCCGGCCTGGCTGCAGCTGGGCAGCA  
GGGGTAGGGGTAGGGAGCCTCCCCTCCCTGTATCACCCCTCCCTACACA  
CAC  
ACACACTGCCTCCCATCCTTCCCTCATGCCCGCCAGTGCACAGGGAAGGG  
CTTGGCCAGCGCTGTTGAGGGGTCCCCTCTGGAATGCACTGAATAAAGCA  
CGTGCAAGGACTCCCGGAGCCTGTGCAGCCTTGGTGGCAAATATCTCATC  
TGCCGGCCCCCAGGACAAGTGGTATGACCAGTGATAATGCCCAAGGAC  
AAGGGGCGTGCCTGGCGCCAGTGGAGTAATTTATGCCTTAGTCTTGTTTT  
GAGGTAGAAATGCAAGGGGGACACATGAAAGGCATCAGTCCCCCTGTGC  
ATAGTACGACCTTTACTGTCGTATTTTTGAAAAATTAAAAATACAGTGTTT  
AAAAACAA 3'*

Predicted pairing of target region (top) and miRNA (bottom)

5' ....ACUCACACA**U**UCCCC - **CACCAGCU**.... Position 724-730 of ITGA11 3'UTR  
3' GCCCGACUAAGUGUUGUGGUCGA has-miR-138-5p

Mutant sequences: 724-730 CACCAGCT→GTGGTCGT

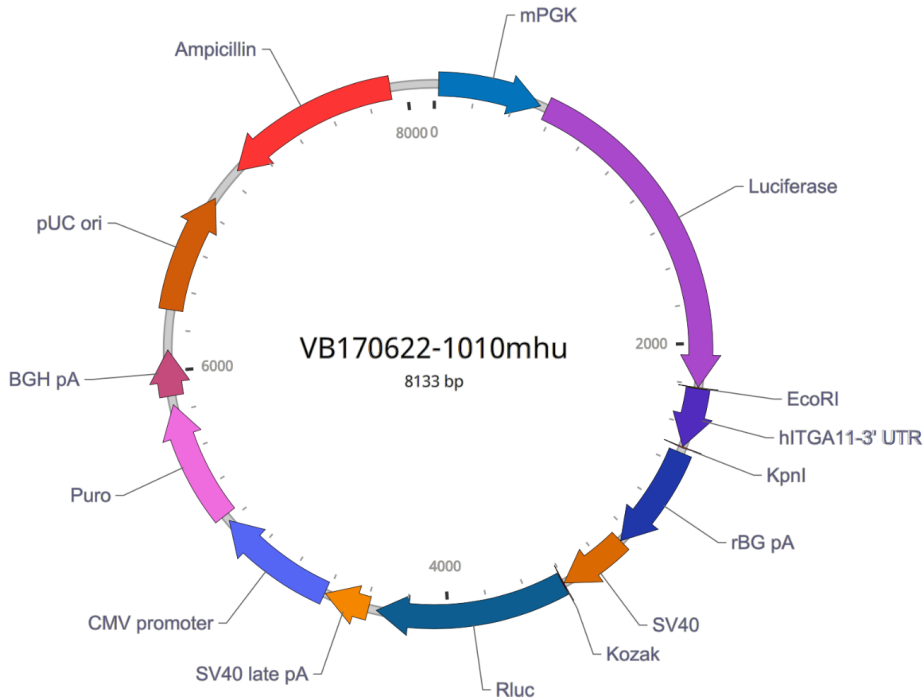


**Figure 10.** Vector map for plasmid DNA used in miRNA target reporter assay.

### 3.12 miRNA *in situ* hybridization and pan-cytokeratin immunohistochemistry double staining

In order to study if tumor stromal miRNAs could serve as novel biomarkers in OSCC stratification and prognosis, *in situ* hybridization (ISH) for miRNAs was optimized for FFPE sections from OSCC lesions. OSCC tissue sections were hybridized with lock nucleic acid based and digoxigenin (DIG) labeled complimentary oligonucleotides specific to miRNAs (Exiqon, Denmark). DIG bound oligonucleotides were then specifically bound to anti-DIG antibodies linked with alkaline phosphatase (ALP). Subsequently, miRNAs were visualized by ALP reaction to its substrate (Nitro blue tetrazolium chloride/5-Bromo-4-chloro-3-indolyl phosphate (NBT-BCIP)) yielding blue precipitate. Levamisole was used to block endogenous ALP activity. No probe

and scramble oligonucleotide were used as negative controls; small nuclear RNA-U6 was used as positive control.

Detection probes	Company	Catalogue no
hsa-miR-204-5p	Exiqon, Denmark	619857-360
hsa-miR-21-5p	Exiqon, Denmark	38102-15
hsa-miR-138-5p	Exiqon, Denmark	38511-15
hsa-miR-155-5p	Exiqon, Denmark	88072-15
U6	Exiqon, Denmark	99002-01
Scramble-miR	Exiqon, Denmark	99004-15

**Table 4.** List of miRNA detection oligonucleotide probes for ISH (miRCURY LNA<sup>TM</sup>; 5'-DIG and 3'-DIG labeled).

Poorly differentiated cancer cells and single tumor cells in OSCC are difficult to identify only with counterstaining. Therefore, in order to exclude epithelium from stromal miRNA quantification, OSCC tissue sections were further optimized for combined miRNA ISH and pan-cytokeratins (pan-CK) immunohistochemistry (IHC). Cytokeratins in OSCC tissue sections were specifically bound to monoclonal mouse anti-human CK antibodies. Secondary antibodies conjugated to horseradish peroxidase (HRP) were targeted to anti-human CK antibodies and visualized using diaminobenzidine (DAB) reaction to HRP. Endogenous peroxidase activity in the tissues was blocked with 3% hydrogen peroxide solution.

CKs are good markers of epithelial tumors. However, we have also found pan-CK negative OSCC tumors, in line with an another study in which a rare case of pan-CK negative small cell lung carcinoma was found [131]. Pan-CK staining was combined to miRNA ISH in four different sequential combinations of miRNA ISH and pan-CK IHC for finding the most optimal methodological flow of stainings, as illustrated in Fig 1 in Paper II.

### 3.13 miRNA quantification in OSCC tissues

miRNA staining in double stained OSCC tissues were digitally quantified using scanned images of stained tissue sections by Hamamatsu NanoZoomer-XR, Japan. Freely available ImageJ and pay lincensing Aperio ImageScope (AperioI) were used for quantification and compared. First, RGB vectors for NBT-BCIP, DAB and fast red were acquired using tissue images with individual staining. Obtained RGB vectors were integrated into java for Color Deconvolution, which was used for color separation. The color deconvolution of the stains used in double staining method is illustrated in Fig 5 in Paper II. Color threshold for NBT-BCIP was set to 195 at which there was minimal signal loss and maximum background removal. Thereafter, positive pixel area percentage (PPAP), and integrated optical density (IOD) per area in the stroma were measured. Mean pixel intensity was converted to OD using the function  $OD = \log_{10}(255/\text{mean pixel intensity})$ , IOD was obtained as product of OD and positive pixel area stained and normalized to region of interest. PPAP and IOD were quantified in the tissue regions of approximately 0.4-0.8 mm<sup>2</sup>. Similar regions in the tissue sections, stained by different combination methods, were selected for comparison.

### 3.14 TCGA miRNA data analysis

TCGA miRNA sequence data (n=488) for miR-204 and miR-138 in HNSCC, matched or unmatched normal tissues, and the corresponding clinical data (n=528) were extracted from Firebrowse database (TCGA data version 2016\_01\_28 for HNSC; <http://firebrowse.org/?cohort=HNSC#>). Non-oral cancer cases, oral cancer cases with history of neoadjuvant therapy and HPV-positive cases were excluded from the cohort. After exclusion criteria 277 and 251 cases of oral cancer and 25 and 21 normal oral tissues remained for miR-138 and miR-204 data analysis respectively.

### 3.15 Statistical analysis

Student's paired T-test and unpaired T-test were used to test significant differences in means between matched and unmatched groups respectively. One-way ANOVA

---

compared means among three or more groups. D'Agostino & Pearson test ( $p > 0.05$ ) was applied to check normal distribution of data. For non-normal continuous variables medians were compared (Wilcoxon for paired and Mann-Whitney for unpaired comparison between two, and Kruskal-Wallis for unpaired comparison among groups). All tests were performed using GraphPad Prism Version 7.

Overall survival (OS) and recurrence free survival (RFS) analysis for clinicopathological and miRNA parameters in OSCC was carried using log-rank test (Mantel-Cox), and plotted using Kaplan-Meier method. Univariate and multivariate Cox's proportional regression analysis was performed to identify independent predictors of OS and RFS as described in Paper II. Before regression analysis, proportional hazard assumption was tested with log minus log function plot. Also, normality tests (Kolmogorov-Smirnov, Shapiro-Wilk, histogram and Q-Q plot) were performed and outliers removed for miR-204 expression data (IOD and PPAP). Pearson's chi-square test was carried to find association of miRNAs with clinicopathological parameters. The tests were carried using IBM SPSS Statistics Version 25.



## 4. Results

### 4.1 Paper I

#### 4.1.1 miRNA array

Unsupervised hierarchical sample clustering of CAFs and NOFs for global miRNA expression identified separate clusters of CAFs and NOFs, but with some degree of inter-clustering. This demonstrates heterogeneity of CAFs regarding miRNA expression, and it is in line with a previous study from our lab where CAFs heterogeneity was identified at the transcriptome level [83]. Two of the CAFs clustered together with NOFs, and one of the NOFs clustered together with CAFs. Significance analysis of microarrays (SAM) analysis resulted in 12 significantly differentially regulated miRNAs ( $q < 0.01$ ). Four of the miRNAs: miR-138-5p, miR-378a-3p, miR-190b and miR-582-5p were significantly up-regulated, while miR-224-5p, miR-16-2-3p, miR-155-5p, miR-92b-3p, miR-204-5p, miR-504-5p, miR-1270, and miR-3611 were significantly down-regulated in CAFs compared to NOFs. qRT-PCR validation of some of the selected miRNAs, miR-204-5p, miR-138-5p and miR-582-5p confirmed the results of microarray for those miRNAs.

#### 4.1.2 Identification of *ITGA11* as a target for miR-204 in CAFs

When we looked at the known and predicted targets of the 12 miRNAs found differentially expressed in CAFs versus NOFs in our study, our attention was drawn towards miR-204 and miR-138 because of their predicted target sites in *ITGA11*, a CAF-specific molecule our lab had interest from before. Our lab had identified *ITGA11* to be upregulated in OSCC stroma [88] and in CAFs compared to NOFs [83], and had a focus on investigating the role of integrin  $\alpha 11$  in OSCC [132].

Prediction of miRNA response elements in *ITGA11* using different miRNA target prediction tools showed conserved pairing of miR-204 seed region in the 3'UTR length of *ITGA11*. The prediction also showed poorly conserved site for miR-138 in the 3'UTR length of *ITGA11* [129].

---

In our study, miR-204 expression was in inverse correlation with *ITGA11* in three of the matched fibroblast pairs. Modulation of miRNAs in CAFs and NOFs using miRNA mimics and inhibitors showed regulation of *ITGA11* by miR-204. Increased expression of miR-204 using the mimic resulted in decreased expression of *ITGA11* both at the mRNA and protein levels. On the contrary, inhibition of miR-204 resulted in increased expression of *ITGA11*, both at the miRNA and protein level, which suggested that regulation of *ITGA11* by miR-204 could be direct. miRNA target reporter assay confirmed direct targeting of *ITGA11* by miR-204 in the CAFs. Co-transfection of miR-204 mimics and the reporter vector bearing 3' UTR length of *ITGA11* into the CAFs resulted in significantly reduced luciferase activity by 77.85%, compared to the control bearing mutation in the seed binding motif of 3' UTR length of *ITGA11*.

#### 4.1.3 Functional role of miR-204 in CAFs

Increased expression of miR-204 resulted in decreased CAFs migration in 2D monolayer cultures and in co-cultures with OSCC cells, and decreased collagen I contraction. Ectopic expression of miR-204 by miR-204 mimics in the CAFs did significantly impair the migration abilities of OSCC cells towards CAFs in 2D assay and significantly decreased the depth of invasion of OSCC cells in 3D organotypic assay.

When CAFs were treated with miR-204 mimics, a significant decrease in CAF-related (FAP, TGF $\beta$ 1, TGFBR2) and migration-related (FAK, pFAK and ROCK2) molecules was observed. Of interest, a decrease in EGFR expression in CAFs was also observed after miR-204 mimics treatment. An increase in these molecules was observed when the CAFs were treated with miR-204 mimics. These molecular changes detected in CAFs after miR-204 modulation indicate a role of miR-204 on impairing the CAF phenotype.

## 4.2 Paper II

### 4.2.1 Combined miRNA ISH and IHC staining and quantification

We used chromogen-based multiplexing techniques to simultaneously detect and visualize the expression of miRNA and protein in the same tissue section. ISH of miRNA and IHC of pan-CK were performed on the same tissue sections in different order sequences, and although some effects of IHC on ISH and vice versa were observed, the methods were comparable regarding the ability to visualize the miRNA and protein. Whether there was co-localization or not, miRNAs and proteins were accessible to either probes or antibody and were visualized to a degree that was quantifiable.

### 4.2.2 miRNA-204 as a prognostic marker in OSCC

The combined ISH and IHC multiplexing methodology we established was further used to investigate miR-204 as a putative prognostic marker in a cohort of 160 HPV-negative OSCC cases with complete clinical data from Haukeland University Hospital. Using this method, we were able to precisely and separately quantify the expression of miR-204 in the tumour islands and in the tumour stroma. A heterogenous expression of miR-204 was observed both in the epithelial and stromal compartment, but a strong correlation was observed between the expression of miR-204 in the tumour cells and in the stroma of the same lesion. Nevertheless, miR-204 expression in the tumor stroma was found to be overall increased at the tumor front and it was associated with a lower recurrence rate ( $p=0.033$ ) and improved survival ( $p=0.048$ ) in our cohort. The expression of miR-204 correlated with similar outcomes also when adjusted for age and tumor stage in a multivariate Cox regression model. These observations are in line with the tumor suppressive roles of miR-204 from Paper I.

---

## 4.3 Paper III

### 4.3.1 Functional role of miR-138 in CAFs

Increasing miR-138 expression by use of mimics in the fibroblasts decreased their proliferation and altered their morphology. Both CAFs and NOFs became stellar in shape and bigger in size post miR-138 transfection, compared to the mimic controls. Transfection of miR-138 mimics decreased fibroblasts motility (invasion) through the collagen I gel and resulted in significantly reduced collagen contraction ability in both CAFs and NOFs. Reversing the miR-138 expression by using inhibitors resulted in the opposite effect. Inhibition of miR-138 in both CAFs and NOFs increased invasion of two OSCC cell lines (UK1 and Luc4), while transfection of both fibroblasts with the mimics of miR-138 almost completely impaired the invasion of both UK1 and Luc4.

The ectopic expression of miR-138 induced decreased expression of proliferation related molecules (CCND1 and EGFR), known CAF-related markers (FAP, TGF $\beta$ 1 and TGFBR2), and molecules of the focal adhesion pathway (FAK and AKT). No change in the levels of integrin  $\alpha$ 11 was detected after transfection with mimics or inhibitors. The luciferase gene reporter assay also did not identify *ITGA11* as a target of miR-138.

### 4.3.2 Heterogenous expression of miR-138 in OSCC tissues

Detection of miR-138 in OSCC tissues by *in situ* hybridization demonstrated miR-138 expression only in a subset of OSCC lesions. Of 53 OSCC tissues stained for miR-138, only 10 (18.9%) stained positive for miR-138: 9 (17%) in the tumour compartment and 5 (9.43%) the tumour stroma. From the seven cases of the positively stained tissues containing both tumor and normal/peritumor region, the miR-138 staining was stronger in the tumor cells compared to the respective normal/peritumour epithelial compartment in five of the cases. Only one of the OSCC cases displayed weaker staining in the tumour cells compared to the respective normal/peritumour epithelial compartment, while there was no difference in another one. Therefore, of the 31 tissues containing both tumor and normal/peritumor

compartments, miR-138 expression was increased in 5 (16.12%) and decreased in 1(3.22%) in the tumor compared to the normal/peritumour areas. Compared to the OSCC tissues, out of the six NHOM tissues, 3 (50%) stained positive for miR-138, and the staining was localized only in the epithelium.

Overall, miR-138 expression displayed a marked heterogeneity in both epithelial and stromal compartments. Except association of miR-138 with lower recurrence and invasion depth, no correlations with clinico-pathological parameters were detected in our cohort or in the TCGA data set.

Heterogeneity of miR-138 expression was also observed in strains of CAFs and NOFs by qRT-PCR.

---

## 5. Discussion

While miRNAs have been extensively investigated in cancer, limited data exist on the altered expression of miRNAs in CAFs versus normal fibroblasts [133], and the data available is often inconsistent between different types of cancers or between clinical samples and experimental settings.

One of the first and most investigated miRNA deregulated in CAFs is miR-21. miR-21 was found frequently upregulated in CAFs across various cancer types including lung, colon, pancreas and OSCC, and demonstrated to be a key regulator of tumor progression and resistance to therapy [134-136] [137, 138] [139]. Of interest, miRNA arrays performed on CAFs from breast [140], lung [141], prostate [142], and our own present study on OSCC-derived CAFs (Paper I) have revealed diverse patterns of miRNA alterations in CAFs, none of them including miR-21. Albeit performed on small number of CAF strains, the results from these miRNA array studies indicate a heterogeneous expression pattern of CAFs between different cancer types.

Identification of reproducible cancer-specific miRNA signatures in CAFs thus remains still a challenge.

Conflicting results between clinical and experimental samples have been also reported, such as in the case of miR-106b [143]. Many of the findings in miRNA research exhibit considerable contradictions that cannot be fully accounted for by the classical regulatory network models and feedback loops, which primarily focus on one-to-one regulatory interactions between molecules involved. An expanded model to understand the regulatory role of miRNAs that takes into account the dynamics of miRNA members as influenced by intracellular and extracellular environmental factors has been proposed [144]. Regulation of miRNA expression is then dependent on the systemic context and doesn't follow the regulation pattern of single molecules, making thus the dysregulation miRNA pattern extremely complex and little reproducible.

Nevertheless, the unsupervised clustering analysis for the data we obtained from the miRNA array analyses identified two separate clusters, one for CAFs and another for

NOFs, although one of the NOF strains exhibited a miRNA expression profile similar to the CAFs, and two of the CAF strains displayed a miRNA expression profile similar to that of NOFs (Paper I). Despite statistically significant difference in miRNAs expression in CAFs group compared to NOFs groups, miRNA expression in a subset of CAFs contradicted the general trend of miRNA alteration, indicating CAF heterogeneity. We have previously demonstrated fibroblast heterogeneity by gene microarray analysis of CAFs derived from OSCC lesions [83].

qRT-PCR profiling of miRNAs also revealed that expression of individual miRNAs, such as miR-204-5p expression, was quite heterogeneous (Paper I). Although generally found to be downregulated in CAFs, miR-204-5p expression was higher in two of the CAF strains compared to their NOF match. While these differences observed between matched and unmatched CAFs-NOFs demand statistical significance, this might also explain differences in the biology of miRNA regulation between NOFs from normal mucosa of a cancer patient and NOFs from a healthy, non-cancer volunteer. Normal cells evolve progressively to neoplastic stage, and the transformed epithelial cells and underlying TME co-evolve [38], meaning that, it is not just the epithelial cells that have undergone genetic and epigenetic transformations, but also the stroma underlying the transformed epithelial cells is changing and these changes could have already been impinged on apparently normal tissues of OSCC patients that are known to display the phenomenon of field cancerization. In this respect, Ganci F et al showed that miRNA regulation was different from tumor to peri-tumor region and from peri-tumor to normal surrounding in HNSCC [145].

Increased heterogeneity of isolated CAFs when seeded on plastic in 2D might as well be related to selection of certain populations that survive in culture. One then might question the representability of the fibroblasts isolated from the tumors in cell culture. Changes in cells phenotype upon transitioning from tissue to cell culture [126] or from 2D to 3D culture models [83] has also been reported. Thus the use of culture conditions as close as possible to the *in vivo* situation, including use of 3D collagen/hydrogel or 3D organotypic co-cultures seems relatively more natural.

---

Earlier studies have reported tumor suppressive functions for miR-204 when expressed in cancer cells (reviewed in the introduction of Paper I). However, it was unknown how miR-204 expression in CAFs can modulate the behavior of CAF. In order to find the role of miR-204 in CAFs, CAFs and respective matched NOFs isolated from two OSCC patients were miR-204 modulated and subjected to proliferation, migration, invasion and molecular detection assays (Paper I). Increasing miR-204 expression with miR-204 mimics in CAFs impaired adjacent OSCC cell invasion in 3D models. On the other hand, when miR-204 function was inhibited in paired NOFs, invasion of OSCC cells grown on NOF-populated 3D collagen gels increased significantly. These findings, coupled to the decreased collagen contraction and migration of CAFs [146] when treated with miR-204 mimics, indicated a tumor suppressive role of miR-204 expression in CAF in OSCC by affecting fibroblast motility.

Previously, our research demonstrated the tumor-promoting role of integrin  $\alpha 11$  in CAF in OSCC [132]. Integrin  $\alpha 11$  expression was increased in CAFs compared to NOFs in all five matched pairs, confirming previous results on non-matched CAFs and NOFs [83]. miRNA target prediction analysis showed that *ITGA11* hosts a target site for miR-204. Therefore, we performed luciferase miRNA target reporter assay, and found *ITGA11* is directly targeted by miR-204, affecting *ITGA11* expression at both transcript and protein level (Paper I). This suggests that the tumor suppressive effect of miR-204 may be mediated via *ITGA11*, although miR-204 is only one of the several miRNAs that could regulate *ITGA11*, and miR-204 has also been documented to affect other pathways of cancer. Several other CAF-related molecules were found to be modulated by miR-204 (Paper I), suggesting also a more complex role of miR-204 in regulating the CAF phenotype than only through *ITGA11*.

Our molecular analysis showed that modulation of miR-204 expression significantly altered FAK and ROCK2 expression (Paper I), both molecules playing an important role in cell motility and CAF motile phenotype. Rho-associated coiled-coil containing protein kinase 2 (ROCK2) is an oncoprotein that controls cytoskeleton organization and cell motility, and ROCK2 overexpression has been reported in OSCC-CAF.



Previous studies showed a prognostic value of ROCK2 in OSCC and its association with CAF density [147].

In order to detect and quantify miRNA expression in clinical settings, we established a combination of multiplexed miRNA ISH and protein IHC protocols on a single tissue section and validated it on a large OSCC cohort (Paper II). By doing so, we found that higher expression of miR-204 in the stroma at the tumor front predicted better patient survival and lower recurrence in OSCC (Paper II).

Detecting and analyzing the spatial distribution patterns of miRNA and/or protein not only provide information about the specific anatomical location within cell and tissue compartments but can also offer valuable mechanistic insights [148]. Although we did not use this method for investigating a miRNA and its target, the coupling of ISH with IHC gives this possibility, to visually correlate miRNA levels with their corresponding targeted protein levels. Moreover, the semi-quantitative quantification of miRNA expression can enhance the physiological significance of *in vitro* findings and enable comparative measurements between different tumor regions, elucidating their relevance to cancer progression [148].

In our study, we used a combination of miRNA ISH staining for miR-204 and protein IHC staining for pan-cytokeratin to identify the epithelial tumor compartment from the tumor stromal compartment, focusing on studying miRNA expression in the tumor stroma. Various methods have been previously established for combining these two methods, utilizing either fluorophores [149] or chromogens [150]. However, there was a lack of information regarding the influence of IHC on miRNA ISH staining and vice versa.

All the different combinations of miRNA ISH and pan-CK IHC successfully detected miRNA and pan-CK in a single section, although there were variations in color metrics depending on the order of the staining steps. Generally, when the chromogen for pan-CK (DAB) preceded the chromogen for miRNA ISH (NBT/BCIP), the brown color appeared darker, and vice versa. Nonetheless, the combined staining methods were specific and comparable to the control method (Paper II).

---

We next went to optimize a digital method for quantification of the combined ISH-IHC method and provided a detailed systematic guide to digital quantification (Paper II). Surprisingly, given the importance of tissue-based biomarkers quantified through IHC in patient stratification and the recent advancements in digital quantification and image analysis, there are still very few digital image analysis-based algorithms used in clinical pathology, such as those for Her2, neu, p53, and Ki-67 quantification that have been cleared by the FDA for diagnostic use [151]. The limited number of approved image analysis algorithms may be attributed to inter- and intra-tumor heterogeneity and the complexity of biological factors.

Quantification of miR-204 in our study revealed a high expression of miR-204 in the stroma of both tumor center and the tumor front. However, only the miR-204 in the stroma of the tumor front exhibited a significant association with improved overall survival (OS) and recurrence-free survival (RFS). Interestingly, compared to the stroma of the surrounding normal oral mucosa, we found an elevated expression of miR-204, which aligns with previous studies conducted in OSCC and other cancer types [152]. We hypothesize that the increase in miR-204 expression in the stroma is a response to early-stage cancer progression and may serve as a prognostic biomarker. However, further *in vitro* and *in vivo* investigations are necessary to fully elucidate the role and dynamics of miR-204 expression in CAFs on OSCC progression.

On the other hand, the investigation of miR-138 expression in OSCC tissue samples showed no associations of miR-138 expression with clinico-pathological parameters (except recurrence and depth of invasion); the study demonstrated a marked heterogeneity in miR-138 expression within OSCC tissues (Paper III). While miR-138 was expressed in tumor compartment in only 17% of the OSCC, it was expressed in normal epithelium in 50% in the NHOM tissues. Indeed, the absence of miR-138 staining in relatively higher percentage (83%) of the tumour samples compared to NHOM can be taken as an indication of tumour suppressive role of miR-138, in line with previous observations in OSCC [153]. However, in contradiction to the

proposed tumor suppressive role of miR-138, five out of 31 OSCC tissues showed increased staining in the tumor cells, compared to the normal/peritumour epithelia.

Surprisingly, overall expression of miR-138 in HNSCC was higher compared to control epithelium in TCGA data set. In addition, miR-138 expression did not show any specific association with tumour stages or lymph node involvement in TCGA data set available for HNSCC (Paper III). Taken together, the overall data from the clinical cohort of OSCC in this study and from the HNSCC cohort in TCGA does not support miR-138 as a biomarker in OSCC.

Previously, our study and others have demonstrated a tumor-supporting role of CAFs in OSCC [83, 154] and their association with poor prognosis [155]. In order to understand, if miR-138 expression in CAFs can modulate the established tumor-supporting role of CAFs, total miR-138 was quantified in matched and separate CAFs and NOFs. The result delineated heterogeneity in regulation of miR-138 in CAFs. While miR-138 was up regulated in CAFs compared to NOFs in unmatched pairs, and also in two of the OSCC tissues hybridized to miR-138, it was down regulated in CAFs compared to NOFs in matched pairs. Despite differential regulation of miR-138 observed in CAFs, increased ectopic expression of miR-138 in both CAFs and NOFs impaired the tumor promoting ability of the studied OSCC cells UK1 and Luc4 in 3D-coculture model. On the other hand, inhibition of miR-138 in both CAFs and NOFs augmented invasion of both OSCC cell lines. Therefore, this study showed that, regardless of fibroblasts used (CAF or NOF), and differences in the expression of miR-138 in between CAFs and NOFs, expression of miR-138 in the fibroblasts reflects in inhibition of invasion of adjacent OSCC cells (Paper III). This outcome may suggest, why miR-138 expression is reduced in CAFs compared to NOFs in mono-layer culture in matched pairs, although it does not explain the observed increased expression of miR-138 in fibroblasts in the tumor stroma compared to the fibroblasts in adjacent peritumor or normal compartment in two of the OSCC tissues investigated. Nonetheless, the increase in miR-138 in CAFs was observed in only two out of 31 OSCC tissues. Overall, the co-culture assay indicated a tumor suppressive function of miR-138 in oral fibroblasts (Paper III).

---

Different functional assays were further carried out to understand the mechanism by which alteration in miR-138 function in the fibroblasts modulates invasion capabilities by OSCC cells (Paper III). Firstly, we observed that proliferation of both CAFs and NOFs was decreased by miR-138. At the molecular level, this was explained by negative regulation of *CCND1* transcripts by miR-138. miR-138 has been previously shown to inhibit cell growth and cell cycle progression by targeting *CCND1* [156] and *CCND3* [157]. However, miR-138 inhibition has also been linked to decrease in proliferation and increase in apoptosis of glioma cells [158].

Another major impact found in this study was the ability of miR-138 to change the spindle shaped CAFs and NOFs into stellar morphology in monolayer culture (Paper III). Previous studies on OSCC cells are in line with the observed change in the cell morphology and showed an association to downregulation of RhoC and ROCK2 by miR-138 [159].

Most importantly, ectopic miR-138 expression in fibroblasts reduced the collagen contraction induced by fibroblasts and significantly reduced invasion of CAF through the collagen I matrix towards the cancer cells. This was associated with decrease in the expression of miR-138 targets such as FAK and ROCK2, but not integrin  $\alpha 11$  in fibroblasts (Paper III). Taken together, these findings indicate a tumor suppressive role for miR-138 in CAFs by indirectly impairing the invasion of OSCC through altered movement of CAFs across collagen I matrix (Paper III). These findings need confirmation in *in vivo* models and further mechanistic studies.

## 6. Conclusions

1. This study revealed the landscape of miRNA deregulation in CAFs in OSCC and identified 12 differentially expressed miRNAs between CAFs and NOFs.
2. A role for miR-204 in impairing the CAF phenotype was demonstrated.
3. This study showed for the first time that miR-204 targets *ITGA11* in OSCC-derived CAFs.
4. The tumor suppressive function of miRNA 204 in OSCC-derived CAFs was accompanied by concomitant alteration in several molecules involved in CAF migration in addition to regulation of *ITGA11* expression.
5. A robust multiplex combined *in situ* hybridization and immunohistochemistry for concomitant miRNA and protein detection has been established.
6. Using this newly established double staining method, miR-204 was found to be an independent prognostic factor for OSCC.
7. Another miRNA differentially expressed in CAFs versus NOFs, the miR-138, also impaired CAF phenotype and invasion of adjacent OSCC cells in 3D-cultures.
8. The tumor suppressive functions of miR-138 were found to be associated with molecules involved in FAK axis and not through regulation of *ITGA11*.
9. Expression of miR-138 showed marked heterogeneity in OSCC lesions and was not related to any clinico-pathological parameters in univariate / multivariate analysis.

---

## 7. Further perspectives

1. To utilize animal models, such as xenograft or genetically engineered mouse models, to assess the *in vivo* effects of miR-204 and miR-138 modulation in fibroblasts or miR-204 and miR-138 alone on OSCC tumorigenesis, metastasis, and therapeutic responses.
2. To use or design miR-204 and miR-138 based drugs that specifically target fibroblasts *in vitro* and *in-vivo* pre-clinical OSCC models.
3. To perform mechanistic studies to investigate the molecular mechanisms underlying the regulatory roles of miR-204 and miR-138 in OSCC.
4. To explore integrative study involving miR-204, miR-138 and other differentially regulated miRNAs with common pathways target that has higher potential to change the course of OSCC.
5. To explore the use of targeting mir-204 and miR-138 in combination therapies in pre-clinical models. Given the role of these miRNAs on mitigating OSCC cell invasion, investigations on whether the modulation of miR204 and miR138 can enhance the efficacy of standard therapies, such as chemotherapy or radiation.
6. In the context of the current development of immunotherapy, one could also think to investigate the interplay between miR-204 and miR-138 expression in CAFs with other tumor microenvironment components such as immune cells. This would imply assessment on how these miRNAs influence the CAF-immune cells interaction, immune responses, and the development of a favorable or suppressive microenvironment in OSCC.

---

## Source of data

- [1] L. Dobrossy, "Epidemiology of head and neck cancer: Magnitude of the problem," (in English), *Cancer and Metastasis Reviews*, vol. 24, no. 1, pp. 9-17, Jan 2005, doi: DOI 10.1007/s10555-005-5044-4.
- [2] W. H. O. International Agency for Research on Cancer. "Global Cancer Observatory." <https://gco.iarc.fr/> (accessed Feb 16, 2022).
- [3] J. Ferlay *et al.*, "Estimating the global cancer incidence and mortality in 2018: GLOBOCAN sources and methods," *Int J Cancer*, vol. 144, no. 8, pp. 1941-1953, Apr 15 2019, doi: 10.1002/ijc.31937.
- [4] P. E. Petersen, "Strengthening the prevention of oral cancer: the WHO perspective," (in English), *Community Dentistry and Oral Epidemiology*, vol. 33, no. 6, pp. 397+, Dec 2005, doi: DOI 10.1111/j.1600-0528.2005.00251.x.
- [5] S. S. Hecht and D. Hoffmann, "Tobacco-Specific Nitrosamines, an Important Group of Carcinogens in Tobacco and Tobacco-Smoke," (in English), *Carcinogenesis*, vol. 9, no. 6, pp. 875-884, Jun 1988, doi: DOI 10.1093/carcin/9.6.875.
- [6] T. Pflaum *et al.*, "Carcinogenic compounds in alcoholic beverages: an update," (in English), *Archives of Toxicology*, vol. 90, no. 10, pp. 2349-2367, Oct 2016, doi: 10.1007/s00204-016-1770-3.
- [7] M. Wang, E. J. McIntee, G. Cheng, Y. Shi, P. W. Villalta, and S. S. Hecht, "Identification of DNA adducts of acetaldehyde," *Chem Res Toxicol*, vol. 13, no. 11, pp. 1149-57, Nov 2000, doi: 10.1021/tx000118t.
- [8] J. S. Chang, J. R. Hsiao, and C. H. Chen, "ALDH2 polymorphism and alcohol-related cancers in Asians: a public health perspective," *J Biomed Sci*, vol. 24, no. 1, p. 19, Mar 3 2017, doi: 10.1186/s12929-017-0327-y.
- [9] H. Sung *et al.*, "Global Cancer Statistics 2020: GLOBOCAN Estimates of Incidence and Mortality Worldwide for 36 Cancers in 185 Countries," *CA Cancer J Clin*, vol. 71, no. 3, pp. 209-249, May 2021, doi: 10.3322/caac.21660.
- [10] A. Y. Han, E. C. Kuan, J. Mallen-St Clair, J. E. Alonso, A. Arshi, and M. A. St John, "Epidemiology of Squamous Cell Carcinoma of the Lip in the United States: A Population-Based Cohort Analysis," *JAMA Otolaryngol Head Neck Surg*, vol. 142, no. 12, pp. 1216-1223, Dec 1 2016, doi: 10.1001/jamaoto.2016.3455.
- [11] K. K. Ang *et al.*, "Human Papillomavirus and Survival of Patients with Oropharyngeal Cancer," (in English), *New England Journal of Medicine*, vol. 363, no. 1, pp. 24-35, Jul 1 2010, doi: 10.1056/NEJMoa0912217.
- [12] A. Lewis, R. Kang, A. Levine, and E. Maghami, "The New Face of Head and Neck Cancer: The HPV Epidemic," *Oncology (Williston Park)*, vol. 29, no. 9, pp. 616-26, Sep 2015. [Online]. Available: <https://www.ncbi.nlm.nih.gov/pubmed/26384796>.
- [13] Z. Yang, P. Sun, K. R. Dahlstrom, N. Gross, and G. Li, "Joint effect of human papillomavirus exposure, smoking and alcohol on risk of oral squamous cell carcinoma," *BMC Cancer*, vol. 23, no. 1, p. 457, May 19 2023, doi: 10.1186/s12885-023-10948-6.

- 
- [14] N. Sathish, X. Wang, and Y. Yuan, "Human Papillomavirus (HPV)-associated Oral Cancers and Treatment Strategies," *J Dent Res*, vol. 93, no. 7 Suppl, pp. 29S-36S, Jul 2014, doi: 10.1177/0022034514527969.
- [15] A. A. Kumar V, and Aster J, *Robbins Basic Pathology, 10th Edition*. Elsevier, 2018.
- [16] D. Hanahan and R. A. Weinberg, "Hallmarks of cancer: the next generation," *Cell*, vol. 144, no. 5, pp. 646-74, Mar 4 2011, doi: 10.1016/j.cell.2011.02.013.
- [17] N. Cancer Genome Atlas, "Comprehensive genomic characterization of head and neck squamous cell carcinomas," *Nature*, vol. 517, no. 7536, pp. 576-82, Jan 29 2015, doi: 10.1038/nature14129.
- [18] S. Negrini, V. G. Gorgoulis, and T. D. Halazonetis, "Genomic instability - an evolving hallmark of cancer," (in English), *Nature Reviews Molecular Cell Biology*, vol. 11, no. 3, pp. 220-228, Mar 2010, doi: 10.1038/nrm2858.
- [19] M. A. Gonzalez-Moles, S. Warnakulasuriya, M. Lopez-Ansio, and P. Ramos-Garcia, "Hallmarks of Cancer Applied to Oral and Oropharyngeal Carcinogenesis: A Scoping Review of the Evidence Gaps Found in Published Systematic Reviews," *Cancers (Basel)*, vol. 14, no. 15, Aug 8 2022, doi: 10.3390/cancers14153834.
- [20] J. Califano *et al.*, "Genetic progression model for head and neck cancer: Implications for field cancerization," (in English), *Cancer Research*, vol. 56, no. 11, pp. 2488-2492, Jun 1 1996. [Online]. Available: <Go to ISI>://WOS:A1996UN25000008.
- [21] S. Warnakulasuriya and G. Lodi, "Oral potentially malignant disorders: Proceedings from an expert symposium," *Oral Dis*, vol. 27, no. 8, pp. 1859-1861, Nov 2021, doi: 10.1111/odi.13999.
- [22] B. J. Braakhuis, C. R. Leemans, and R. H. Brakenhoff, "A genetic progression model of oral cancer: current evidence and clinical implications," *J Oral Pathol Med*, vol. 33, no. 6, pp. 317-22, Jul 2004, doi: 10.1111/j.1600-0714.2004.00225.x.
- [23] D. P. Slaughter, H. W. Southwick, and W. Smejkal, "Field cancerization in oral stratified squamous epithelium; clinical implications of multicentric origin," *Cancer*, vol. 6, no. 5, pp. 963-8, Sep 1953, doi: 10.1002/1097-0142(195309)6:5<963::aid-cnrcr2820060515>3.0.co;2-q.
- [24] B. J. Braakhuis, M. P. Tabor, J. A. Kummer, C. R. Leemans, and R. H. Brakenhoff, "A genetic explanation of Slaughter's concept of field cancerization: evidence and clinical implications," *Cancer Res*, vol. 63, no. 8, pp. 1727-30, Apr 15 2003. [Online]. Available: <https://www.ncbi.nlm.nih.gov/pubmed/12702551>.
- [25] M. P. Tabor *et al.*, "Persistence of genetically altered fields in head and neck cancer patients: Biological and clinical implications," (in English), *Clinical Cancer Research*, vol. 7, no. 6, pp. 1523-1532, Jun 2001. [Online]. Available: <Go to ISI>://WOS:000169310600007.
- [26] K. R. Dionne, S. Warnakulasuriya, R. B. Zain, and S. C. Cheong, "Potentially malignant disorders of the oral cavity: current practice and future directions in the clinic and laboratory," *Int J Cancer*, vol. 136, no. 3, pp. 503-15, Feb 1 2015, doi: 10.1002/ijc.28754.



- 
- [27] N. K. Cervigne *et al.*, "Identification of a microRNA signature associated with progression of leukoplakia to oral carcinoma," *Hum Mol Genet*, vol. 18, no. 24, pp. 4818-29, Dec 15 2009, doi: 10.1093/hmg/ddp446.
- [28] E. Chattopadhyay *et al.*, "Expression deregulation of mir31 and CXCL12 in two types of oral precancers and cancer: importance in progression of precancer and cancer," *Sci Rep*, vol. 6, p. 32735, Sep 6 2016, doi: 10.1038/srep32735.
- [29] D. A. Gaykalova *et al.*, "Novel insight into mutational landscape of head and neck squamous cell carcinoma," *PLoS One*, vol. 9, no. 3, p. e93102, 2014, doi: 10.1371/journal.pone.0093102.
- [30] D. A. Gaykalova *et al.*, "Correction: Novel Insight into Mutational Landscape of Head and Neck Squamous Cell Carcinoma," *PLoS One*, vol. 15, no. 5, p. e0233409, 2020, doi: 10.1371/journal.pone.0233409.
- [31] C. India Project Team of the International Cancer Genome, "Mutational landscape of gingivo-buccal oral squamous cell carcinoma reveals new recurrently-mutated genes and molecular subgroups," *Nat Commun*, vol. 4, p. 2873, 2013, doi: 10.1038/ncomms3873.
- [32] N. Stransky *et al.*, "The mutational landscape of head and neck squamous cell carcinoma," *Science*, vol. 333, no. 6046, pp. 1157-60, Aug 26 2011, doi: 10.1126/science.1208130.
- [33] S. C. Su *et al.*, "Exome Sequencing of Oral Squamous Cell Carcinoma Reveals Molecular Subgroups and Novel Therapeutic Opportunities," *Theranostics*, vol. 7, no. 5, pp. 1088-1099, 2017, doi: 10.7150/thno.18551.
- [34] Y. Ju *et al.*, "Genomic Landscape of Head and Neck Squamous Cell Carcinoma Across Different Anatomic Sites in Chinese Population," *Front Genet*, vol. 12, p. 680699, 2021, doi: 10.3389/fgene.2021.680699.
- [35] H. N. Dongre *et al.*, "Targeted Next-Generation Sequencing of Cancer-Related Genes in a Norwegian Patient Cohort With Head and Neck Squamous Cell Carcinoma Reveals Novel Actionable Mutations and Correlations With Pathological Parameters," *Front Oncol*, vol. 11, p. 734134, 2021, doi: 10.3389/fonc.2021.734134.
- [36] I. C. Mackenzie and W. H. Binnie, "Recent advances in oral mucosal research," *J Oral Pathol*, vol. 12, no. 6, pp. 389-415, Dec 1983, doi: 10.1111/j.1600-0714.1983.tb00353.x.
- [37] D. E. Costea, O. Tsinkalovsky, O. K. Vintermyr, A. C. Johannessen, and I. C. Mackenzie, "Cancer stem cells - new and potentially important targets for the therapy of oral squamous cell carcinoma," *Oral Dis*, vol. 12, no. 5, pp. 443-54, Sep 2006, doi: 10.1111/j.1601-0825.2006.01264.x.
- [38] W. RA, *Biology of Cancer*. Garland Publishing Inc, 2013.
- [39] J. Ferlay *et al.*, "Cancer incidence and mortality worldwide: Sources, methods and major patterns in GLOBOCAN 2012," (in English), *International Journal of Cancer*, vol. 136, no. 5, pp. E359-E386, Mar 1 2015, doi: 10.1002/ijc.29210.
- [40] M. K. Mayland, D. G. Sessions, and J. Lenox, "The influence of lymph node metastasis in the treatment of squamous cell carcinoma of the oral cavity, oropharynx, larynx, and hypopharynx: N0 versus N+," (in English), *Laryngoscope*, vol. 115, no. 4, pp. 629-639, Apr 2005, doi: 10.1097/01.mlg.0000161338.54515.b1.

- 
- [41] S. P. Barnali Majumdar, Sachin C Sarode, Gargi S Sarode, and Roopa S Rao, "Clinico-pathological prognosticators in oral squamous cell carcinoma: An update. ," *Translational Research in Oral Oncology* 2017, doi: 10.1177/2057178X17738912.
- [42] D. Adelstein *et al.*, "NCCN Guidelines Insights: Head and Neck Cancers, Version 2.2017," *J Natl Compr Canc Netw*, vol. 15, no. 6, pp. 761-770, Jun 2017, doi: 10.6004/jnccn.2017.0101.
- [43] AJCC, *AJCC cancer staging handbook*. . Springer 2017.
- [44] J. A. Woolgar, "Histopathological prognosticators in oral and oropharyngeal squamous cell carcinoma," *Oral Oncol*, vol. 42, no. 3, pp. 229-39, Mar 2006, doi: 10.1016/j.oraloncology.2005.05.008.
- [45] R. H. Spiro, A. G. Huvos, G. Y. Wong, J. D. Spiro, C. A. Gnecco, and E. W. Strong, "Predictive value of tumor thickness in squamous carcinoma confined to the tongue and floor of the mouth," *Am J Surg*, vol. 152, no. 4, pp. 345-50, Oct 1986, doi: 10.1016/0002-9610(86)90302-8.
- [46] H. International Consortium for Outcome Research in *et al.*, "Primary tumor staging for oral cancer and a proposed modification incorporating depth of invasion: an international multicenter retrospective study," *JAMA Otolaryngol Head Neck Surg*, vol. 140, no. 12, pp. 1138-48, Dec 2014, doi: 10.1001/jamaoto.2014.1548.
- [47] L. L. Matos, R. A. Dedivitis, M. A. V. Kulcsar, E. S. de Mello, V. A. F. Alves, and C. R. Cernea, "External validation of the AJCC Cancer Staging Manual, 8th edition, in an independent cohort of oral cancer patients," *Oral Oncol*, vol. 71, pp. 47-53, Aug 2017, doi: 10.1016/j.oraloncology.2017.05.020.
- [48] W. M. Lydiatt *et al.*, "Head and Neck cancers-major changes in the American Joint Committee on cancer eighth edition cancer staging manual," *CA Cancer J Clin*, vol. 67, no. 2, pp. 122-137, Mar 2017, doi: 10.3322/caac.21389.
- [49] J. N. Myers, J. S. Greenberg, V. Mo, and D. Roberts, "Extracapsular spread. A significant predictor of treatment failure in patients with squamous cell carcinoma of the tongue," *Cancer*, vol. 92, no. 12, pp. 3030-6, Dec 15 2001, doi: 10.1002/1097-0142(20011215)92:12<3030::aid-cnrc10148>3.0.co;2-p.
- [50] V. B. Wreesmann *et al.*, "Influence of extracapsular nodal spread extent on prognosis of oral squamous cell carcinoma," *Head Neck*, vol. 38 Suppl 1, no. Suppl 1, pp. E1192-9, Apr 2016, doi: 10.1002/hed.24190.
- [51] E. D. S. Dolens *et al.*, "The Impact of Histopathological Features on the Prognosis of Oral Squamous Cell Carcinoma: A Comprehensive Review and Meta-Analysis," *Front Oncol*, vol. 11, p. 784924, 2021, doi: 10.3389/fonc.2021.784924.
- [52] A. Almangush *et al.*, "Clinical significance of tumor-stroma ratio in head and neck cancer: a systematic review and meta-analysis," *BMC Cancer*, vol. 21, no. 1, p. 480, Apr 30 2021, doi: 10.1186/s12885-021-08222-8.
- [53] P. C. Rodrigues *et al.*, "Clinicopathological prognostic factors of oral tongue squamous cell carcinoma: a retrospective study of 202 cases," *Int J Oral Maxillofac Surg*, vol. 43, no. 7, pp. 795-801, Jul 2014, doi: 10.1016/j.ijom.2014.01.014.

- 
- [54] M. Bryne, H. S. Koppang, R. Lilleng, and A. Kjaerheim, "Malignancy grading of the deep invasive margins of oral squamous cell carcinomas has high prognostic value," *J Pathol*, vol. 166, no. 4, pp. 375-81, Apr 1992, doi: 10.1002/path.1711660409.
- [55] M. Bryne, "Is the invasive front of an oral carcinoma the most important area for prognostication?," *Oral Dis*, vol. 4, no. 2, pp. 70-7, Jun 1998, doi: 10.1111/j.1601-0825.1998.tb00260.x.
- [56] F. A. Sawair, C. R. Irwin, D. J. Gordon, A. G. Leonard, M. Stephenson, and S. S. Napier, "Invasive front grading: reliability and usefulness in the management of oral squamous cell carcinoma," *J Oral Pathol Med*, vol. 32, no. 1, pp. 1-9, Jan 2003, doi: 10.1034/j.1600-0714.2003.00060.x.
- [57] A. Brandwein-Gensler *et al.*, "Oral squamous cell carcinoma - Histologic risk assessment, but not margin status, is strongly predictive of local disease-free and overall survival," (in English), *American Journal of Surgical Pathology*, vol. 29, no. 2, pp. 167-178, Feb 2005. [Online]. Available: <Go to ISI>://WOS:000226586000003.
- [58] A. Almagush *et al.*, "Depth of invasion, tumor budding, and worst pattern of invasion: Prognostic indicators in early-stage oral tongue cancer," (in English), *Head and Neck-Journal for the Sciences and Specialties of the Head and Neck*, vol. 36, no. 6, pp. 811-818, Jun 2014, doi: 10.1002/hed.23380.
- [59] D. Chatterjee *et al.*, "Tumor Budding and Worse Pattern of Invasion Can Predict Nodal Metastasis in Oral Cancers and Associated With Poor Survival in Early-Stage Tumors," *Ear Nose Throat J*, vol. 98, no. 7, pp. E112-E119, Aug 2019, doi: 10.1177/0145561319848669.
- [60] N. Xie *et al.*, "Tumor budding correlates with occult cervical lymph node metastasis and poor prognosis in clinical early-stage tongue squamous cell carcinoma," *J Oral Pathol Med*, vol. 44, no. 4, pp. 266-72, Apr 2015, doi: 10.1111/jop.12242.
- [61] I. H. Bjerkli *et al.*, "Tumor budding score predicts lymph node status in oral tongue squamous cell carcinoma and should be included in the pathology report," *PLoS One*, vol. 15, no. 9, p. e0239783, 2020, doi: 10.1371/journal.pone.0239783.
- [62] R. Keerthi, A. Dutta, S. Agarwal, V. Kani, and A. Khatua, "Perineural Invasion of Oral Squamous Cell Carcinoma: A New Hurdle for Surgeons," *J Maxillofac Oral Surg*, vol. 17, no. 1, pp. 59-63, Mar 2018, doi: 10.1007/s12663-016-0943-1.
- [63] X. Yang *et al.*, "Prognostic impact of perineural invasion in early stage oral tongue squamous cell carcinoma: Results from a prospective randomized trial," *Surg Oncol*, vol. 27, no. 2, pp. 123-128, Jun 2018, doi: 10.1016/j.suronc.2018.02.005.
- [64] L. Y. Lee *et al.*, "Prognostic impact of extratumoral perineural invasion in patients with oral cavity squamous cell carcinoma," *Cancer Med*, vol. 8, no. 14, pp. 6185-6194, Oct 2019, doi: 10.1002/cam4.2392.
- [65] I. H. Bjerkli *et al.*, "A combined histo-score based on tumor differentiation and lymphocytic infiltrate is a robust prognostic marker for mobile tongue cancer,"

- 
- Virchows Arch*, vol. 477, no. 6, pp. 865-872, Dec 2020, doi: 10.1007/s00428-020-02875-9.
- [66] D. Borsetto *et al.*, "Prognostic Significance of CD4+ and CD8+ Tumor-Infiltrating Lymphocytes in Head and Neck Squamous Cell Carcinoma: A Meta-Analysis," *Cancers (Basel)*, vol. 13, no. 4, Feb 13 2021, doi: 10.3390/cancers13040781.
- [67] A. Almagush *et al.*, "Reply to 'Comment on 'Prognostic biomarkers for oral tongue squamous cell carcinoma: a systematic review and meta-analysis'," *Br J Cancer*, vol. 118, no. 5, p. e12, Mar 6 2018, doi: 10.1038/bjc.2017.491.
- [68] A. Almagush *et al.*, "Prognostic biomarkers for oral tongue squamous cell carcinoma: a systematic review and meta-analysis," *Br J Cancer*, vol. 117, no. 6, pp. 856-866, Sep 5 2017, doi: 10.1038/bjc.2017.244.
- [69] G. Cervino *et al.*, "Molecular Biomarkers Related to Oral Carcinoma: Clinical Trial Outcome Evaluation in a Literature Review," *Dis Markers*, vol. 2019, p. 8040361, 2019, doi: 10.1155/2019/8040361.
- [70] P. G. Meliante *et al.*, "Diagnostic Predictors of Immunotherapy Response in Head and Neck Squamous Cell Carcinoma," *Diagnostics (Basel)*, vol. 13, no. 5, Feb 23 2023, doi: 10.3390/diagnostics13050862.
- [71] I. J. Fidler, "Timeline - The pathogenesis of cancer metastasis: the 'seed and soil' hypothesis revisited," (in English), *Nature Reviews Cancer*, vol. 3, no. 6, pp. 453-458, Jun 2003, doi: 10.1038/nrc1098.
- [72] S. Paget, "The distribution of secondary growths in cancer of the breast. 1889," *Cancer metastasis reviews*, vol. 8, no. 2, pp. 98-101, Aug 1989. [Online]. Available: <http://www.ncbi.nlm.nih.gov/pubmed/2673568>.
- [73] M. M. Mueller and N. E. Fusenig, "Tumor-stroma interactions directing phenotype and progression of epithelial skin tumor cells," *Differentiation*, vol. 70, no. 9-10, pp. 486-497, 2002. [Online]. Available: <http://dx.doi.org/10.1046/j.1432-0436.2002.700903.x>.
- [74] D. C. Radisky and M. J. Bissell, "Cancer. Respect thy neighbor!," *Science*, vol. 303, no. 5659, pp. 775-7, Feb 6 2004. [Online]. Available: [http://www.ncbi.nlm.nih.gov/entrez/query.fcgi?cmd=Retrieve&db=PubMed&dopt=Citation&list\\_uids=14764858](http://www.ncbi.nlm.nih.gov/entrez/query.fcgi?cmd=Retrieve&db=PubMed&dopt=Citation&list_uids=14764858).
- [75] C. Zeltz, I. Primac, P. Erusappan, J. Alam, A. Noel, and D. Gullberg, "Cancer-associated fibroblasts in desmoplastic tumors: emerging role of integrins," *Seminars in cancer biology*, vol. 62, pp. 166-181, May 2020, doi: 10.1016/j.semcancer.2019.08.004.
- [76] M. R. Junttila and F. J. de Sauvage, "Influence of tumour micro-environment heterogeneity on therapeutic response," (in English), *Nature*, vol. 501, no. 7467, pp. 346-354, Sep 19 2013, doi: 10.1038/nature12626.
- [77] D. F. Quail and J. A. Joyce, "Microenvironmental regulation of tumor progression and metastasis," (in English), *Nature Medicine*, vol. 19, no. 11, pp. 1423-1437, Nov 2013, doi: 10.1038/nm.3394.
- [78] X. Zhang, T. Meng, S. Cui, D. Liu, Q. Pang, and P. Wang, "Roles of ubiquitination in the crosstalk between tumors and the tumor microenvironment (Review)," *Int J Oncol*, vol. 61, no. 1, Jul 2022, doi: 10.3892/ijo.2022.5374.

- 
- [79] C. D. Dongre H, "Tumor-Fibroblast Interactions in Carcinomas," in *Biomarkers of the Tumor Microenvironment*, W. Akslen L, R Ed.: Springer, 2022.
- [80] B. Peltanova, M. Raudenska, and M. Masarik, "Effect of tumor microenvironment on pathogenesis of the head and neck squamous cell carcinoma: a systematic review," *Mol Cancer*, vol. 18, no. 1, p. 63, Mar 30 2019, doi: 10.1186/s12943-019-0983-5.
- [81] R. Kalluri, "The biology and function of fibroblasts in cancer," (in English), *Nature Reviews Cancer*, vol. 16, no. 9, pp. 582-598, Sep 2016, doi: 10.1038/nrc.2016.73.
- [82] U. M. Polanska and A. Orimo, "Carcinoma-associated fibroblasts: Non-neoplastic tumour-promoting mesenchymal cells," (in English), *Journal of Cellular Physiology*, vol. 228, no. 8, pp. 1651-1657, Aug 2013, doi: 10.1002/jcp.24347.
- [83] D. E. Costea *et al.*, "Identification of two distinct carcinoma-associated fibroblast subtypes with differential tumor-promoting abilities in oral squamous cell carcinoma," *Cancer Res*, vol. 73, no. 13, pp. 3888-901, Jul 1 2013, doi: 10.1158/0008-5472.CAN-12-4150.
- [84] C. Gaggioli *et al.*, "Fibroblast-led collective invasion of carcinoma cells with differing roles for RhoGTPases in leading and following cells," (in English), *Nature Cell Biology*, vol. 9, no. 12, pp. 1392-U92, Dec 2007, doi: 10.1038/ncb1658.
- [85] A. J. Daly, L. McIlreavey, and C. R. Irwin, "Regulation of HGF and SDF-1 expression by oral fibroblasts - Implications for invasion of oral cancer," (in English), *Oral Oncology*, vol. 44, no. 7, pp. 646-651, Jul 2008, doi: 10.1016/j.oraloncology.2007.08.012.
- [86] S. Kawashiri *et al.*, "Significance of Stromal Desmoplasia and Myofibroblast Appearance at the Invasive Front in Squamous Cell Carcinoma of the Oral Cavity," (in English), *Head and Neck-Journal for the Sciences and Specialties of the Head and Neck*, vol. 31, no. 10, pp. 1346-1353, Oct 2009, doi: 10.1002/hed.21097.
- [87] M. G. Kellermann *et al.*, "Myofibroblasts in the stroma of oral squamous cell carcinoma are associated with poor prognosis," (in English), *Histopathology*, vol. 51, no. 6, pp. 849-853, Dec 2007, doi: 10.1111/j.1365-2559.2007.02873.x.
- [88] H. Parajuli *et al.*, "Integrin alpha11 is overexpressed by tumour stroma of head and neck squamous cell carcinoma and correlates positively with alpha smooth muscle actin expression," *J Oral Pathol Med*, vol. 46, no. 4, pp. 267-275, Apr 2017, doi: 10.1111/jop.12493.
- [89] N. Fujii *et al.*, "Cancer-associated fibroblasts and CD163-positive macrophages in oral squamous cell carcinoma: their clinicopathological and prognostic significance," *J Oral Pathol Med*, vol. 41, no. 6, pp. 444-51, Jul 2012, doi: 10.1111/j.1600-0714.2012.01127.x.
- [90] D. Marsh *et al.*, "Stromal features are predictive of disease mortality in oral cancer patients," (in English), *Journal of Pathology*, vol. 223, no. 4, pp. 470-481, Mar 2011, doi: 10.1002/path.2830.
- [91] A. K. Patel *et al.*, "A subtype of cancer-associated fibroblasts with lower expression of alpha-smooth muscle actin suppresses stemness through BMP4 in

- 
- oral carcinoma," *Oncogenesis*, vol. 7, no. 10, p. 78, Oct 5 2018, doi: 10.1038/s41389-018-0087-x.
- [92] M. Mellone *et al.*, "Induction of fibroblast senescence generates a non-fibroblastic myofibroblast phenotype that differentially impacts on cancer prognosis," *Aging (Albany NY)*, vol. 9, no. 1, pp. 114-132, Dec 15 2016, doi: 10.18632/aging.101127.
- [93] E. Sahai *et al.*, "A framework for advancing our understanding of cancer-associated fibroblasts," *Nat Rev Cancer*, vol. 20, no. 3, pp. 174-186, Mar 2020, doi: 10.1038/s41568-019-0238-1.
- [94] R. Kalluri and M. Zeisberg, "Fibroblasts in cancer," *Nat Rev Cancer*, vol. 6, no. 5, pp. 392-401, May 2006, doi: 10.1038/nrc1877.
- [95] K. P. Lim *et al.*, "Fibroblast gene expression profile reflects the stage of tumour progression in oral squamous cell carcinoma," *J Pathol*, vol. 223, no. 4, pp. 459-69, Mar 2011, doi: 10.1002/path.2841.
- [96] K. Louault, R. R. Li, and Y. A. DeClerck, "Cancer-Associated Fibroblasts: Understanding Their Heterogeneity," *Cancers (Basel)*, vol. 12, no. 11, Oct 24 2020, doi: 10.3390/cancers12113108.
- [97] J. H. Choi *et al.*, "Single-cell transcriptome profiling of the stepwise progression of head and neck cancer," *Nat Commun*, vol. 14, no. 1, p. 1055, Feb 24 2023, doi: 10.1038/s41467-023-36691-x.
- [98] S. V. Puram *et al.*, "Single-Cell Transcriptomic Analysis of Primary and Metastatic Tumor Ecosystems in Head and Neck Cancer," *Cell*, vol. 171, no. 7, pp. 1611-1624 e24, Dec 14 2017, doi: 10.1016/j.cell.2017.10.044.
- [99] D. P. Bartel, "Metazoan MicroRNAs," *Cell*, vol. 173, no. 1, pp. 20-51, Mar 22 2018, doi: 10.1016/j.cell.2018.03.006.
- [100] K. A. Cottrell, P. Szczesny, and S. Djuranovic, "Translation efficiency is a determinant of the magnitude of miRNA-mediated repression," (in English), *Scientific Reports*, vol. 7, Nov 2 2017, doi: ARTN 1488410.1038/s41598-017-13851-w.
- [101] D. R. Hogg and L. W. Harries, "Human genetic variation and its effect on miRNA biogenesis, activity and function," *Biochem Soc Trans*, vol. 42, no. 4, pp. 1184-9, Aug 2014, doi: 10.1042/BST20140055.
- [102] D. P. Bartel, "MicroRNAs: Genomics, biogenesis, mechanism, and function," (in English), *Cell*, vol. 116, no. 2, pp. 281-297, Jan 23 2004, doi: Doi 10.1016/S0092-8674(04)00045-5.
- [103] G. A. Calin *et al.*, "Human microRNA genes are frequently located at fragile sites and genomic regions involved in cancers," *Proceedings of the National Academy of Sciences of the United States of America*, vol. 101, no. 9, pp. 2999-3004, Mar 2 2004, doi: 10.1073/pnas.0307323101.
- [104] K. Ruan, X. Fang, and G. Ouyang, "MicroRNAs: novel regulators in the hallmarks of human cancer," *Cancer Lett*, vol. 285, no. 2, pp. 116-26, Nov 28 2009, doi: 10.1016/j.canlet.2009.04.031.
- [105] N. Tran, C. J. O'Brien, J. Clark, and B. Rose, "Potential Role of Micro-Rnas in Head and Neck Tumorigenesis," (in English), *Head and Neck-Journal for the Sciences and Specialties of the Head and Neck*, vol. 32, no. 8, pp. 1099-1111, Aug 2010, doi: 10.1002/hed.21356.

- 
- [106] A. J. Min, C. Zhu, S. P. Peng, S. Rajthala, D. E. Costea, and D. Sapkota, "MicroRNAs as Important Players and Biomarkers in Oral Carcinogenesis," (in English), *Biomed Research International*, 2015, doi: Artn 18690410.1155/2015/186904.
- [107] N. Sethi, A. Wright, H. Wood, and P. Rabbitts, "MicroRNAs and head and neck cancer: Reviewing the first decade of research," (in English), *European Journal of Cancer*, vol. 50, no. 15, pp. 2619-2635, Oct 2014, doi: 10.1016/j.ejca.2014.07.012.
- [108] N. Sethi, A. Wright, H. Wood, and P. Rabbitts, "MicroRNAs and head and neck cancer: reviewing the first decade of research," (in eng), *Eur J Cancer*, vol. 50, no. 15, pp. 2619-35, Oct 2014, doi: 10.1016/j.ejca.2014.07.012.
- [109] S. C. Peng *et al.*, "MicroRNAs MiR-218, MiR-125b, and Let-7g predict prognosis in patients with oral cavity squamous cell carcinoma," (in eng), *PLoS One*, vol. 9, no. 7, p. e102403, 2014, doi: 10.1371/journal.pone.0102403.
- [110] C. Rajan *et al.*, "MiRNA expression profiling and emergence of new prognostic signature for oral squamous cell carcinoma," *Sci Rep*, vol. 11, no. 1, p. 7298, Mar 31 2021, doi: 10.1038/s41598-021-86316-w.
- [111] G. Troiano, F. Mastrangelo, V. C. A. Caponio, L. Laino, N. Cirillo, and L. Lo Muzio, "Predictive Prognostic Value of Tissue-Based MicroRNA Expression in Oral Squamous Cell Carcinoma: A Systematic Review and Meta-analysis," *J Dent Res*, vol. 97, no. 7, pp. 759-766, Jul 2018, doi: 10.1177/0022034518762090.
- [112] P. P. Medina, M. Nolde, and F. J. Slack, "OncomiR addiction in an in vivo model of microRNA-21-induced pre-B-cell lymphoma," (in eng), *Nature*, vol. 467, no. 7311, pp. 86-90, Sep 2 2010, doi: 10.1038/nature09284.
- [113] L. B. Frankel, N. R. Christoffersen, A. Jacobsen, M. Lindow, A. Krogh, and A. H. Lund, "Programmed cell death 4 (PDCD4) is an important functional target of the microRNA miR-21 in breast cancer cells," (in eng), *J Biol Chem*, vol. 283, no. 2, pp. 1026-33, Jan 11 2008, doi: 10.1074/jbc.M707224200.
- [114] M. Dillhoff, J. Liu, W. Frankel, C. Croce, and M. Bloomston, "MicroRNA-21 is Overexpressed in Pancreatic Cancer and a Potential Predictor of Survival," *Journal of Gastrointestinal Surgery*, journal article vol. 12, no. 12, p. 2171, July 19 2008, doi: 10.1007/s11605-008-0584-x.
- [115] P. P. Reis *et al.*, "Programmed cell death 4 loss increases tumor cell invasion and is regulated by miR-21 in oral squamous cell carcinoma," (in eng), *Mol Cancer*, vol. 9, p. 238, Sep 10 2010, doi: 10.1186/1476-4598-9-238.
- [116] A. Min, C. Zhu, S. Peng, S. Rajthala, D. E. Costea, and D. Sapkota, "MicroRNAs as Important Players and Biomarkers in Oral Carcinogenesis," *Biomed Res Int*, vol. 2015, p. 186904, 2015, doi: 10.1155/2015/186904.
- [117] D. S. Hong *et al.*, "Phase 1 study of MRX34, a liposomal miR-34a mimic, in patients with advanced solid tumours," *Br J Cancer*, vol. 122, no. 11, pp. 1630-1637, May 2020, doi: 10.1038/s41416-020-0802-1.
- [118] M. S. Beg *et al.*, "Phase I study of MRX34, a liposomal miR-34a mimic, administered twice weekly in patients with advanced solid tumors," *Invest New Drugs*, vol. 35, no. 2, pp. 180-188, Apr 2017, doi: 10.1007/s10637-016-0407-y.

- 
- [119] M. Ito, Y. Miyata, and M. Okada, "Current clinical trials with non-coding RNA-based therapeutics in malignant diseases: A systematic review," *Transl Oncol*, vol. 31, p. 101634, May 2023, doi: 10.1016/j.tranon.2023.101634.
- [120] L. J. Harper, K. Piper, J. Common, F. Fortune, and I. C. Mackenzie, "Stem cell patterns in cell lines derived from head and neck squamous cell carcinoma," (in English), *Journal of Oral Pathology & Medicine*, vol. 36, no. 10, pp. 594-603, Nov 2007, doi: 10.1111/j.1600-0714.2007.00617.x.
- [121] A. Biddle *et al.*, "Cancer stem cells in squamous cell carcinoma switch between two distinct phenotypes that are preferentially migratory or proliferative," *Cancer Res*, vol. 71, no. 15, pp. 5317-26, Aug 1 2011, doi: 10.1158/0008-5472.CAN-11-1059.
- [122] D. G. Altman, L. M. McShane, W. Sauerbrei, and S. E. Taube, "Reporting Recommendations for Tumor Marker Prognostic Studies (REMARK): explanation and elaboration," *PLoS Med*, vol. 9, no. 5, p. e1001216, 2012, doi: 10.1371/journal.pmed.1001216.
- [123] Z. Zhang *et al.*, "Metabolic reprogramming of normal oral fibroblasts correlated with increased glycolytic metabolism of oral squamous cell carcinoma and precedes their activation into carcinoma associated fibroblasts," *Cell Mol Life Sci*, vol. 77, no. 6, pp. 1115-1133, Mar 2020, doi: 10.1007/s00018-019-03209-y.
- [124] D. E. Costea, A. O. Dimba, L. L. Loro, O. K. Vintermyr, and A. C. Johannessen, "The phenotype of in vitro reconstituted normal human oral epithelium is essentially determined by culture medium," *J Oral Pathol Med*, vol. 34, no. 4, pp. 247-52, Apr 2005, doi: 10.1111/j.1600-0714.2005.00308.x.
- [125] D. E. Costea, L. L. Loro, E. A. Dimba, O. K. Vintermyr, and A. C. Johannessen, "Crucial effects of fibroblasts and keratinocyte growth factor on morphogenesis of reconstituted human oral epithelium," *J Invest Dermatol*, vol. 121, no. 6, pp. 1479-86, Dec 2003, doi: 10.1111/j.1523-1747.2003.12616.x.
- [126] M. Anders, R. Hansen, R. X. Ding, K. A. Rauen, M. J. Bissell, and W. M. Korn, "Disruption of 3D tissue integrity facilitates adenovirus infection by deregulating the coxsackievirus and adenovirus receptor," *Proc Natl Acad Sci USA*, vol. 100, no. 4, pp. 1943-8, Feb 18 2003, doi: 10.1073/pnas.0337599100.
- [127] E. Cukierman, R. Pankov, D. R. Stevens, and K. M. Yamada, "Taking cell-matrix adhesions to the third dimension," *Science*, vol. 294, no. 5547, pp. 1708-12, Nov 23 2001, doi: 10.1126/science.1064829.
- [128] A. Abbott, "Cell culture: Biology's new dimension," (in English), *Nature*, vol. 424, no. 6951, pp. 870-872, Aug 21 2003, doi: 10.1038/424870a.
- [129] V. Agarwal, G. W. Bell, J. W. Nam, and D. P. Bartel, "Predicting effective microRNA target sites in mammalian mRNAs," (in English), *Elife*, vol. 4, Aug 12 2015, doi: ARTN e05005  
10.7554/eLife.05005.
- [130] W. J. Kent *et al.*, "The human genome browser at UCSC," (in English), *Genome Research*, vol. 12, no. 6, pp. 996-1006, Jun 2002, doi: 10.1101/gr.229102.
- [131] T. Terada, "Cytokeratin-negative small cell lung carcinoma," *Rare Tumors*, vol. 3, no. 4, p. e38, Oct 21 2011, doi: 10.4081/rt.2011.e38.



- 
- [132] H. Parajuli, "Role of integrin  $\alpha 1$  in oral carcinogenesis," PhD, University of Bergen, 2016.
- [133] X. Wang, X. Wang, M. Xu, and W. Sheng, "Effects of CAF-Derived MicroRNA on Tumor Biology and Clinical Applications," *Cancers (Basel)*, vol. 13, no. 13, Jun 24 2021, doi: 10.3390/cancers13133160.
- [134] A. Savardashtaki, Z. Shabaninejad, A. Movahedpour, R. Sahebnasagh, H. Mirzaei, and M. R. Hamblin, "miRNAs derived from cancer-associated fibroblasts in colorectal cancer," *Epigenomics*, vol. 11, no. 14, pp. 1627-1645, Nov 2019, doi: 10.2217/epi-2019-0110.
- [135] L. L. Matos *et al.*, "Cancer-associated fibroblast regulation by microRNAs promotes invasion of oral squamous cell carcinoma," *Oral Oncol*, vol. 110, p. 104909, Nov 2020, doi: 10.1016/j.oraloncology.2020.104909.
- [136] N. Hedback *et al.*, "MiR-21 Expression in the Tumor Stroma of Oral Squamous Cell Carcinoma: An Independent Biomarker of Disease Free Survival," (in English), *Plos One*, vol. 9, no. 4, Apr 22 2014, doi: ARTN e95193  
10.1371/journal.pone.0095193.
- [137] T. R. Donahue *et al.*, "Stromal microRNA-21 levels predict response to 5-fluorouracil in patients with pancreatic cancer," *J Surg Oncol*, vol. 110, no. 8, pp. 952-9, Dec 2014, doi: 10.1002/jso.23750.
- [138] A. Kunita *et al.*, "MicroRNA-21 in cancer-associated fibroblasts supports lung adenocarcinoma progression," *Sci Rep*, vol. 8, no. 1, p. 8838, Jun 11 2018, doi: 10.1038/s41598-018-27128-3.
- [139] B. E. Kadera *et al.*, "MicroRNA-21 in pancreatic ductal adenocarcinoma tumor-associated fibroblasts promotes metastasis," *PLoS One*, vol. 8, no. 8, p. e71978, 2013, doi: 10.1371/journal.pone.0071978.
- [140] L. Zhao *et al.*, "MiRNA expression analysis of cancer-associated fibroblasts and normal fibroblasts in breast cancer," *Int J Biochem Cell Biol*, vol. 44, no. 11, pp. 2051-9, Nov 2012, doi: 10.1016/j.biocel.2012.08.005.
- [141] J. Zhang *et al.*, "miR-101 represses lung cancer by inhibiting interaction of fibroblasts and cancer cells by down-regulating CXCL12," *Biomed Pharmacother*, vol. 74, pp. 215-21, Aug 2015, doi: 10.1016/j.biopha.2015.08.013.
- [142] V. Doldi *et al.*, "Integrated gene and miRNA expression analysis of prostate cancer associated fibroblasts supports a prominent role for interleukin-6 in fibroblast activation," *Oncotarget*, vol. 6, no. 31, pp. 31441-60, Oct 13 2015, doi: 10.18632/oncotarget.5056.
- [143] M. Schoepp, A. J. Strose, and J. Haier, "Dysregulation of miRNA Expression in Cancer Associated Fibroblasts (CAFs) and Its Consequences on the Tumor Microenvironment," *Cancers (Basel)*, vol. 9, no. 6, May 24 2017, doi: 10.3390/cancers9060054.
- [144] J. Haier, A. Strose, C. Matuszcak, and R. Hummel, "miR clusters target cellular functional complexes by defining their degree of regulatory freedom," *Cancer Metastasis Rev*, vol. 35, no. 2, pp. 289-322, Jun 2016, doi: 10.1007/s10555-016-9617-1.

- 
- [145] F. Ganci *et al.*, "Altered peritumoral microRNA expression predicts head and neck cancer patients with a high risk of recurrence," (in English), *Modern Pathology*, vol. 30, no. 10, pp. 1387-1401, Oct 2017, doi: 10.1038/modpathol.2017.62.
- [146] C. Gaggioli *et al.*, "Fibroblast-led collective invasion of carcinoma cells with differing roles for RhoGTPases in leading and following cells," *Nat Cell Biol*, vol. 9, no. 12, pp. 1392-400, Dec 2007, doi: 10.1038/ncb1658.
- [147] M. R. Dourado, C. E. de Oliveira, I. Sawazaki-Calone, E. Sundquist, R. D. Coletta, and T. Salo, "Clinicopathologic significance of ROCK2 expression in oral squamous cell carcinomas," *J Oral Pathol Med*, vol. 47, no. 2, pp. 121-127, Feb 2018, doi: 10.1111/jop.12651.
- [148] L. Chen and H. Jin, "MicroRNAs as novel biomarkers in the diagnosis of non-small cell lung cancer: a meta-analysis based on 20 studies," *Tumour Biol*, vol. 35, no. 9, pp. 9119-29, Sep 2014, doi: 10.1007/s13277-014-2188-2.
- [149] A. D. Chaudhuri, S. V. Yelamanchili, and H. S. Fox, "Combined fluorescent in situ hybridization for detection of microRNAs and immunofluorescent labeling for cell-type markers," *Front Cell Neurosci*, vol. 7, p. 160, 2013, doi: 10.3389/fncel.2013.00160.
- [150] G. J. Nuovo, "In situ detection of microRNAs in paraffin embedded, formalin fixed tissues and the co-localization of their putative targets," *Methods*, vol. 52, no. 4, pp. 307-15, Dec 2010, doi: 10.1016/j.ymeth.2010.08.009.
- [151] F. Aeffner *et al.*, "Introduction to Digital Image Analysis in Whole-slide Imaging: A White Paper from the Digital Pathology Association," *J Pathol Inform*, vol. 10, p. 9, 2019, doi: 10.4103/jpi.jpi\_82\_18.
- [152] C. C. Yu, P. N. Chen, C. Y. Peng, C. H. Yu, and M. Y. Chou, "Suppression of miR-204 enables oral squamous cell carcinomas to promote cancer stemness, EMT traits, and lymph node metastasis," (in English), *Oncotarget*, vol. 7, no. 15, pp. 20180-20192, Apr 12 2016, doi: DOI 10.18632/oncotarget.7745.
- [153] M. Manikandan, A. K. D. M. Rao, K. S. Rajkumar, R. Rajaraman, and A. K. Munirajan, "Altered levels of miR-21, miR-125b-2\*, miR-138, miR-155, miR-184, and miR-205 in oral squamous cell carcinoma and association with clinicopathological characteristics," (in English), *Journal of Oral Pathology & Medicine*, vol. 44, no. 10, pp. 792-800, Nov 2015, doi: 10.1111/jop.12300.
- [154] K. J. Bienkowska, C. J. Hanley, and G. J. Thomas, "Cancer-Associated Fibroblasts in Oral Cancer: A Current Perspective on Function and Potential for Therapeutic Targeting," *Front Oral Health*, vol. 2, p. 686337, 2021, doi: 10.3389/froh.2021.686337.
- [155] M. R. Dourado, E. N. S. Guerra, T. Salo, D. W. Lambert, and R. D. Coletta, "Prognostic value of the immunohistochemical detection of cancer-associated fibroblasts in oral cancer: A systematic review and meta-analysis," *J Oral Pathol Med*, vol. 47, no. 5, pp. 443-453, May 2018, doi: 10.1111/jop.12623.
- [156] X. Liu *et al.*, "MiR-138 suppressed nasopharyngeal carcinoma growth and tumorigenesis by targeting the CCND1 oncogene," (in English), *Cell Cycle*, vol. 11, no. 13, pp. 2495-2506, Jul 1 2012, doi: 10.4161/cc.20898.
- [157] W. Wang, L. J. Zhao, Y. X. Tan, H. Ren, and Z. T. Qi, "MiR-138 induces cell cycle arrest by targeting cyclin D3 in hepatocellular carcinoma," (in English),

- Carcinogenesis*, vol. 33, no. 5, pp. 1113-1120, May 2012, doi: 10.1093/carcin/bgs113.
- [158] X. H. Chan *et al.*, "Targeting glioma stem cells by functional inhibition of a prosurvival oncomiR-138 in malignant gliomas," *Cell Rep*, vol. 2, no. 3, pp. 591-602, Sep 27 2012, doi: 10.1016/j.celrep.2012.07.012.
- [159] L. Jiang *et al.*, "Downregulation of the Rho GTPase signaling pathway is involved in the microRNA-138-mediated inhibition of cell migration and invasion in tongue squamous cell carcinoma," *Int J Cancer*, vol. 127, no. 3, pp. 505-12, Aug 1 2010, doi: 10.1002/ijc.25320.



Article

# Profiling and Functional Analysis of microRNA Deregulation in Cancer-Associated Fibroblasts in Oral Squamous Cell Carcinoma Depicts an Anti-Invasive Role of microRNA-204 via Regulation of Their Motility

Saroj Rajthala <sup>1,2</sup>, Anjie Min <sup>1,3</sup>, Himalaya Parajuli <sup>1,2</sup> , Kala Chand Debnath <sup>1,2</sup>, Borghild Ljøkjel <sup>4</sup>, Kristin Marie Hoven <sup>4</sup>, Arild Kvalheim <sup>5</sup>, Stein Lybak <sup>4</sup>, Evelyn Neppelberg <sup>4,6</sup>, Olav Karsten Vintermyr <sup>1,7</sup>, Anne Christine Johannessen <sup>1,2,7</sup>, Dipak Sapkota <sup>8</sup> and Daniela Elena Costea <sup>1,2,7,\*</sup>

- <sup>1</sup> Gade Laboratory for Pathology, Department of Clinical Medicine, Faculty of Medicine, University of Bergen, 5020 Bergen, Norway; saroj.rajthala@uib.no (S.R.); william0732@csu.edu.cn (A.M.); himalaya.parajuli@uib.no (H.P.); kcdebnath.cdc@gmail.com (K.C.D.); olav.karsten.vintermyr@helse-bergen.no (O.K.V.); anne.johannessen@uib.no (A.C.J.)
- <sup>2</sup> Centre for Cancer Biomarkers (CCBio), Faculty of Medicine, University of Bergen, 5020 Bergen, Norway
- <sup>3</sup> Department of Oral Maxillofacial Surgery, Xiangya Hospital, Central South University, Changsha 410008, China
- <sup>4</sup> Head and Neck Clinic, Haukeland University Hospital, 5021 Bergen, Norway; borghild.ljokjel@helse-bergen.no (B.L.); kristin.marie.hoven@helse-bergen.no (K.M.H.); stein.lybak@helse-bergen.no (S.L.); evelyn.neppelberg@helse-bergen.no (E.N.)
- <sup>5</sup> Oral Surgery Private Referral Practice “Tannteam”, 5221 Nesttun, Norway; ari-kval@online.no
- <sup>6</sup> Department of Oral Surgery, Institute of Clinical Dentistry, University of Bergen, 5020 Bergen, Norway
- <sup>7</sup> Department of Pathology, Haukeland University Hospital, 5020 Bergen, Norway
- <sup>8</sup> Department of Oral Biology, University of Oslo, 0372 Oslo, Norway; dipak.sapkota@odont.uio.no
- \* Correspondence: Daniela.costea@uib.no; Tel.: +47-559-72565



**Citation:** Rajthala, S.; Min, A.; Parajuli, H.; Debnath, K.C.; Ljøkjel, B.; Hoven, K.M.; Kvalheim, A.; Lybak, S.; Neppelberg, E.; Vintermyr, O.K.; et al. Profiling and Functional Analysis of microRNA Deregulation in Cancer-Associated Fibroblasts in Oral Squamous Cell Carcinoma Depicts an Anti-Invasive Role of microRNA-204 via Regulation of Their Motility. *Int. J. Mol. Sci.* **2021**, *22*, 11960. <https://doi.org/10.3390/ijms222111960>

Academic Editor: Young-Ho Ahn

Received: 12 October 2021

Accepted: 2 November 2021

Published: 4 November 2021

**Publisher's Note:** MDPI stays neutral with regard to jurisdictional claims in published maps and institutional affiliations.



**Copyright:** © 2021 by the authors. Licensee MDPI, Basel, Switzerland. This article is an open access article distributed under the terms and conditions of the Creative Commons Attribution (CC BY) license (<https://creativecommons.org/licenses/by/4.0/>).

**Abstract:** *Background:* Knowledge on the role of miR changes in tumor stroma for cancer progression is limited. This study aimed to investigate the role of miR dysregulation in cancer-associated fibroblasts (CAFs) in oral squamous cell carcinoma (OSCC). *Methodology:* CAF and normal oral fibroblasts (NOFs) were isolated from biopsies of OSCC patients and healthy individuals after informed consent and grown in 3D collagen gels. Total RNA was extracted. Global miR expression was profiled using Illumina version 2 panels. The functional impact of altered miR-204 expression in fibroblasts on their phenotype and molecular profile was investigated using mimics and inhibitors of miR-204. Further, the impact of miR-204 expression in fibroblasts on invasion of adjacent OSCC cells was assessed in 3D-organotypic co-cultures. *Results:* Unsupervised hierarchical clustering for global miR expression resulted in separate clusters for CAF and NOF. SAM analysis identified differential expression of twelve miRs between CAF and NOF. Modulation of miR-204 expression did not affect fibroblast cell proliferation, but resulted in changes in the motility phenotype, expression of various motility-related molecules, and invasion of the adjacent OSCC cells. 3' UTR miR target reporter assay showed ITGA11 to be a direct target of miR-204. *Conclusions:* This study identifies differentially expressed miRs in stromal fibroblasts of OSCC lesions compared with normal oral mucosa and it reveals that one of the significantly downregulated miRs in CAF, miR-204, has a tumor-suppressive function through inhibition of fibroblast migration by modulating the expression of several different molecules in addition to directly targeting ITGA11.

**Keywords:** oral squamous cell carcinoma; miR-204; fibroblasts; tumor stroma; ITGA11

## 1. Introduction

Oral cancer represents a significant proportion of head and neck cancer and is an important cause of morbidity and mortality worldwide [1]. It was recently estimated

that an alarming 109% increase in the number of incident lip and oral cavity cancers over a 28 y period has occurred (from around 186,000 in 1990 to 389,800 in 2017) [2]. Oral squamous cell carcinoma (OSCC) that arises from oral epithelium represents 90% of the oral cancers [3]. Although few studies showed an improvement in survival for OSCC during the last years [4], owing to recent advances in treatment of SCC [5,6], many studies have reported that the five-year survival for OSCC remained low during the last decades, and thus it requires a better understanding of its biology for designing even more innovative treatment modalities [7,8].

The discovery of micro-RNAs (miRs) as regulators of gene expression [9–11], and evidence of their importance for development and disease [12], has led to a burst of miR studies in cancers, including OSCC. Since then, several miRs have been shown to have either tumor-promoting or tumor-suppressive roles [13]. For example, miR-21, miR-146a, miR-155, and miR-134 have been shown to exhibit oncogenic functions, while miR-7, miR-99a, and miR-218 have been proven to exhibit tumor suppressive functions (reviewed in [14]) in OSCC.

With regards to changes in miR expression in tumors, miRs have been suggested as potential diagnostic and prognostic biomarkers in several cancers. Changes in miR expression in various biological samples such as tumor biopsies, serum/plasma, and saliva have been reported. For example, miR-21 has been reported to be increased in both plasma and tissues in OSCC, and miR-29a has been shown to be decrease in serum of OSCC patients. More than that, miRs have also been regarded as potential targets for therapeutic intervention (reviewed in [14–16]).

Several lines of evidence support now that it is not only the intrinsic properties of the epithelial cells that drive carcinogenesis. Rather, the invasion potential of transformed cancer cells is largely influenced by the tumor microenvironment composed of fibroblasts, immune cells, blood and lymph vessels, muscles, fat, nerves, extracellular matrix, and soluble factors [17,18]. Fibroblasts are the most abundant mesenchyme-derived cell type in the stroma responsible for the structural framework of tissues. Cancer-associated fibroblasts (CAFs), which can be derived from several sources, such as neighboring normal fibroblasts, pericytes, endothelial cells, or from mesenchymal stem cells from bone marrow, have been shown to play an important role in supporting tumor initiation and invasion in both *in vitro* cell culture studies [19–21] and *in vivo* animal studies [19]. In addition, CAF have been associated with lymph node metastasis [22,23] and poor prognosis [22–26].

While most studies focused on miR changes in tumor cells or tumor as a whole, including in the OSCC studies, our knowledge on miR alterations in the tumor microenvironment, and in particular in CAFs, is very sparse. Given the impact of both miRs and CAFs in tumor progression, miR dysregulation in CAFs could be a major factor in determining the behavior of tumor cells. Thus, this study was aimed at investigating miR dysregulation in CAFs in OSCC. Our previous transcriptomic study that compared the same CAF and NOF strains used in this study identified altered expression of integrin alpha 11 (ITGA11) in CAFs [19]. We have also validated this finding on patient material, by detected significantly increased expression of ITGA11 in the stroma of head and neck squamous cell carcinoma compared with normal oral mucosa controls [24]. This further led our investigation towards miR-204, one of the miRs identified by the microarray study presented here to have an altered expression in CAFs and to have a predicted target site at 3' UTR of ITGA11.

Several studies have shown decreased expression of miR-204 in tumor tissues compared with normal tissues [27–30], but none investigated specifically its alterations in CAFs. An anti-tumorigenic effect of miR-204 has been demonstrated in cell culture and in animal studies [27–31], using cancer cells, but not CAFs. Lower expression of miR-204 has been observed in oral premalignant lesions [32] and OSCC tumors compared with normal tissues [33,34], and the anti-tumor effect of miR-204 has also been demonstrated *in vitro* in OSCC cells, but not in OSCC-derived CAFs [35]. In a recent study on a cohort of 169 patients with human papilloma virus (HPV)-negative primary OSCC, we showed that presence of miR-204 in the stroma at the tumor front predicted better overall survival and

recurrence free survival [36]. Nevertheless, none of these previous studies investigated the dysregulation of miR-204 in CAFs and its impact on the behavior of OSCC cells. Therefore, this study sought also to explore the functional role of expression of miR-204 in CAFs on OSCC progression.

## 2. Results

### 2.1. miR Array Identifies Twelve miRs with Differential Expression in CAFs versus NOFs

Unsupervised hierarchical clustering performed on all the samples (unmatched CAFs and NOFs grown in 3D collagen gels) based upon global miR expression resulted in separate clusters of CAFs (lilac ring) and NOFs (black ring), although with some minor inter-clustering; two CAF strains clustered together with NOFs, and one strain of NOF clustered together with CAFs (Figure 1A). SAM analysis identified twelve significantly (FDR = 0) differentially regulated miRs (Figure 1B). Different subgroups for CAFs and NOFs were observed when clustered for the twelve significantly differentially regulated miRs by fibroblast type (Figure 1B). Four of the miRs: miR-138-5p, miR-378a-3p, miR-190b, and miR-582-5p were significantly up-regulated, while miR-224-5p, miR-16-2-3p, miR-155-5p, miR-92b-3p, miR-204-5p, miR-504-5p, miR-1270, and miR-3611 were significantly down-regulated in CAFs compared with NOFs (Figure 1B).

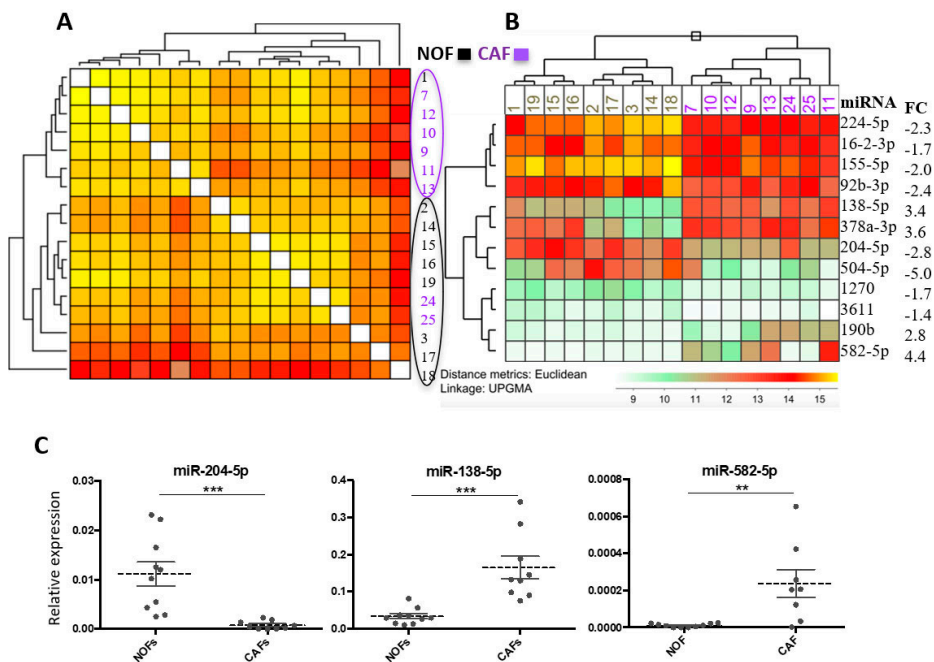


**Figure 1.** (A) Unsupervised hierarchical sample clustering of CAFs and NOFs for miR expression. (B) Clustering analysis by fibroblast type for 12 significantly differentially regulated miRs (SAM analysis). Significantly altered miRs (FDR = 0) and corresponding fold changes (FCs) on the right. (C) miR validation of microarray results by qRT-PCR (\*\*  $p < 0.005$ , \*\*\*  $p < 0.0005$ ).

## 2.2. Validation of Altered Expression of miR-204 in Cultured Fibroblasts and Patient Material

qRT-PCR validation of some of the dysregulated miRs (miR-204-5p, miR-138-5p, and miR-582-5p) confirmed the results of the miR array analysis (Figure 1C). Unlike down-regulation of miR-204 expression in CAFs compared with unmatched NOFs, the alterations in the expression of miR-204 in CAFs compared with NOFs were more heterogeneous when investigated on matched CAF and NOF pairs from OSCC patients grown in 2D cultures. Three (ID 8m, 10m, and 21m) of the five fibroblast pairs showed reduced expression of miR-204 in CAFs compared with NOFs (Figure 2A), while in two pairs' (ID 7m and 15m) miR-204 expression in was increased in CAFs versus NOFs.

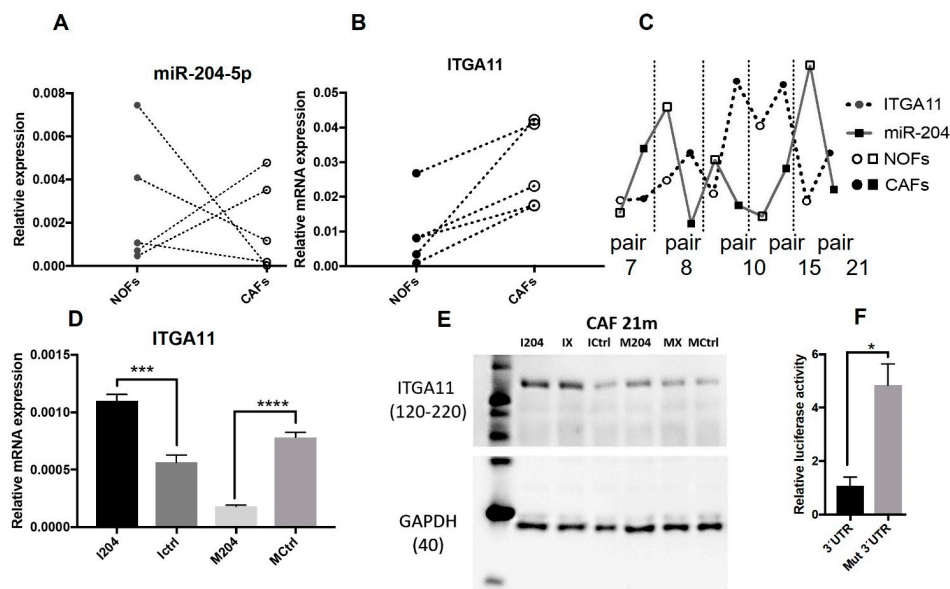


**Figure 2.** ITGA11 and its regulation by miR-204: relative expression of (A) miR-204 and (B) ITGA11 in NOFs compared with matched CAFs (connected by dotted lines), and the corresponding (C) expression correlation between miR-204 and ITGA11. (D) mRNA and (E) protein (Western blot image) regulation of ITGA11 by miR204, 48 h post transfection. (F) Luciferase activity in CAFs in one with miR-204 target site and another with mutated sequence in 3' UTR for ITGA11 in miR target reporter assay (\*  $p < 0.05$ , \*\*\*  $p < 0.0005$ , \*\*\*\*  $p < 0.00005$ , unpaired Student's  $t$ -test,  $n = 4$ ).

When TCGA data on expression of miR-204 in tumor as a whole were analyzed, a statistically significant difference in expression of miR-204 between OSCC lesions and normal human oral mucosa was not observed (Figure 3A). However, statistically significant ( $p < 0.001$ ) down-regulation of miR-204 was observed when OSCC lesions were compared with their matched normal oral mucosa (Figure 3B). Despite statistically insignificant differences among OSCC pathological stages, a trend for decreased expression from stage I to more advanced stages was observed (Figure 3C).

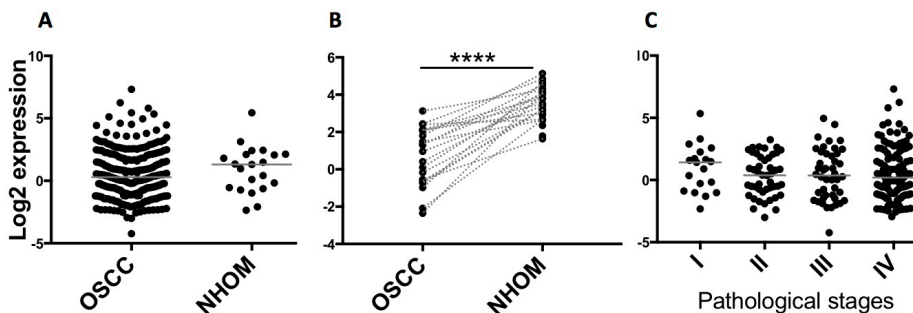


**Figure 3.** Graphs showing expression of miR-204 in OSCC (TCGA data): (A) No significant difference between miR-204 expression in OSCC compared with normal tissues (Mann-Whitney test;  $n = 251$  OSCC,  $n = 21$  NHOM). (B) A significant difference was detected between miR-204 expression in matched OSCC-NHOM cases (paired  $t$ -test;  $n = 20$ , matched cases are linked by a dotted line, \*\*\*\*  $p < 0.00005$ ). (C) No significant difference in miR-204 expression among different OSCC stages (Kruskal-Wallis test showed no significant difference between different stages, although a trend for decreased expression from stage I to more advanced stages could be observed).

### 2.3. *ITGA11* Is a Direct Target of miR-204 in Fibroblasts

The same CAF and NOF strains analyzed here were previously investigated for their transcriptomic differences [19]. mRNA for *ITGA11* was identified as one of the core mRNAs upregulated in CAFs versus NOFs. Prediction of miR targets for *ITGA11* using TargetScan 7.2 showed conserved pairing of miR-204 seed region in the 3' UTR length of *ITGA11* [33]. qRT PCR showed that *ITGA11* transcript was significantly higher in CAFs compared with NOFs in all five fibroblast matched pairs investigated here (Figure 2B). An inverse correlation between expressions of miR-204 and *ITGA11* was observed in three out of five matched fibroblast pairs (ID 8m, 10m, and 21m (Figure 2C)).

Furthermore, increased expression of miR-204 in fibroblasts using mimics resulted in decreased expression of *ITGA11* both at the mRNA (Figure 2D) and protein (Figure 2E) level. On the contrary, inhibition of miR-204 resulted in increased expression of *ITGA11*, both at the mRNA and protein level, pointing also towards a direct regulation of *ITGA11* by miR-204.

Finally, miR target reporter assay confirmed the direct targeting of *ITGA11* by miR-204 in CAFs. Co-transfection of miR-204 mimics and the reporter vector bearing 3' UTR length of *ITGA11* into CAFs resulted in significantly reduced luciferase activity by 77.85%, compared with the control bearing mutation in the miR-204 seed binding motif of 3' UTR length of *ITGA11* (Figure 2F).

### 2.4. miR-204 Modulates the Expression of Several CAF-Related Molecules

Transfection of CAFs with miR-204 mimics induced a significant decrease in mRNA and protein levels of several molecules that are considered to be characteristic of CAF phenotype, such as FAP and TGF $\beta$ -related molecules (TGF $\beta$ 1 and TGFBR2) [37] (Figure 4A–C, Figure S1). Expression levels of mRNA for EGFR were also downregulated, while miR-204 mimics were transfected (Figure 4D). Opposite effects after transfection with miR-204 inhibitors were not observed. In NOFs, a significant effect of miR-204 mimics was observed for TGFBR2 only (Figure 4G), while inhibition of miR-204 led to a significant increase in expression of TGFBR1 and EGFR (Figure 4F,H).



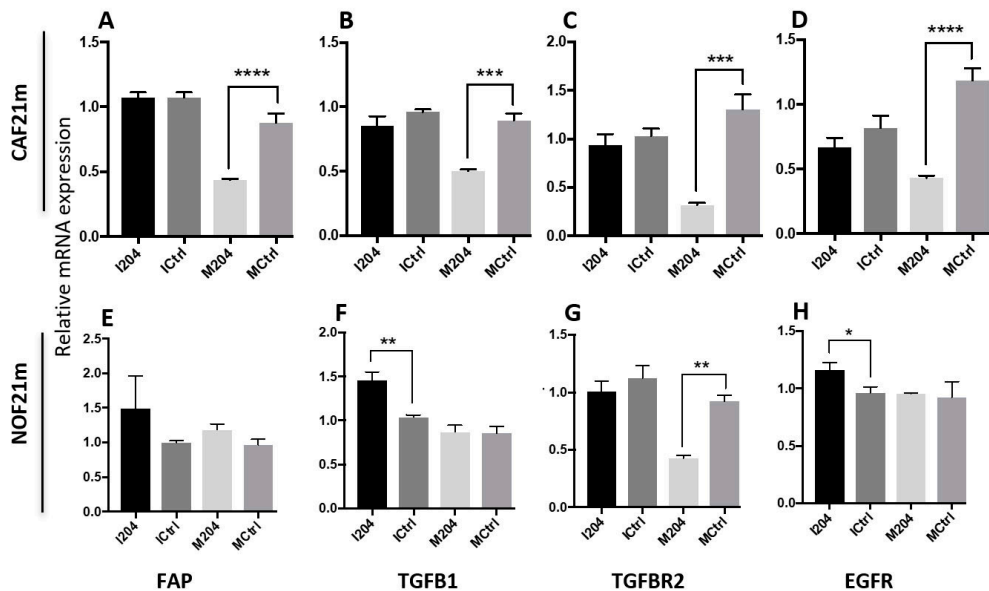


**Figure 4.** Regulation of CAF-related transcripts by miR-204 ( $* p < 0.05$ ,  $** p < 0.005$ ,  $*** p < 0.0005$ , and  $**** p < 0.0001$ , unpaired Student’s *t*-test,  $n = 3$ ). (A,E) FAP expression; (B,F) TGFβ1 expression; (C,G) TGFβ2 expression; and (D,H) EGFR expression in CAF21m and NOF21m respectively.

2.5. miR-204 Decreases Migration and Collagen Contraction Abilities of CAFs

Proliferation of CAFs was not altered on increasing expression of miR-204 using miR mimics (Figure 5A). Migration and collagen contraction are essential attributes of CAFs, proven to be essential for adjacent OSCC cell invasion [20]. Increased expression of miR-204 resulted in decreased migration of CAFs alone (Figure 5B1) or in interaction with OSCC cell line UK1 (Figure 5B2) in 2D monolayer migration assay. Increased expression of miR-204 in the fibroblasts resulted in decreased collagen I gel contraction (Figure 5C).

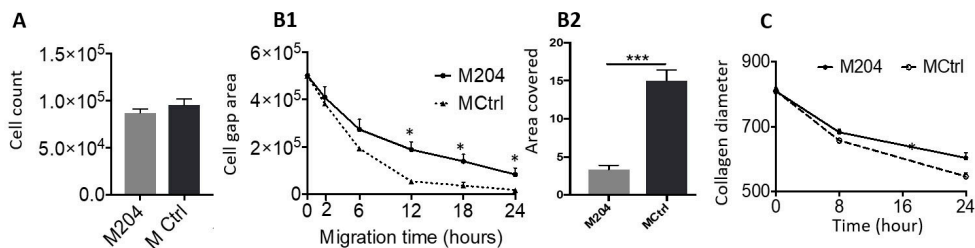


**Figure 5.** Regulation of (A) CAF proliferation, (B1) CAF migration alone, and (B2) in interaction with UK1 and (C) CAF collagen contraction ability post miR-204 transfection ( $n = 6$ ) ( $* p < 0.05$ ,  $*** p < 0.0005$ ).

2.6. Expression of miR-204 in Fibroblasts Inhibits Invasion and Migration of Adjacent OSCC Cells

When co-cultured in 2D monolayers with CAFs treated with miR-204 inhibitors, only minimal effects on migration of OSCC cell line UK1 were observed (Figure 6A). When UK1 were co-cultured with CAFs treated with miR-204 mimics, UK1 cells showed a significant reduction of migration across the gap area towards the CAF region (Figure 6B). In 3D organotypic co-culture models, increased expression of miR-204 in CAFs significantly reduced the depth of invasion by UK1 cells, while inhibitors of miR-204 in NOFs significantly increased the depth of invasion of OSCC cell line Luc4 (Figure 6C,D).

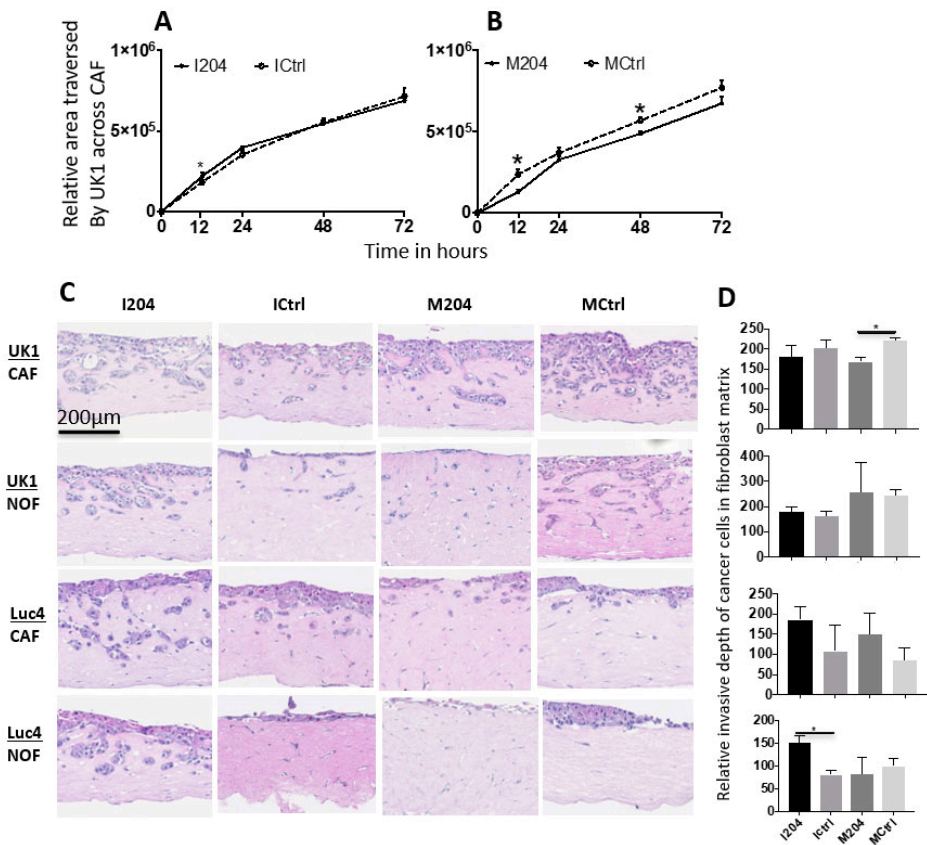


**Figure 6.** (A,B) Graphs showing quantification of the area traversed by UK1 across the gap towards CAFs at different time points from the baseline post miR-204 modulation in CAFs in UK1-CAF monolayer co-culture ( $n = 4$ ). (C) Representative pictures from 3D organotypic cultures showing the invasion by OSCC cell lines UK1 and Luc4 in post miR-204 modulated fibroblasts-populated collagen matrices and (D) the corresponding graphs depicting the quantification of invasion depths ( $n = 4$ , unpaired *t*-test, \*  $p < 0.05$ ).

### 2.7. miR-204 in Fibroblasts Regulates Several Molecules Involved in Cell Migration

Increased miR-204 expression in CAFs significantly decreased the levels of PTK2 (FAK) and ROCK2 transcripts (Figure 7A). Moreover, at the protein level, FAK and its active form, phosphorylated FAK (pFAK), were decreased upon increased miR-204 (Figure 7B,C).

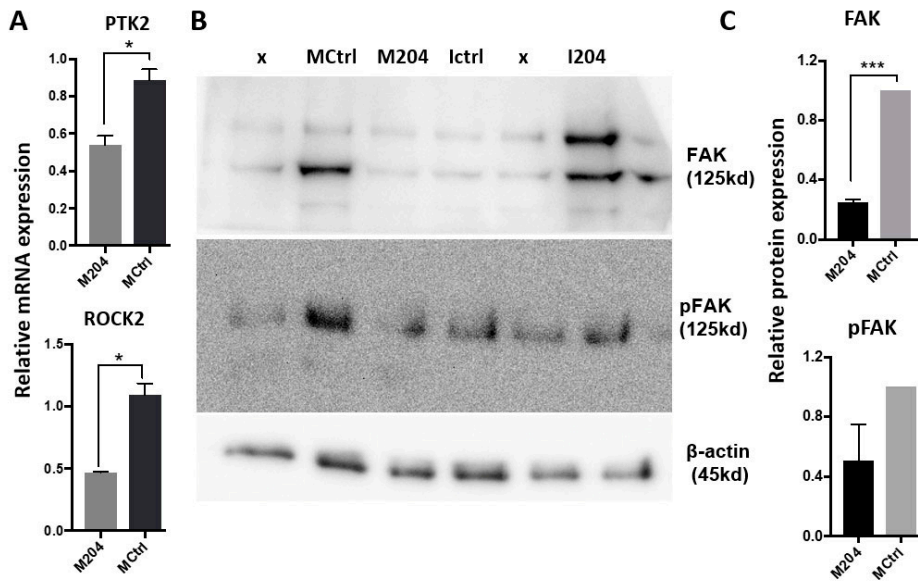


**Figure 7.** Changes in (A) mRNA and (B) protein expression following miR-204 modulation in CAFs. Western blot image (B) and the semi-quantification of protein blots using ImageJ (C) (\*  $p < 0.05$ , \*\*\*  $p < 0.0005$ ).

### 3. Discussion

In this study several miRs were identified to have a differential expression in CAFs compared with NOFs, as demonstrated by the segregation of CAF and NOF strains in two separate clusters by unsupervised clustering analysis of the miRs expression in the miR array. Nevertheless, one of the NOF strains exhibited a miR expression profile similar to CAF strains, and two of the CAF strains displayed a miR expression profile similar to that of NOF strains. We have previously demonstrated CAF heterogeneity at transcriptomic level by gene microarray analysis [19]. The present study points towards CAF heterogeneity regarding miR expression as well. One possible explanation for this variation could be the fact that the fibroblasts used for miR array in this study were primary cells in their early passages, and that these differences most likely reflect the patient-to-patient biological variation and heterogeneity. Nevertheless, there could be other reasons for this heterogeneity such as selection in culture. While miR-204 expression was increased in almost all cases of NOFs isolated from healthy, non-cancer patients compared with the CAFs isolated from OSCC lesions, miR-204 expression was much lower in two of the CAF–NOF pairs, in which NOFs were isolated from the morphologically normal mucosa of OSCC patients. While these differences might point to differences in the biology of miR regulation between NOFs from non-cancer-related and cancer-bearing individuals, the possible alteration of NOFs in OSCC cancer patients cannot be excluded, taking into consideration the field cancerization phenomenon common for the oral mucosa of OSCC patients, in which pre-malignant or even malignant alterations in the apparently normal tissue surrounding the tumor are

quite common [38]. In this line, a study by Ganci F.; et al. showed that miR regulation was different from tumor to peri-tumor region and from peri-tumor to normal surrounding in HNSCC [39]. The tumor cells and tumor microenvironment (TME) co-evolve [26], meaning that transformations in all TME components including fibroblasts take place alongside neoplastic transformation of the epithelium from early stages. Increased heterogeneity of fibroblasts when seeded on plastic as 2D monolayers might as well be related to the selection of certain populations that survive in culture. One then might question the representability of the fibroblasts isolated from the tissues in cell culture for the fibroblast population in that tumor or tissue. Changes in cells' phenotype upon transitioning from tissue to cell culture have also been reported [40], thus use of culture conditions as close as possible to the in vivo situation, such as 3D collagen gels or 3D organotypic co-cultures, is essential.

The major limitation of our study is the use of a limited number of fibroblast strains, although comparable with previously published studies on miRNA array in CAFs versus NOFs. Few other miRNA array studies on pairs of CAFs versus normal fibroblasts (NF) have been previously performed [41–44]. Significantly dysregulated miRNA candidates in CAF in our OSCC study were distinct from those miRNA identified by the previous studies, and this could be attributed to different localization of the cancers from which fibroblasts were isolated. The eight miRNA found significantly downregulated in CAFs in our study, among which was also miR-204, affected TGF $\beta$  signaling, adherens junction, and proteoglycans in cancer pathways among other pathways significantly affected by them, as shown by KEGG pathway analysis by Diana MirPath v.3 using a database of experimentally supported miRNA–gene interactions: TarBase v.7 and [45]. Among the pathways significantly affected by the four miRNAs found to be upregulated in CAFs versus NOFs in our study were p53 signaling, cell cycle, and proteoglycans in cancer pathways.

For validation on different data sets, we first explored GEO datasets on miR-expression in CAFs versus NOFs in different cancers. We identified three studies that had compared miRNA expression in CAFs versus NOFs. With GEO2R analysis, we did not match any significantly deregulated miRNA candidates identified in our OSCC study with those in prostate CAFs ( $n = 3$ ) versus NOFs ( $n = 3$ ) (GSE68166; GPL10558). Another dataset (GSE97545) in lung cancer could not be analyzed. The data from the third published study on miRNA array in CAFs versus NOFs in OSCC were not made publicly available, so we could not investigate that dataset either [43]. Therefore, we sought next to explore the expression of the miR, thus we further focused our attention in this study on miR-204, in OSCC versus normal oral mucosa in the TCGA database. In spite of the fact that TCGA miRNA data were derived from the whole OSCC tissues, a decrease in miR-204 expression in OSCC compared with normal tissues (statistically significant for matched, paired lesions) was observed, which is in line with the decreased miR-204 in CAFs compared with NOFs observed in our study.

Among the twelve dysregulated miRNA identified in our study, we focused further on miR-204 in functional and molecular assays owing to a possible link that we found in silico between this particular miRNA and integrin alpha11, which has been identified as one of the top genes significantly up-regulated in CAFs derived from OSCC in our previous transcriptomic study [19]. Supportive of our choice was also the fact that earlier studies have suggested tumor-suppressive functions by miR-204, as described in the Introduction. Reduced expression of miR-204 in cancers, likening or leading to aggressiveness and metastasis of cancer cells, was previously reported. We have previously investigated miR204 expression and its correlation with clinical-pathological parameters and survival in a cohort of 169 HPV-negative OSCC patient cohort [36]. Data from that cohort showed a correlation between the expression of miR-204 in tumor center and the degree of differentiation, namely higher miR-204 expression in well-differentiated OSCC lesions. However, we could not find any correlation between the differentiation degree of the OSCC lesions from which the CAFs were derived and the expression of miR204 in the isolated CAFs, probably owing to the heterogeneity of the CAFs within a tumor or because of the low number of cases in which we isolated CAFs for analysis in the present study.

However, it was previously unknown how miR regulation in CAFs in general, and miR-204 expression in particular, can modulate the tumor promoting function by CAFs. In order to identify the role of miR-204 in CAFs, CAFs and respective matched NOFs from two OSCC patients were miR-204 modulated and used to populate the collagen matrix of a 3D organotypic model in which OSCC cells could be tested for their invasive potential. Increasing miR-204 expression in CAFs suppressed OSCC cell invasion. On the contrary, when miR-204 expression was inhibited in paired NOFs, invasion of OSCC cells increased significantly. These findings, coupled with the decreased collagen contraction and migration of CAFs when treated with miR204 mimics, indicate a tumor suppressive role of miR-204 expression in CAFs in OSCC by affecting fibroblast motility [20].

Our previous work on transcriptomic analysis of the same CAF and NOF strains showed upregulation of ITGA11 in CAF derived from OSCC lesions [19]. Moreover, we described a correlation with a CAF phenotype for CAFs expressing high levels of ITGA11 [24] and a tumor-promoting role of ITGA11 when expressed in CAFs [46]; integrin  $\alpha 11$  is a collagen I receptor, and it has been involved in cell motility [47]. In this study, integrin  $\alpha 11$  expression was increased in CAF compared with NOF strains in all five matched pairs, confirming the previous results on non-matched CAFs and NOFs [19]. miR target prediction analysis showed that ITGA11 contains a target site for miR-204. Therefore, we performed luciferase miR target reporter assay and demonstrated that, indeed, ITGA11 is directly targeted by miR-204, affecting ITGA11 expression at both transcript and protein levels. Together with our data on miR-204 affecting fibroblast cell motility, this suggests that the tumor suppressive effect of miR-204 is mediated via ITGA11. Nevertheless, miR-204 is only one of the several miRs that regulate ITGA11. In addition, miR-204 has also been documented to affect other molecules and pathways of cancer. In this line, we show in this study that several other CAF-related molecules were modulated by miR-204, endorsing also a more complex role of miR-204 in regulating the CAF phenotype than only through ITGA11.

Our molecular analysis targeted towards motility-related molecules showed that modulation of miR-204 expression significantly altered, in addition to ITGA11, the mRNA levels of FAK and ROCK2, two other molecules playing an important role in cell motility and CAF motile phenotype. FAK has been shown to be involved in actin filaments-based protrusions, named filopodia via polymerization and bundling of linear actin filaments within fan like lamellipodia, and thereby affecting cell adhesion and motility [48]. FAK may be activated by integrins, receptor tyrosine kinases (RTKs), mechanical stimuli, cytokine and G-protein coupled receptors (GPCRs), and changes of intracellular pH (H<sup>+</sup>) [48]. This study adds one more level of complexity in the regulation of FAK, showing that, in addition to post-translational modifications, expression of FAK transcripts and total FAK protein levels are regulated by miR-204. ROCK2 is another oncoprotein that controls cytoskeleton organization and cell motility. ROCK2 overexpression has been reported in OSCC-CAF and it has been shown to have a prognostic value for OSCC and to be associated with CAF density [49]. Our current findings that miR-204 targets several motility-related molecules corroborate well with our functional results showing that miR-204 alters the motility of fibroblasts, and are in line with previous observations of miR-204 affecting cell motility, although this has been shown previously in cancer cells only [50]. Furthermore, the alterations in CAF motility observed when miR-204 mimics were used were followed by impaired OSCC cell invasion, in line with the previous studies pointing to the essential role of CAF motility for fibroblast-led collective OSCC cell invasion [20]. This is an intricate mechanism suggesting a tumor-suppressive role for miR-204 through regulation of CAF motility via restriction of several motility-related molecules and direct regulation of the collagen receptor integrin  $\alpha 11$ .

## 4. Materials and Methods

### 4.1. Patient Material

CAFs were isolated from biopsies of OSCC primary lesions of patients ( $n = 13$ ) diagnosed at Haukeland University Hospital, Bergen, Norway, prior to any treatment. Matched normal oral fibroblasts (NOFs) were also isolated from biopsies taken from morphologically cancer-free regions of oral mucosa of five of the OSCC patients ( $n = 5$ ) (Supplementary Table S1). Tissues from the patients who underwent neoadjuvant therapy and/or later were confirmed HPV-positive were not included in the study. NOFs from biopsies of normal oral mucosa of healthy, cancer-free volunteers ( $n = 9$ ) were also obtained. Outliers, one each from the CAF and NOF groups, were removed in miR-microarray data analysis. Written consent was obtained from both OSCC patients and healthy donors. Tissues were collected in Dulbecco's modified Eagle's medium (DMEM; D6429, Sigma), supplemented with 2% antibiotic-antimycotic (AB/AM; 100 U/mL penicillin, 100 µg/mL Streptomycin, and 25 ng/mL Amphotericin B; all from Invitrogen, Waltham, MA, USA). Ethical approval was obtained from the regional ethical committee in Norway (West Norway; REKVest 3.2006.2620, REKVest 3.2006.1341).

### 4.2. Fibroblast Isolation and Cell Culture

Tissues collected were thoroughly washed in the collecting medium. Bleeding and necrotic areas of the tissues were removed using a sterile scalpel and washed thoroughly again. Tissues were cut into approximately 2–4 mm<sup>3</sup> bits, and then placed on 6 cm culture dish. Tissue bits (explants) were slightly air-dried (approximately 1–2 min) to facilitate explants to attach on the surface of the dish. Thereafter, explants were carefully covered with complete growth medium, DMEM with 10% heat inactivated newborn calf serum (NBCS; 31765068, Gibco, Amarillo, TX, USA) supplemented with 1% AB/AM. The culture dishes were then incubated in a growth chamber maintained at 37 °C and 5% CO<sub>2</sub>. Few days later, cells with epithelial morphology that grew from the explant were scrapped off under a microscope using pipette tips. Alternatively, cells with fibroblast morphology were trypsin selected (trypsin detached fibroblasts earlier compared with epithelial cells; 1–2 min vs. 4–7 min). CAFs and NOFs obtained were further propagated in complete DMEM medium without AB/AM. All functional assays were performed in matched fibroblast pair 21.

OSCC cell lines UK1 [51] and Luc4 [52] were grown in DMEM/Nutrient Mixture F-12 Ham (DMEM/F12; D8437, Sigma, St. Gallen, Switzerland), supplemented with 10% NBCS, 0.4 µg/mL hydrocortisone (H0888, Sigma), 1 × Insulin–Transferrin–Selenium (41400-04, Thermofisher Scientific), 50 µg/mL L-ascorbic acid (A7631, Sigma), and 10 ng/mL epidermal growth factor (E9644, Sigma).

### 4.3. Total RNA Isolation and Small RNA Enrichment for miR Microarray

RNA was isolated using miRVana RNA extraction kit (AM1561, Thermo Fisher Scientific, Dreieich, Germany) following the manufacturer's protocol. In brief, sub-confluent cell cultures were washed with tepid phosphate buffered saline (PBS), lysed with lysis/binding buffer and phenol/chloroform was extracted. For total RNA isolation, the aqueous phase with RNA from phenol/chloroform extraction was treated with 1.25 volume of 100% ethanol. RNA was then captured in glass fiber filter cartridge and collected in 100 µL of preheated (95 °C) nuclease free elution solution (0.1 mM EDTA).

For the enrichment of small RNAs (~200 nucleotides and less) for miR microarray, 50 µg of total RNA was mixed with five volumes of lysis/binding buffer. To the RNA mixture was added 1/10 volume of homogenate additive, after which it was mixed well and left on ice for 10 min. The RNA mixture was then mixed thoroughly with 1/3 volume of 100% ethanol to allow capture of larger RNA in the filter cartridge. The filtrate with small RNAs was collected, 2/3 volume of 100% ethanol was added, and it was passed through a new filter cartridge. The cartridge was washed with Wash Solutions and, finally, small RNA was collected in elution solution.

The purity and quantity of the isolated RNAs were measured using NanoDrop® ND-1000 Spectrophotometer and ND-1000 V3.5.2 software (Nanodrop Technologies, Wilmington, DE, USA). RNA was quantified using the principle that an absorbance reading of 1 at 260 nm wavelength is equivalent to 40 µg/mL of RNA. The blank measurement was made with 1 µL of elution buffer; 1 µL of the RNA samples were pipetted on the measurement pedestal and the absorbance was taken at 260 nm, 280 nm, and 230 nm wavelength. Purity was assessed assuming that the pure RNA has an A260/A280 of 2.1 and A260/A230 of 2. Isolated RNAs were stored at −80 °C.

#### 4.4. miR Microarray

CAFs and NOFs at early passages ( $p < 5$ ) were grown in 3D in collagen gels (rat tail, BD Biosciences, Franklin Lakes, NJ, USA) containing DMEM, NBCS, and reconstitution buffer (2.2g NaHCO<sub>3</sub> + 0.6 g NaOH + 4.766 mL HEPES in 100 mL double distilled water H<sub>2</sub>O) at a volume ratio of 7:1:1:1, respectively, at the concentration of  $4 \times 10^5$  cells/mL. After 5 days in 3D culture, cells were harvested. Then, 100 ng of enriched small RNAs isolated from the cells was converted cDNA and fed into Illumina microarray version 2 panel with miR-specific oligos. The samples were profiled for 1146 human miRs expression (>97% coverage from miRBase release 12). Using J-Express [31,53], the data file from miR microarray was normalized; outliers; one each from CAFs and NOFs were removed; and, with significant analysis of microarray (SAM), significantly differentially expressed miRs in between CAFs and NOFs were identified. The differentially regulated miRs were further validated by miR specific reverse transcription (Applied Biosystems, Waltham, MS, USA) and quantitative real time PCR (qRT-PCR) using Taqman assays (Supplementary Table S2).

#### 4.5. Reverse Transcription

For miR quantification, miRs specific primers were used to synthesize specific miR cDNAs (TaqMan MicroRNA Reverse Transcriptase kit, Applied Biosystems). In brief, 10 ng of total RNA was mixed with miR specific primer, dNTPs, reverse transcription buffer, RNase inhibitor, and reverse transcriptase to the final reaction mixture volume of 15 µL. The reaction mixture was then subjected to a thermal cycle of 16 °C for 30 min, 42 °C for 30 min, and 85 °C for 5 min in Mastercycler Gradient thermal cycler (Eppendorf).

For mRNA quantification, reverse transcription of total RNA into cDNA was carried using Taqman Reverse Transcription kit (Applied Biosystems). In brief, 100 ng of RNA was mixed with reverse transcription buffer, random hexamers, MgCl<sub>2</sub>, dNTPs, RNase inhibitor, and reverse transcriptase and adjusted to a final volume of 25 µL with RNase free water. The reaction mixture was subjected heated at 20 °C for 10 min, 48 °C for 30 min, and 90 °C for 5 min.

#### 4.6. Quantitative Real-Time Polymerase Chain Reaction (qRT-PCR)

miRs and mRNAs were quantified by qRT-PCR using Taqman Gene Expression assays in ABI Prism 7900 HT sequence detector system (Applied Biosystems). In 384-well reaction plates (Thermo Fisher Scientific), PCR reaction volume of 10 µL in each well was prepared by mixing 1 µL of cDNA with 1 µL Taqman assay, 5 µL Universal Master Mix, and 3 µL RNase free water. The plate was then run at 50 °C for 2 min, 95 °C for 10 min, and 40 cycles of 95 °C for 15 s and 60 °C for 1 min. Each sample was run in triplicate. A threshold cycle of mRNA obtained was normalized to endogenous controls GAPDH. GAPDH was further verified with 18S and RPL13A. miR expression was normalized to RNU48. Relative expressions were calculated using the  $2^{-\Delta\Delta Ct}$  method.

#### 4.7. TCGA Data Analysis

TCGA data on miR-204 expression in head and neck squamous cell carcinoma (HNSCC) and normal oral tissues and the associated clinical data were obtained from Firebrowse database version 2016\_01\_28 (<http://www.firebrowse.org>; accessed on 30 April 2020). HPV-positive cases, non-oral cancer cases, and cases with history of neoadjuvant

therapy were excluded from the cohort. Therefore 251 OSCC and 21 normal oral cases remained after exclusion. Of 21 cases with normal mucosa, data for 20 matched OSCC cases were available.

#### 4.8. miR Target Identification and miR Dual Luciferase Target Reporter Assay

miR target prediction by miR target prediction softwares TargetScan Release 7:1 [54], miRmap [55] and miRDB [56] showed target conserved sites for several miRs in the 3' UTR of ITGA11. Of the three, TargetScan and miRmap predicted target site for miR-204 in the 3' UTR of ITGA11 (3' UTR ITGA11 sequence: 5' GGCTCCAGAGGAGACTTTGAGTTGATG GGGGCCAGACACCAGTCCAGGTAGTGTGAGACCCAGGCCTGTGGCCCCACCGA GCTGGAGCGGAGAGGAAGCCAGCTGGCTTGCACCTTACCTCATCTCCCGAGCAAT GGGCCTGCTCCCTCCAGAATGGAAGTCAAGCTGGTTTAAAGTGGAACTGCCCTAC TGGGAGACTGGGACACCTTTAACACAGACCCCTAGGGATTAAAGGGACACCCCT AACACACCCAGGCCATGCCAAGGCCTCCCTCAGGCTCTGTG 3'). 3'UTR sequence of ITGA11 (NM 001004439.2) with miR-204 binding site was retrieved from UCSC genome browser (<http://genome.ucsc.edu>, accessed on 17 November 2019) [57], and a plasmid vector with luciferase upstream of 3'UTR and renilla as a transfection control under different promoters were designed using VectorBuilder. Non-complimentary mutant sequence was introduced to the miR-204 binding site (236–242 AAAGGGA → ATTCCCT) on 3'UTR of ITGA11 as control. Both vectors were purchased from VectorBuilder. Reduction in luciferase signal normalized to renilla signal compared with mutant control after miR-204 mimics transfection into the cells indicates direct targeting of ITGA11 by miR-204. Luciferase and renilla activity was measured using Dual-Luciferase Reporter Assay (Promega; E1910) following the manufacturer's protocol using a luminometer. In brief,  $5 \times 10^4$  CAFs in each well in 24-well plates were reverse co-transfected with 250 ng of plasmid DNA and miR-204 mimic at a 50 nM concentration in complete DMEM medium using Lipofectamine™ 3000 Transfection Reagent. Then, 48 h after transfection, growth media from cultured cells were removed and washed with PBS solution. Thereafter, the cells were lysed with 100  $\mu$ L of 1X lysis buffer. The cell culture plate was gently rocked for about 15 min to allow cells to lyse completely. Then, 20  $\mu$ L of cell lysates were pipetted into the wells in 96-well plates and dispensed with 100  $\mu$ L of luciferase substrate. Immediately, luciferase activity was read using a Tecan Infinite M200PRO luminometer. The wells were again dispensed with 100  $\mu$ L of 1X Stop & Glo reagent and renilla luciferase activity was read.

#### 4.9. miR-204 Modulation in Cultured Fibroblasts

Fibroblasts were reverse transfected using Lipofectamine™ 3000 Transfection Reagent (L3000015; Invitrogen) with a mimic (C-300563-05, Dharmacon, Lafayette, CO, USA), an inhibitor (IH-300563-07, Dharmacon), and the respective controls (CN-001000-01, IN00105-01-05, Dharmacon) of miR-204-5p at 50 nM concentration in the growth medium. Cells were harvested for RNA or protein extraction or subjected to further experiments after 48 h of transfection. Transfection of miR-204 mimic induced a significant increase in miR-204 levels in both CAF and NOF strains (Supplementary Figure S1), while transfection of miR-204 inhibitor did not induce a significant change in the miR-204 levels in cultured fibroblasts (Supplementary Figure S2).

#### 4.10. Protein Isolation and Quantification

The cell cultures were washed twice with ice cold PBS buffer, lysed with ice cold RIPA lysis and extraction buffer (89901, Thermo Fisher Scientific), supplemented with  $1 \times$  Halt Protease and Phosphatase Inhibitor (78442, Thermo Fisher Scientific), and scrapped using sterile scrapers. The lysates were then collected in ice-cold Eppendorf tubes and centrifuged at 14,000 rpm for 15 min. Protein supernatants were aliquoted in new Eppendorf tubes and stored at  $-80$  °C until use.

Total protein in the lysates was measured by DC protein assay (5000111, BioRad, Hercules, CA, USA) in a 96-well microplate, using the manufacturer's protocol. In brief,



20  $\mu\text{L}$  of reagent S was mixed with 1 mL of reagent A to give a working reagent A'. Then, 1.5  $\mu\text{g}/\text{mL}$  of BSA was diluted in twofold to use as standards. Five microlitres of protein samples and standards were then pipetted into a microtiter plate, and 25  $\mu\text{L}$  of reagent A' and 200  $\mu\text{L}$  of reagent B were added. The plate was gently agitated to mix the reagents, incubated at room temperature for 15 min, and the optical density was measured at 750 nm wavelength using (BIO-TEKR). All the samples were measured in triplicates, and blanks were included.

#### 4.11. Western Blotting

Fifteen micrograms of protein were mixed with 4 $\times$  NuPAGE LDS sample buffer (NP0007, Invitrogen) and 10 $\times$  NuPAGE sample reducing agent (NP0004, Invitrogen) to the final concentration of 1 $\times$ . The protein mixture was heated at 95  $^{\circ}\text{C}$  for 5 min and run on NuPAGE Novex 10% Bis-Tris Protein Gel (NP0303, Invitrogen) in 1 $\times$  NuPAGE MOPS SDS Running Buffer (NP0001, Invitrogen) at 160 Volt for 90 min. Then, 500  $\mu\text{L}$  of NuPAGE Antioxidant (NP0005) was added in the upper chamber immediately before applying the voltage. Precision Plus Protein Dual Color Standard (1610374, Biorad) was used as a protein weight marker. The resolved protein in the gel was then blotted into methanol activated (for 1 min) Amersham Hybond P 0,45 PVDF membrane (10600069, GE Healthcare, Chicago, IL, USA) using filter paper sandwich in 1 $\times$  NuPAGE transfer buffer (NP0006, Invitrogen) with 10% methanol and 0.2% Antioxidant at 40 Volt for 1 h. Then, 200  $\mu\text{L}$  of antioxidant was added in the upper chamber immediately before applying the voltage.

After completion of the blotting, PVDF membrane was blocked with 5% dry milk or 3% BSA prepared in 1 $\times$  Pierce TBS Tween 20 Buffer for 30 min. The PVDF membrane was then incubated with primary antibody in 5% non-fat dry milk or 3% BSA for overnight at 4  $^{\circ}\text{C}$ . Thereafter, the membrane blot was washed with TBS-Tween three times for 10 min each and incubated with secondary antibody for one hour at room temperature (anti-rabbit from Cell Signalling, #7074, and anti-mouse from Cell Signalling, #7076). The membrane was then washed with TBS-Tween four times for 10 min each and, finally, visualized using SuperSignal West Pico Chemiluminescent Substrate (34080, ThermoFisher) in Image Reader LAS 1000 (Fujifilm). Relative protein amounts in each protein bands in the captured images were quantified using ImageJ using Gel commands. Antibodies used for Western blotting are listed in Supplementary Table S3.

#### 4.12. Migration Assay (2D Co-Culture)

Two-well silicone inserts (80209, ibidi) were placed in the center of 24-well plates. Fibroblasts or OSCC cells ( $2 \times 10^4$  cells) were plated, and reverse transfected with miR mimics and inhibitors) into each well. Silicone inserts were removed 48 h post-transfection to create a uniform cell-free gap of 50  $\mu\text{m}$  between the edges of two cell-rich zones. The wells were then imaged at two-hour time interval using IncuCyte Zoom using a 4 $\times$  objective (EssenBioScience, Ann Arbor, MI, USA). The cell-free unoccupied area was measured using MRI Wound Healing Tool in ImageJ.

#### 4.13. Collagen Contraction Assay

Ninety-six-well plates were blocked overnight with 2% BSA in PBS in 37  $^{\circ}\text{C}$  incubation chamber. Forty-eight hours post-miR modulations, fibroblasts at  $5 \times 10^5/\text{mL}$  density were uniformly suspended in collagen type I matrix, as described above. Subsequently, 100  $\mu\text{L}$  of collagen cell suspension was added into each well and allowed to gel for 90 min. The gels were then floated with 100  $\mu\text{L}$  of DMEM medium, and the change in gel dimensions was measured at different time points.

#### 4.14. 3D Organotypic Co-Cultures

Fibroblasts at a density of  $5 \times 10^5$  cells/mL were re-suspended in collagen type I (rat tail, 354239, BD Biosciences, Franklin Lakes, NJ, USA) matrix, and uniformly mixed with DMEM, NBCS, and sterile reconstitution buffer in the volume ratio of 7:1:1:1, respectively.

Then, 700  $\mu$ L of the collagen cell suspension was dispensed into each well in 24-well plates and allowed to gel in a humidified incubator at 37 °C. After two hours, the gels were added to 1 mL of fibroblast growth medium to allow the cells to grow until next day. The next day,  $5 \times 10^5$  OSCC cells were added on the top of each fibroblast gel. Another day, the gels were transferred on the metal grids layered with a filter paper. Organotypic growth medium (DMEM and Ham's F12 Nutrient mixture (31765068, Thermo Fisher Scientific) in ratio 1:3, and supplemented with Insulin-Transferrin-Selenium, hydrocortisone, and L-ascorbic acid, as mentioned above, and NBCS replaced with 0.1% Bovine Albumin Fraction (V15260-037, Thermo Fisher Scientific)) was added to reach the level of filter paper to allow gels to grow at the air–medium interface. Medium was changed at each alternative day. Ten days after culture on grid, gels were fixed overnight in 4% buffered formalin and embedded in paraffin.

#### 4.15. Quantification of Invasion of OSCC Cells in 3D-Organotypic Models

Tissue gels embedded in paraffin blocks were cut into 5  $\mu$ m sections and stained with hematoxylin and eosin. Invasion depth of OSCC cells in the stained organotypic sections was measured using NDP.view2 (Hamamatsu, Naka Ward, Sunayamacho, Japan). Invasion depth was measured as the vertical distance of invaded cancer cells from the reconstructed basement membrane (horizontal line along the non-invading cells). Twenty measurements at each 50  $\mu$ m distance along the tissue were taken and averaged. Non-uniform thick, curved, or tapered ends of the 3D organotypic tissues as a result of differential contraction by the fibroblasts were excluded in the analysis.

#### 4.16. Statistical Analysis

SAM analysis was performed to detect differentially regulated miRNAs using J-Express (University of Bergen, Norway), a freely available software for analyzing microarray gene expression data [58]. Differentially expressed miRs with false discovery rate (FDR) = 0 were considered to be significantly modulated miRs. For functional assays, and miR, mRNA, or protein expressions data, paired and unpaired *t*-tests were applied to find the significant difference in means ( $p < 0.05$ ). For non-normally distributed data (D'Augustino & Pearson test;  $p > 0.05$ ), non-parametric comparisons (Mann–Whitney for unpaired comparison between two, and Kruskal–Wallis for unpaired comparison among groups) were carried out to find significant differences in median expression. Parametric and non-parametric analyses were carried out as required using GraphPad Prism 7 (GraphPad, San Diego, CA, USA).

## 5. Conclusions

This study demonstrates for the first time miR dysregulation in OSCC-derived CAFs compared with NOFs and identifies twelve differentially expressed miR in CAFs isolated from OSCC lesions compared with fibroblasts isolated from normal mucosa. One of the dysregulated miRs, miR-204, was further investigated, and we show here for the first time that miR-204 directly targets the ITGA11, and that its tumor-suppressive function is mediated via alteration of CAF motility through regulating several other motility-related molecules in addition to ITGA11.

**Supplementary Materials:** The following are available online at <https://www.mdpi.com/article/10.3390/ijms222111960/s1>.

**Author Contributions:** Conceptualization, S.R., A.M., H.P., S.L., E.N., O.K.V., A.C.J., D.S. and D.E.C.; data curation, S.R.; formal analysis, S.R. and D.S.; funding acquisition, D.E.C.; investigation, S.R., H.P., K.C.D., B.L., K.M.H., A.K., S.L. and E.N.; methodology, S.R., A.M., H.P., K.C.D. and D.S.; project administration, A.C.J., D.S. and D.E.C.; supervision, O.K.V., A.C.J., D.S. and D.E.C.; validation, S.R.; visualization, S.R.; writing—original draft, S.R.; writing—review & editing, S.R., A.M., H.P., K.C.D., B.L., K.M.H., A.K., S.L., E.N., O.K.V., A.C.J., D.S. and D.E.C. All authors have read and agreed to the published version of the manuscript.

**Funding:** This work was supported by the Research Council of Norway through its Centers of Excellence funding scheme (Grant No. 22325), The Western Norway Regional Health Authority (Helse Vest Grant No. 911902/2013 and 912260/2019), and The Norwegian Centre for International Cooperation in Education (project number CPEA-LT-2016/10106).

**Institutional Review Board Statement:** Ethical approval was obtained from the regional ethical committee in Norway (West Norway; REKVest 3.2006.2620, REKVest 3.2006.1341).

**Informed Consent Statement:** Informed consent was obtained from all subjects involved in the study.

**Data Availability Statement:** The datasets for this study are available here. GEO accession GSE172287: Go to <https://www.ncbi.nlm.nih.gov/geo/query/acc.cgi?acc=GSE172287>.

**Acknowledgments:** We are thankful to Hans-Richard Brattbakk from the Genomics Core Facility, Faculty of Medicine, University of Bergen for the help on analysis of miRNA-microarray data.

**Conflicts of Interest:** The authors declare no conflict of interest.

## References

1. Ferlay, J.; Colombet, M.; Soerjomataram, I.; Mathers, C.; Parkin, D.; Piñeros, M.; Znaor, A.; Bray, F. Estimating the global cancer incidence and mortality in 2018: GLOBOCAN sources and methods. *Int. J. Cancer* **2019**, *144*, 1941–1953. [[CrossRef](#)] [[PubMed](#)]
2. Du, M.; Nair, R.; Jamieson, L.; Liu, Z.; Bi, P. Incidence Trends of Lip, Oral Cavity, and Pharyngeal Cancers: Global Burden of Disease 1990–2017. *J. Dent. Res.* **2020**, *99*, 143–151. [[CrossRef](#)] [[PubMed](#)]
3. Dobrossy, L. Epidemiology of head and neck cancer: Magnitude of the problem. *Cancer Metastasis Rev.* **2005**, *24*, 9–17. [[CrossRef](#)] [[PubMed](#)]
4. Karnov, K.K.S.; Grønhoj, C.; Jensen, D.H.; Wessel, I.; Charabi, B.W.; Specht, L.; Kjaer, A.; von Buchwald, C. Increasing incidence and survival in oral cancer: A nationwide Danish study from 1980 to 2014. *Acta Oncol.* **2017**, *56*, 1204–1209. [[CrossRef](#)]
5. Bennardo, L.; Bennardo, F.; Giudice, A.; Passante, M.; Dastoli, S.; Morrone, P.; Provenzano, E.; Patruno, C.; Nisticò, S. Local Chemotherapy as an Adjuvant Treatment in Unresectable Squamous Cell Carcinoma: What Do We Know So Far? *Curr. Oncol.* **2021**, *28*, 2317–2325. [[CrossRef](#)]
6. Pentangelo, G.; Nisticò, S.; Provenzano, E.; Cisale, G.; Bennardo, L. Topical 5% imiquimod sequential to surgery for HPV-related squamous cell carcinoma of the lip. *Medicina* **2021**, *57*, 563. [[CrossRef](#)] [[PubMed](#)]
7. Malik, U.U.; Zarina, S.; Pennington, S.R. Oral squamous cell carcinoma: Key clinical questions, biomarker discovery, and the role of proteomics. *Arch. Oral Biol.* **2016**, *63*, 53–65. [[CrossRef](#)]
8. Ragin, C.C.R.; Taioli, E. Survival of squamous cell carcinoma of the head and neck in relation to human papillomavirus infection: Review and meta-analysis. *Int. J. Cancer* **2007**, *121*, 1813–1820. [[CrossRef](#)] [[PubMed](#)]
9. Lee, R.C.; Feinbaum, R.L.; Ambros, V. The *C. elegans* heterochronic gene lin-4 encodes small RNAs with antisense complementarity to lin-14. *Cell* **1993**, *75*, 843–854. [[CrossRef](#)]
10. Wightman, B.; Ha, I.; Ruvkun, G. Posttranscriptional regulation of the heterochronic gene lin-14 by lin-4 mediates temporal pattern formation in *C. elegans*. *Cell* **1993**, *75*, 855–862. [[CrossRef](#)]
11. Lee, R.C.; Ambros, V. An Extensive Class of Small RNAs in *Caenorhabditis elegans*. *Science* **2001**, *294*, 862–864. [[CrossRef](#)] [[PubMed](#)]
12. Bartel, D.P. MicroRNAs: Genomics, Biogenesis, Mechanism, and Function. *Cell* **2004**, *116*, 281–297. [[CrossRef](#)]
13. Zhang, B.H.; Pan, X.P.; Cobb, G.P.; Anderson, T.A. microRNAs as oncogenes and tumor suppressors. *Dev. Biol.* **2007**, *302*, 1–12. [[CrossRef](#)]
14. Min, A.; Zhu, C.; Peng, S.; Rajthala, S.; Costea, D.E.; Sapkota, D. MicroRNAs as Important Players and Biomarkers in Oral Carcinogenesis. *Biomed. Res. Int.* **2015**, *2015*, 186904. [[CrossRef](#)] [[PubMed](#)]
15. Tran, N.; O'Brien, C.J.; Clark, J.; Rose, B. Potential Role of Micro-Rnas in Head and Neck Tumorigenesis. *Head Neck J. Sci. Spec. Head Neck* **2010**, *32*, 1099–1111. [[CrossRef](#)] [[PubMed](#)]
16. Sethi, N.; Wright, A.; Wood, H.; Rabbitts, P. MicroRNAs and head and neck cancer: Reviewing the first decade of research. *Eur. J. Cancer* **2014**, *50*, 2619–2635. [[CrossRef](#)]
17. Fidler, I.J. Timeline-The pathogenesis of cancer metastasis: The 'seed and soil' hypothesis revisited. *Nat. Rev. Cancer* **2003**, *3*, 453–458. [[CrossRef](#)] [[PubMed](#)]
18. Hanahan, D.; Weinberg, R.A. Hallmarks of cancer: The next generation. *Cell* **2011**, *144*, 646–674. [[CrossRef](#)] [[PubMed](#)]
19. Costea, D.E.; Hills, A.; Osman, A.H.; Thurlow, J.; Kalna, G.; Huang, X.; Pena Murillo, C.; Parajuli, H.; Suliman, S.; Kulasekara, K.K.; et al. Identification of two distinct carcinoma-associated fibroblast subtypes with differential tumor-promoting abilities in oral squamous cell carcinoma. *Cancer Res.* **2013**, *73*, 3888–3901. [[CrossRef](#)]
20. Gaggioli, C.; Hooper, S.; Hidalgo-Carcedo, C.; Grosse, R.; Marshall, J.F.; Harrington, K.; Sahai, E. Fibroblast-led collective invasion of carcinoma cells with differing roles for RhoGTPases in leading and following cells. *Nat. Cell Biol.* **2007**, *9*, 1392–1400. [[CrossRef](#)] [[PubMed](#)]
21. Daly, A.J.; McIlreavey, L.; Irwin, C.R. Regulation of HGF and SDF-1 expression by oral fibroblasts-Implications for invasion of oral cancer. *Oral Oncol.* **2008**, *44*, 646–651. [[CrossRef](#)]

22. Kawashiri, S.; Tanaka, A.; Noguchi, N.; Hase, T.; Nakaya, H.; Ohara, T.; Kato, K.; Yamamoto, E. Significance of stromal desmoplasia and myofibroblast appearance at the invasive front in squamous cell carcinoma of the oral cavity. *Head Neck J. Sci. Spec. Head Neck* **2009**, *31*, 1346–1353. [[CrossRef](#)] [[PubMed](#)]
23. Kellermann, M.G.; Sobral, L.M.; da Silva, S.D.; Zecchin, K.G.; Graner, E.; Lopes, M.A.; Nishimoto, I.; Kowalski, L.P.; Coletta, R.D. Myofibroblasts in the stroma of oral squamous cell carcinoma are associated with poor prognosis. *Histopathology* **2007**, *51*, 849–853. [[CrossRef](#)] [[PubMed](#)]
24. Parajuli, H.; Teh, M.T.; Abrahamson, S.; Christoffersen, I.; Neppelberg, E.; Lybak, S.; Osman, T.; Johannessen, A.C.; Gullberg, D.; Skarstein, K.; et al. Integrin alpha11 is overexpressed by tumour stroma of head and neck squamous cell carcinoma and correlates positively with alpha smooth muscle actin expression. *J. Oral Pathol. Med.* **2017**, *46*, 267–275. [[CrossRef](#)] [[PubMed](#)]
25. Fujii, N.; Shomori, K.; Shiomi, T.; Nakabayashi, M.; Takeda, C.; Ryoike, K.; Ito, H. Cancer-associated fibroblasts and CD163-positive macrophages in oral squamous cell carcinoma: Their clinicopathological and prognostic significance. *J. Oral Pathol. Med.* **2012**, *41*, 444–451. [[CrossRef](#)] [[PubMed](#)]
26. Marsh, D.; Suchak, K.; Moutasim, K.A.; Vallath, S.; Hopper, C.; Jerjes, W.; Upile, T.; Kalavrezos, N.; Violette, S.M.; Weinreb, P.H.; et al. Stromal features are predictive of disease mortality in oral cancer patients. *J. Pathol.* **2011**, *223*, 470–481. [[CrossRef](#)]
27. Xia, Y.; Zhu, Y.; Ma, T.; Pan, C.F.; Wang, J.; He, Z.C.; Li, Z.; Qi, X.T.; Chen, Y.J. miR-204 functions as a tumor suppressor by regulating SIX1 in NSCLC. *Febs Lett.* **2014**, *588*, 3703–3712. [[CrossRef](#)] [[PubMed](#)]
28. Sacconi, A.; Biagioni, F.; Canu, V.; Mori, F.; Di Benedetto, A.; Lorenzon, L.; Ercolani, C.; Di Agostino, S.; Cambria, A.M.; Germoni, S.; et al. miR-204 targets Bcl-2 expression and enhances responsiveness of gastric cancer. *Cell Death Dis.* **2012**, *3*, e423. [[CrossRef](#)]
29. Hong, B.S.; Ryu, H.S.; Kim, N.; Kim, J.; Lee, E.; Moon, H.; Kim, K.H.; Jin, M.S.; Kwon, N.H.; Kim, S.; et al. Tumor suppressor miRNA-204-5p regulates growth, metastasis, and immune microenvironment remodeling in breast cancer. *Cancer Res.* **2019**, *79*, 1520–1534.
30. Bao, W.; Wang, H.H.; Tian, F.J.; He, X.Y.; Qiu, M.T.; Wang, J.Y.; Zhang, H.J.; Wang, L.H.; Wan, X.P. A TrkB-STAT3-miR-204-5p regulatory circuitry controls proliferation and invasion of endometrial carcinoma cells. *Mol. Cancer* **2013**, *12*, 155. [[CrossRef](#)]
31. Imam, J.S.; Plyler, J.R.; Bansal, H.; Prajapati, S.; Bansal, S.; Rebeles, J.; Chen, H.I.H.; Chang, Y.F.; Panneerdoss, S.; Zoghi, B.; et al. Genomic loss of tumor suppressor miRNA-204 promotes cancer cell migration and invasion by activating AKT/mTOR/Rac1 signaling and actin reorganization. *PLoS ONE* **2012**, *7*, e52397.
32. Schneider, A.; Victoria, B.; Lopez, Y.N.; Suchorska, W.; Barczak, W.; Sobecka, A.; Golusinski, W.; Masternak, M.M.; Golusinski, P. Tissue and serum microRNA profile of oral squamous cell carcinoma patients. *Sci. Rep.* **2018**, *8*, 675. [[CrossRef](#)]
33. Tsai, S.C.; Huang, S.F.; Chiang, J.H.; Chen, Y.F.; Huang, C.C.; Tsai, M.H.; Tsai, F.J.; Kao, M.C.; Yang, J.S. The differential regulation of microRNAs is associated with oral cancer. *Oncol. Rep.* **2017**, *38*, 1613–1620. [[CrossRef](#)] [[PubMed](#)]
34. Chattopadhyay, E.; Singh, R.; Ray, A.; Roy, R.; De Sarkar, N.; Paul, R.R.; Pal, M.; Aich, R.; Roy, B. Expression deregulation of mir31 and CXCL12 in two types of oral precancers and cancer: Importance in progression of precancer and cancer. *Sci. Rep.* **2016**, *6*, 32735. [[CrossRef](#)]
35. Yu, C.C.; Chen, P.N.; Peng, C.Y.; Yu, C.H.; Chou, M.Y. Suppression of miR-204 enables oral squamous cell carcinomas to promote cancer stemness, EMT traits, and lymph node metastasis. *Oncotarget* **2016**, *7*, 20180–20192. [[CrossRef](#)]
36. Rajthala, S.; Dongre, H.; Parajuli, H.; Min, A.; Nginamau, E.S.; Kvalheim, A.; Lybak, S.; Sapkota, D.; Johannessen, A.C.; Costea, D.E. Combined In situ hybridization and immunohistochemistry on archival tissues reveals stromal microRNA-204 as prognostic biomarker for oral squamous cell carcinoma. *Cancers* **2021**, *13*, 1307. [[CrossRef](#)] [[PubMed](#)]
37. Sahai, E.; Astsaturov, I.; Cukierman, E.; DeNardo, D.G.; Egeblad, M.; Evans, R.M.; Fearon, D.; Greten, F.R.; Hingorani, S.R.; Hunter, T.; et al. A framework for advancing our understanding of cancer-associated fibroblasts. *Nat. Rev. Cancer* **2020**, *20*, 174–186. [[CrossRef](#)] [[PubMed](#)]
38. Tabor, M.P.; Brakenhoff, R.H.; van Houten, V.M.M.; Kummer, J.A.; Snel, M.H.J.; Snijders, P.J.F.; Snow, G.B.; Leemans, C.R.; Braakhuis, B.J.M. Persistence of genetically altered fields in head and neck cancer patients Biological and clinical implications. *Clin. Cancer Res.* **2001**, *7*, 1523–1532.
39. Ganci, F.; Sacconi, A.; Manciooco, V.; Covello, R.; Benevolo, M.; Rollo, F.; Strano, S.; Valsoni, S.; Biciato, S.; Spriano, G.; et al. Altered peritumoral microRNA expression predicts head and neck cancer patients with a high risk of recurrence. *Mod. Pathol.* **2017**, *30*, 1387–1401. [[CrossRef](#)] [[PubMed](#)]
40. Cukierman, E.; Pankov, R.; Stevens, D.R.; Yamada, K.M. Taking cell-matrix adhesions to the third dimension. *Science* **2001**, *294*, 1708–1712. [[CrossRef](#)] [[PubMed](#)]
41. Doldi, V.; Callari, M.; Giannoni, E.; D’Aiuto, F.; Maffezzini, M.; Valdagni, R.; Chiarugi, P.; Gandellini, P.; Zaffaroni, N. Integrated gene and miRNA expression analysis of prostate cancer associated fibroblasts supports a prominent role for interleukin-6 in fibroblast activation. *Oncotarget* **2015**, *6*, 31441–31460. [[CrossRef](#)]
42. Negrete-Garcia, M.C.; Ramirez-Rodriguez, S.L.; Rangel-Escareno, C.; Munoz-Montero, S.; Kelly-Garcia, J.; Vazquez-Manriquez, M.E.; Santillan, P.; Ramirez, M.M.; Ramirez-Martinez, G.; Ramirez-Venegas, A.; et al. Deregulated MicroRNAs in Cancer-Associated Fibroblasts from Front Tumor Tissues of Lung Adenocarcinoma as Potential Predictors of Tumor Promotion. *Tohoku J. Exp. Med.* **2018**, *246*, 107–120. [[CrossRef](#)] [[PubMed](#)]
43. Shen, Z.; Qin, X.; Yan, M.; Li, R.; Chen, G.; Zhang, J.; Chen, W. Cancer-associated fibroblasts promote cancer cell growth through a miR-7-RASSF2-PAR-4 axis in the tumor microenvironment. *Oncotarget* **2017**, *8*, 1290–1303. [[CrossRef](#)]

44. Yang, T.S.; Yang, X.H.; Chen, X.; Wang, X.D.; Hua, J.; Zhou, D.L.; Zhou, B.; Song, Z.S. MicroRNA-106b in cancer-associated fibroblasts from gastric cancer promotes cell migration and invasion by targeting PTEN. *FEBS Lett.* **2014**, *588*, 2162–2169. [[CrossRef](#)]
45. Vlachos, I.S.; Paraskevopoulou, M.D.; Karagkouni, D.; Georgakilas, G.; Vergoulis, T.; Kanellos, I.; Anastasopoulos, I.L.; Maniou, S.; Karathanou, K.; Kalfakakou, D.; et al. DIANA-TarBase v7.0: Indexing more than half a million experimentally supported miRNA:mRNA interactions. *Nucleic Acids Res.* **2015**, *43*, D153–D159. [[CrossRef](#)] [[PubMed](#)]
46. Zeltz, C.; Alam, J.; Liu, H.; Erusappan, P.M.; Hoschuetzky, H.; Molven, A.; Parajuli, H.; Cukierman, E.; Costea, D.E.; Lu, N.; et al. alpha11beta1 Integrin is Induced in a Subset of Cancer-Associated Fibroblasts in Desmoplastic Tumor Stroma and Mediates In Vitro Cell Migration. *Cancers* **2019**, *11*, 765. [[CrossRef](#)]
47. Velling, T.; Kusche-Gullberg, M.; Sejersen, T.; Gullberg, D. cDNA cloning and chromosomal localization of human alpha(11) integrin: A collagen-binding, I domain-containing, beta(1)-associated integrin alpha-chain present in muscle tissues. *J. Biol. Chem.* **1999**, *274*, 25735–25742. [[CrossRef](#)]
48. Katoh, K. FAK-Dependent Cell Motility and Cell Elongation. *Cells* **2020**, *9*, 192. [[CrossRef](#)] [[PubMed](#)]
49. Dourado, M.R.; de Oliveira, C.E.; Sawazaki-Calone, I.; Sundquist, E.; Coletta, R.D.; Salo, T. Clinicopathologic significance of ROCK2 expression in oral squamous cell carcinomas. *J. Oral Pathol. Med.* **2018**, *47*, 121–127. [[CrossRef](#)] [[PubMed](#)]
50. Ying, Z.; Li, Y.; Wu, J.; Zhu, X.; Yang, Y.; Tian, H.; Li, W.; Hu, B.; Cheng, S.Y.; Li, M. Loss of miR-204 expression enhances glioma migration and stem cell-like phenotype. *Cancer Res.* **2013**, *73*, 990–999. [[CrossRef](#)] [[PubMed](#)]
51. Locke, M.; Heywood, M.; Fawell, S.; Mackenzie, I.C. Retention of intrinsic stem cell hierarchies in carcinoma-derived cell lines. *Cancer Res.* **2005**, *65*, 8944–8950. [[CrossRef](#)]
52. Biddle, A.; Liang, X.; Gammon, L.; Fazil, B.; Harper, L.J.; Emich, H.; Costea, D.E.; Mackenzie, I.C. Cancer stem cells in squamous cell carcinoma switch between two distinct phenotypes that are preferentially migratory or proliferative. *Cancer Res.* **2011**, *71*, 5317–5326. [[CrossRef](#)] [[PubMed](#)]
53. Stavrum, A.K.; Petersen, K.; Jonassen, I.; Dysvik, B. Analysis of gene-expression data using J-Express. *Curr. Protoc. Bioinform.* **2008**, *21*, 1–25. [[CrossRef](#)] [[PubMed](#)]
54. Agarwal, V.; Bell, G.W.; Nam, J.W.; Bartel, D.P. Predicting effective microRNA target sites in mammalian mRNAs. *eLife* **2015**, *4*, e05005. [[CrossRef](#)] [[PubMed](#)]
55. Vejnar, C.E.; Zdobnov, E.M. MiRmap: Comprehensive prediction of microRNA target repression strength. *Nucleic Acids Res.* **2012**, *40*, 11673–11683. [[CrossRef](#)] [[PubMed](#)]
56. Wong, N.; Wang, X. miRDB: An online resource for microRNA target prediction and functional annotations. *Nucleic Acids Res.* **2015**, *43*, D146–D152. [[CrossRef](#)]
57. Kent, W.J.; Sugnet, C.W.; Furey, T.S.; Roskin, K.M.; Pringle, T.H.; Zahler, A.M.; Haussler, D. The human genome browser at UCSC. *Genome Res.* **2002**, *12*, 996–1006. [[CrossRef](#)]
58. Dysvik, B.; Jonassen, I. J-Express: Exploring gene expression data using Java. *Bioinformatics* **2001**, *17*, 369–370. [[CrossRef](#)]

**Supplementary Table S1.** Patient information

<i>ID</i>	<i>Age Gender</i>	<i>site</i>	<i>TNM</i>	<i>Differentiation</i>	<i>Later metastasis</i>	<i>Smoking</i>	<i>Survival (months)</i>
<b><i>Donors of CAF-NOF matched pairs</i></b>							
7m	68, M	gingiva	T4N2M0	middle	bone, lung	yes	20
8m	69, M	floor of mouth	T4N1M0	middle	bone	yes	9
10m	51, M	tongue	T2N2bM0	high	no	-	alive
15m	66, M	gingiva	T4N0M0	poor	-	yes	1
21m	62, M	tongue	T2N1M0	high	lung, liver	yes	8
<b><i>Donors of CAF (un-matched group)</i></b>							
7	80, F	buccal	T2N2M0	high	no	no	12
9	66, F	buccal	T2N2M0	high	no	no	alive
10	49, M	tongue	T3N1M0	middle	no	yes	96
11	57, M	tongue	T4N2M0	middle	-	-	-
12	52, M	tongue	T3N1M0	poor	-	-	-
13	72, M	floor of mouth	T4N1M0	middle	-	yes	-
24	63, F	tongue	T3N1M0	high	bone	no	16
25	42, M	gingiva	T4N1M0	high	lung, bone	no	12

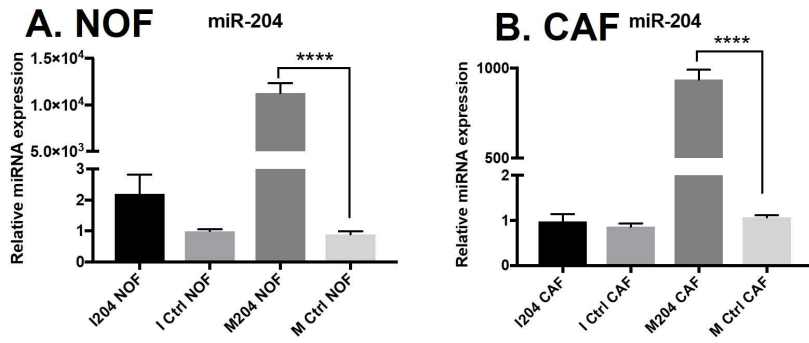
**Supplementary Table S2.** List of Taqman Assays (ThermoFisher, USA)

<i>Genes</i>	<i>Taqman Assay ID</i>
hsa-miR-204-5p	000508
hsa-miR-138-5p	002284
hsa-miR-582-5p	001983
RNU48	001006
ITGA11	Hs00201927_m1
PTK2	Hs01056457_m1
EGFR	Hs01076090_m1
GAPDH	Hs99999905_m1
FAP	Hs00990806_m1
TGFB1	Hs00998130_m1
ROCK2	Hs00178154_m1
18s	Hs99999901_s1
TGFBR2	Hs00559660_m1
RPL13A	Hs04194366_g1

**Supplementary Table S3.** List of antibodies used for western blot.

<b>1<sup>o</sup> Antibodies</b>	<b>Cat No</b>	<b>Dilution</b>	<b>Protein block</b>
ITGA11 [1]	-	1:2000	5% Dry milk
FAK (D2R2E)	#13009, Cell Signalling	1:1000	3%BSA
p-FAK(Tyr397) (D20B1)	#8556, Cell Signalling	1:1000	3%BSA
FAP (SP325	#ab207178 Abcam	1:1000	5% Dry milk
TGFBR2 (E5M6F)	# 41896S, Cell Signalling	1:1000	5% Dry milk
GAPDH	AB9484, Abcam	1:10000	5% Dry milk
B-Actin	#4967, Cell Signalling	1:5000	5% Dry milk

1. Velling T, Kusche-Gullberg M, Sejersen T, Gullberg D: **cDNA cloning and chromosomal localization of human alpha(11) integrin. A collagen-binding, I domain-containing, beta(1)-associated integrin alpha-chain present in muscle tissues.** *J Biol Chem* 1999, **274**(36):25735-25742.





**Supplementary Fig. 1** miR-204 changes in fibroblasts 48 hours post transfection with mimics and inhibitors.





Article

# Combined In Situ Hybridization and Immunohistochemistry on Archival Tissues Reveals Stromal microRNA-204 as Prognostic Biomarker for Oral Squamous Cell Carcinoma

Saroj Rajthala<sup>1,2</sup>, Harsh Dongre<sup>1,2</sup>, Himalaya Parajuli<sup>1,2</sup> , Anjie Min<sup>3</sup>, Elisabeth Sivy Nginamau<sup>1,2,4</sup>, Arild Kvalheim<sup>5</sup>, Stein Lybak<sup>6</sup>, Dipak Sapkota<sup>7</sup>, Anne Christine Johannessen<sup>1,2,4</sup> and Daniela Elena Costea<sup>1,2,4,\*</sup> 

- <sup>1</sup> Gade Laboratory for Pathology, Department of Clinical Medicine, Faculty of Medicine, University of Bergen, N-5020 Bergen, Norway; saroj.rajthala@uib.no (S.R.); harsh.dongre@uib.no (H.D.); himalaya.parajuli@uib.no (H.P.); elisabeth.nginamau@uib.no (E.S.N.); anne.johannessen@uib.no (A.C.J.)
- <sup>2</sup> Centre for Cancer Biomarkers (CCBio), Faculty of Medicine, University of Bergen, N-5020 Bergen, Norway
- <sup>3</sup> Department of Oral Maxillofacial Surgery, Xiangya Hospital, Central South University, Changsha 410083, China; william0732@csu.edu.cn
- <sup>4</sup> Department of Pathology, Haukeland University Hospital, N-5021 Bergen, Norway
- <sup>5</sup> Oral Surgery Private Referral Practice "Tannteam", N-5221 Nesttun, Norway; post@tannteam.no
- <sup>6</sup> Head and Neck Clinic, Haukeland University Hospital, N-5021 Bergen, Norway; stein.lybak@helse-bergen.no
- <sup>7</sup> Institute of Oral Biology, Faculty of Dentistry, University of Oslo, N-0316 Oslo, Norway; dipak.sapkota@odont.uio.no
- \* Correspondence: daniela.costea@uib.no; Tel.: +47-5597-2565



**Citation:** Rajthala, S.; Dongre, H.; Parajuli, H.; Min, A.; Nginamau, E.S.; Kvalheim, A.; Lybak, S.; Sapkota, D.; Johannessen, A.C.; Costea, D.E. Combined In Situ Hybridization and Immunohistochemistry on Archival Tissues Reveals Stromal microRNA-204 as Prognostic Biomarker for Oral Squamous Cell Carcinoma. *Cancers* **2021**, *13*, 1307. <https://doi.org/10.3390/cancers13061307>

Academic Editor: Sven Otto

Received: 6 February 2021

Accepted: 13 March 2021

Published: 15 March 2021

**Publisher's Note:** MDPI stays neutral with regard to jurisdictional claims in published maps and institutional affiliations.



**Copyright:** © 2021 by the authors. Licensee MDPI, Basel, Switzerland. This article is an open access article distributed under the terms and conditions of the Creative Commons Attribution (CC BY) license (<https://creativecommons.org/licenses/by/4.0/>).

**Simple Summary:** In addition to the transformation of epithelial cells, dysfunction of stroma is crucial in carcinogenesis; cancer-associated stroma can regulate the phenotype of cancer cells and thereby influence the clinical outcome. Our study aimed to investigate the correlation of stromal miR-204 with progression of oral squamous cell carcinoma (OSCC) and assert its clinical utility. We first established a chromogen-based method that combined immunohistochemistry and in situ hybridization for exact delimitation of stroma from the tumor islands and concomitant visualization of miRs, and have developed a guide to digital miR quantification using the publicly available tool ImageJ and the licensed software Aperio ImageScope. We have then applied the method for investigating stromal miR-204 as a putative prognostic biomarker on an OSCC cohort and identified expression of miR204 in the stroma at tumor front as an independent prognostic biomarker for this disease.

**Abstract:** Micro-RNAs (miRs) are emerging as important players in carcinogenesis. Their stromal expression has been less investigated in part due to lack of methods to accurately differentiate between tumor compartments. This study aimed to establish a robust method for dual visualization of miR and protein (pan-cytokeratin) by combining chromogen-based in situ hybridization (ISH) and immunohistochemistry (IHC), and to apply it to investigate stromal expression of miR204 as a putative prognostic biomarker in oral squamous cell carcinoma (OSCC). Four different combinations of methods were tested and ImageJ and Aperio ImageScope were used to quantify miR expression. All four dual ISH-IHC methods tested were comparable to single ISH in terms of positive pixel area percentage or integrated optical density of miRs staining. Based on technical simplicity, one of the methods was chosen for further investigation of miR204 on a cohort of human papilloma virus (HPV)-negative primary OSCC ( $n = 169$ ). miR204 stromal expression at tumor front predicted recurrence-free survival ( $p = 0.032$ ) and overall survival ( $p = 0.036$ ). Multivariate Cox regression further confirmed it as an independent prognostic biomarker in OSCC. This study provides a methodological platform for integrative biomarker studies based on simultaneous detection and quantification of miRs and/or protein and reveals stromal miR204 as a prognostic biomarker in OSCC.

**Keywords:** miR204; oral cancer; stroma; biomarker; chromogen; in situ hybridization; immunohistochemistry

## 1. Introduction

In addition to the transformation of epithelial cells, dysfunction of stroma is crucial in carcinogenesis [1,2]. The abnormal stroma surrounding carcinoma cells is referred to as reactive tumor stroma or cancer-associated stroma. Cancer-associated stroma comprises non-cancer cell constituents including cancer-associated fibroblasts, immune cells, adipocytes, endothelial cells, pericytes, nerves, extracellular matrix and secretomes synthesized by cells [1,3]. Cancer-associated stroma can regulate the phenotype of cancer cells and thereby influence the clinical outcome [1].

Better understanding of the role of cancer-associated stroma in carcinoma progression and therapeutic outcome has led to an increasing interest for stromal biomarkers in recent years. With the emergence of micro-RNAs (miRs) as important players in carcinogenesis [4–7], the hunt for new biomarkers has expanded to cancer-specific miRs in several biological specimens including blood [8,9], saliva [10], urine [11], stool [12], and tumors [13]. miRs control gene expression by targeting mRNA for cleavage or translational repression using a protein complex known as RNA-inducing silencing complex [7,14]. Several miRs have been found to promote or suppress cancer progression, and thereby are called oncogenic or tumor suppressor miRs [4–7].

As an example of putative tumor suppressor miR, miR-204 expression has been shown to decrease in several cancers [15–19]. In favor of its role as a tumor suppressor there are several studies showing anti-tumorigenic effects of miR-204 in both in vitro and in vivo animal studies [15–21]. Decreased expression of miR-204 has been associated with poor survival in breast cancer [17], gastric cancer [16], endometrial cancer [19], acute myeloid leukemia [22], medulloblastoma [20], and neuroblastoma [23]. Expression of miR-204 in neuroblastoma cells and gastric cancer cell lines increased their sensitivity to cisplatin [23], 5-fluorouracil, and oxaloplatin, respectively [16]. These studies support the notion that expression of miR-204 in cancer cells could be used both as prognostic marker and for targeted treatment. The same trend of decreased miR-204 expression in cancer cells with disease progression has been also described for oral squamous cell carcinoma (OSCC) [24–26]. Decreased expression of miR-204 in tumor cells was associated with increased lymph node incidence [27] and increased distant metastasis [26] in animal models of OSCC. Similarly, lowered miR-204 expression was shown to predict poor survival in OSCC [27].

Nevertheless, despite these studies on the expression and role of miR-204 in several cancers, including OSCC, there is a complete gap of knowledge in miR-204 function in the tumor stroma of carcinomas, including OSCC. All the above-mentioned studies were based on qRT-PCR, microarray, and sequencing techniques and were thus conducted selectively on cancer cells or on whole tumor tissues, which eludes the spatial distribution and regulation of miR-204 in different tumor compartments. Therefore, our study aimed to investigate the correlation of stromal miR-204 with OSCC progression and assert its clinical utility.

Since single and poorly differentiated invading carcinoma cells are difficult to recognize without specific markers, thus leading to false positive results by erroneously being included in the quantification of the stroma, we aimed firstly to establish robust methods of combining miR in situ hybridization (ISH) with immunohistochemistry (IHC) for epithelial markers, e.g., pan-cytokeratin (pan-CK), for a more precise quantification of miRs in specific tumor compartments. We chose two oncogenic miRs, miR-21 and miR-155, for establishing the method since they were previously reported in the literature to have a biological relevance for OSCC and had different expression patterns which we thought would help in evaluating the double staining method we wanted to establish. Both miR-155 [28,29] and miR-21 [13] were shown to be overexpressed in OSCC tissues and were previously found to predict poor prognosis. Previous studies by single ISH found that miR-21 was primarily expressed in the tumor stroma and in some tumor-associated blood vessels with

no expression in the adjacent normal epithelia or stroma [13], while miR155 was reported to be located in the cancer nests, inflammatory area, and vascular endothelium [28]. Here, we present robust ISH-IHC combination methods and a guide to digital miR quantification using the publicly available tool ImageJ and the licensed software Aperio ImageScope. By applying them to a well-annotated OSCC cohort of patients we show that stromal expression of miR-204 at the tumor front is an independent prognostic biomarker in OSCC.

## 2. Materials and Methods

### 2.1. *In Situ Hybridization (ISH)*

ISH was performed following a modified protocol, while adhering to the staining principles in the Instruction Manual v3.0 (Exiqon A/S Vedbæk, Denmark). In brief, 3 µm formalin fixed paraffin embedded (FFPE) tissue sections were deparaffinized in xylene and rehydrated in a series of decreasing alcohol concentrations. To expose miR probes, we incubated tissue sections with 15 µg/mL Proteinase K solution (90,000; Exiqon) at 37 °C for 10 min, after a titration experiment that established the optimal unmasking treatment while maintaining tissue morphology. Tissues were then pre-hybridized with ISH buffer (90,000;) for 30 min, and then hybridized with locked nucleic acid-based digoxigenin (DIG)-labeled miR binding oligonucleotides at corresponding hybridization temperatures. miR-155-5p (619862-360; Exiqon) was hybridized at 48 °C; miR-21-5p (619870-360; Exiqon) and miR-204-5p (619857-360; Exiqon) were hybridized at 53 °C for 2 h. Optimal hybridization temperature for the individual miR target probes was determined using melting temperature-based temperature series test, and optimal concentration was determined using series of miR target probe concentration. Tissues were then washed stringently in decreasing concentrations of saline-sodium citrate (SSC) buffer (S66391L; MilliporeSigma, Munich, Germany) at corresponding hybridization temperatures. Following stringent wash, tissues were blocked in 2% sheep serum (013-000-121; Jackson ImmunoResearch, West Grove, PA, USA) and 1% bovine serum albumin (BSA). Tissues were then incubated with alkaline phosphatase (ALP)-linked anti-DIG Fc fragments (11093274910; Roche, Basel, Switzerland) at 1:400 concentration overnight at room temperature (RT). The following day, tissues were incubated with ALP substrate-Nitro blue tetrazolium chloride/5-Bromo-4-chloro-3-indolyl phosphate (NBT-BCIP) (11681451001; Roche) at 30 °C for 2 h or at RT overnight. The reaction was stopped using KBTB buffer, counterstained with nuclear fast red and mounted in xylene-based medium Pertex (00871.1000-EX; Histolab Products AB, Västra Frölunda, Sweden). Levamisole (X3021; Agilent Dako, Santa Clara, CA, USA) was used to block endogenous ALP activity. No probe and scramble oligonucleotide were used as negative controls; small nuclear RNA-U6 was used as positive control.

### 2.2. *Immunohistochemistry (IHC)*

FFPE tissue sections were deparaffinized, rehydrated, antigen retrieved using Proteinase K, and blocked in sheep serum and BSA solution as described above in ISH section. p16INK<sup>4a</sup> antigen was retrieved by boiling tissue sections in Tris-EDTA (pH 9) in a microwave oven for 15 minutes. Thereafter, tissue sections were incubated with monoclonal mouse anti-human primary antibody (pan-CK 1:800, Clone MNF116, Agilent Dako; p16INK4a 1:1000, G175-405, BD Pharmingen, New York, NJ, USA) at RT for 1 h. A Dako Envision+ System-HRP (DAB) kit (K4007; Agilent Dako) was used for the subsequent steps. Tissue endogenous peroxidase activity was blocked with peroxidase block for 5 min. Thereafter, sections were incubated with horseradish peroxidase (HRP)-conjugated secondary antibody for 30 min and visualized with diaminobenzidine (DAB) substrate at RT. Tissues were counterstained with fast red and mounted with Pertex.

### 2.3. *Combined miR ISH and IHC staining*

ISH of miR and IHC of pan-CK were performed on the same tissue section following the methods described above, and in different order sequences as illustrated in the flowchart (Figure 1).

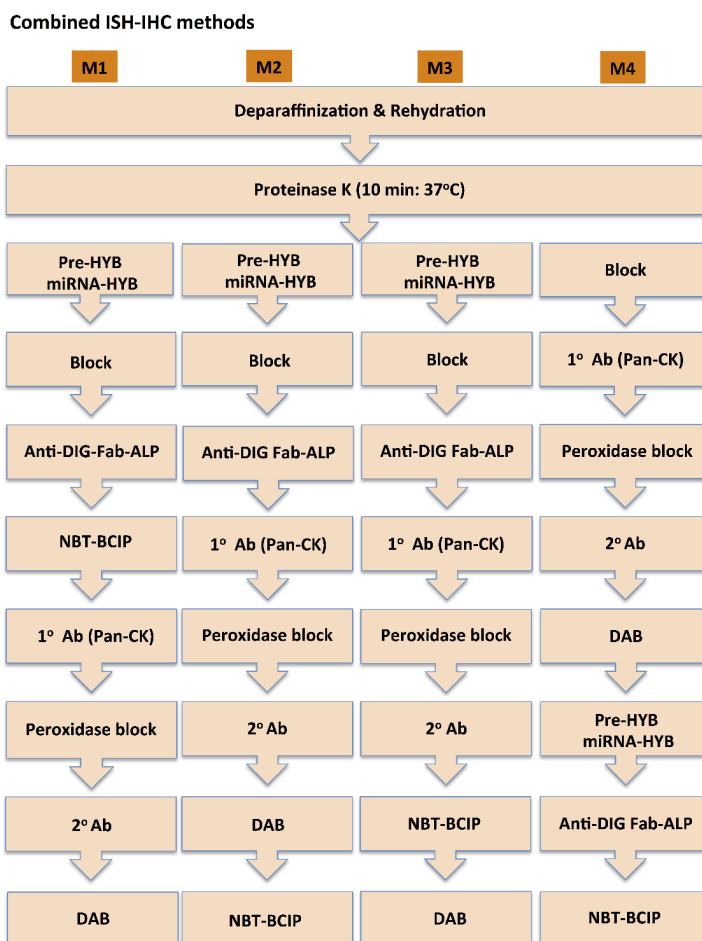


**Figure 1.** Flowchart depicting the ISH-IHC (in situ hybridization with immunohistochemistry) combinations employed in the double staining method.

#### 2.4. Image Acquisition and Quantification

Images for the stained tissues were acquired at 40× objective using a whole slide scanner (Hamamatsu NanoZoomer-XR, Shizuoka, Japan). RGB vectors for NBT-BCIP, DAB and fast red were acquired using images from tissues stained with individual dye using “From ROI” interactive option in the Color Deconvolution plugin for ImageJ. Acquired RGB vectors for the stains were then integrated into Java for Color Deconvolution. Images were then color deconvoluted to resolve miR stain (NBT-BCIP) from fast red and DAB (Figure 1). Color threshold for NBT-BCIP was set to 195 to exclude background, and thereafter, positive pixel area percentage (PPAP) and integrated optical density (IOD; normalized to analysed area) of miR staining were measured. Mean pixel intensity was converted to OD using the function  $OD = \log_{10}(255/\text{mean pixel intensity})$ ; IOD was

obtained as product of OD and positive pixel area stained and normalized to region of interest. The same measurements for the miR staining were made using other software, Aperio (Leica Biosystems, Wetzlar, Germany), using the same principles and criteria used in ImageJ. PPAP and IOD were quantified in the stroma regions of tumor center and tumor front of approximately 0.4–0.8 mm<sup>2</sup>. Five to seven hot spots, i.e., areas with highest staining intensity, were chosen for the quantification. Blood vessels, glands, muscles, and nerves were excluded from the study. For the methodological comparisons, similar regions in the tissue sections stained by different combination methods were chosen. MiR-21 and miR-204 were quantified both at tumor center and invasive tumor front. The invasive tumor front was defined as a 100 µm broad tissue area around the outermost invasive tumor islands.

### 2.5. Study Cohort

The study cohort consisted of patients older than 18 years with primary diagnosis of OSCC between 1998 and 2012 and surgically, radio-, or combinatory treated at Haukeland University Hospital, Bergen, Norway ( $n = 169$ ). Patients with neoadjuvant treatment, missing tissue blocks, and missing clinical information were excluded from the study. The clinical information (age, gender, smoking and alcohol use, localization, TNM stage, co-morbidities, recurrence, last date of follow-up, survival) was obtained from patients' medical electronic journals and is presented in Table S1. FFPE tissue blocks containing the tumor front with surrounding stroma and adjacent normal human oral mucosa (NHOM) were selected for the study. Serial sections of 3–4 µm thickness were cut using a microtome (HistoCore Biocut, Leica Biosystems), mounted on glass slides (Superforst Plus from Thermo Fisher Scientific, Waltham, MA, USA), fixed on slides by incubation at 58 °C for 2 hours and stored at 4 °C until use. RNA contamination was avoided during cutting and handling using gloves and RNase decontaminating solution (RNase Zap, Thermo Fisher, Scientific). Tumor specimens were screened for human papillomavirus (HPV) infection with the surrogate marker p16INK4a by IHC. Nine cases (5.53%) displaying strong nuclear and cytoplasmic staining in more than 70–80% of the tumor cells and were excluded from the study. Finally, a total of 160 HPV-negative OSCC cases (age range: 27–93; mean = 65.25; median = 65) were included in the study. The mean follow-up time was 8.6 years, and the 5-year survival rate was 40%. Adequacy in sample size for the Cox regression was met as suggested by Peduzzi et al. [30]. NHOM from clinically healthy donors was also collected during wisdom tooth extraction ( $n = 14$ ). Informed consents were obtained for the research use of tissues and clinical data. This study was approved by the regional ethical committee in Norway (REKVest 3.2006.2620 REKVest 3.2006.1341) and followed REMARK criteria [31].

### 2.6. Evaluation of Clinical and Pathological Parameters

Staging of OSCC (TNM) was done at the point of diagnosis according to the American Joint Committee on Cancer manual 6th edition. Tumor depth of invasion (DI), which is the distance from a theoretically reconstructed normal mucosal line to the deepest invasion point [32], and tumor budding (TB), which is defined as a single cell or a cluster of less than five cancer cells, were evaluated as described earlier [33]. Worst pattern of invasion (WPI) was scored as described by Brandwein-Gensler et al. [34]. Histological scoring was performed on scanned pan-cytokeratin stained images by an experienced pathologist (E.S.N.).

### 2.7. RNA Extraction and Quantitative Reverse-Transcriptase Polymerase Chain Reaction (qRT-PCR)

Approximately 10% of cohort samples (16 samples) were randomly selected and used for validation of miR-204 expression by using qRT-PCR. Three to four 10 µm freshly cut sections from FFPE samples were collected in RNase-free microtubes and RNA was isolated using miRNeasy FFPEkit (Qiagen, Oslo, Norway) according to the manufacturer's guidelines. The paraffin around tissues was trimmed prior to sectioning, and the sections

were macrodissected in order to select mainly the tumor front, removing the bulk of the tumor center or the normal surrounding tissue. Briefly, each sample was treated with deparaffinization solution, to remove excess paraffin. This was followed by mixing with buffer PKD and Proteinase K digestion with heat treatment (at 56 °C for 15 min and at 80 °C for 15 min). The DNA/RNA phases were separated by centrifugation at 20,000 *g* for 15 min. To further purify RNA, DNase treatment was applied to remove genomic DNA contamination. Each sample was then mixed with ethanol and transferred onto RNeasy MinElute spin columns. Following the manufacturer's protocol of washing with RPE buffer, the RNA was subsequently eluted in 15 µL RNase-free water. RNA concentrations were measured using NanoDrop 1000 (Thermo Fisher Scientific). The RNA yield varied from 50 to 1800 ng/µL and the purity ranged from 1.7 to 1.99 (A260/A280 ratio).

Three RT reactions were performed for each sample (with 200 ng of input RNA for each reaction) in a 15 µL reaction using the TaqMan microRNA reverse transcription kit (Applied Biosystems, Foster City, CA, USA). RT primers were specific for each of the following miR: RNU6B (assay ID: 001093), RNU48 (assay ID: 001006), and hsa-miR-204 (assay ID: 000508). qRT-PCR reactions were performed on cDNA products and thus obtained with TaqMan Fast Advanced master mix II (Applied biosystems) according to the manufacturer's protocol. PCR reactions were performed on a 7500 Fast Real-time PCR system (Applied Biosystems), with each reaction run in duplicates.

For analysis, the expression level of miR-204 was normalized to the mean of internal controls (RNU6B and RNU48) and the relative difference ( $\Delta Ct$ ) was correlated with quantified ISH values (PPAP). Pearson correlation plot was used to establish significance and the data are represented as QQ plots (GraphPad Prism, v9, GraphPad Software, San Diego, CA, USA).

### 2.8. Statistical Analysis

Survival functions (overall survival (OS) and recurrence-free survival (RFS)) of clinicopathological parameters, including miR-204 expression in the tumor stroma, were plotted using the Kaplan–Meir (KM) method. Test of equality for survival distribution of the variables within the parameters was carried using the log-rank test (Mantel–Cox). Risks of clinicopathological parameters in the OS and RFS of the OSCC patients were further examined by univariate survival analysis using Cox's proportional regression. Parameters with variables that exhibited significant risk difference in the OS and RFS in the univariate analysis were entered into the multivariate model to examine the risk adjusted to confounding variables. The proportional hazard assumptions, i.e., if the baseline hazard function was proportional or not, was checked graphically for all parameters with Log minus log function plot before regression analysis. Additionally, time-dependent covariates were modeled to check the proportionality of hazards over time ( $p < 0.05$  indicates change of predictor over time). Tests of independence of clinicopathological parameters with miR-204 expression were assessed using Pearson's chi-squared test. Kolmogorov–Smirnov test, Shapiro–Wilk test, histogram, and Q–Q plots were used to test the normality for the miR expressions. Tumor stroma expressions of miR-204 in the tumor front and tumor center were categorized into higher and lower expression group by the median expression value. Mann–Whitney U or Wilcoxon match-paired signed rank test was performed to find significant differences in miR in between high and low expression groups. Paired Student's t-test was conducted to detect significant differences in mean of the PPAP and IOD for the miR expression in between control (single miR ISH) and double staining methods. The statistical analysis was performed using GraphPad Prism Version 7.0 (GraphPad Software) or IBM SPSS Statistics Version 25.0 (IBM Corp, Armonk, NY, USA).

## 3. Results

### 3.1. miRs Expression and Their Co-Localization with pan-CK

Diverse spatial distribution of the expression of the investigated miRs was observed in OSCC tissues. miR-21 staining was confined to reactive tumor stroma (Figure 2), with

higher staining intensity at tumor center compared to tumor front (Figure 2). The staining was observed almost exclusively in the cytoplasm of cells with a fibroblast-like appearance. Expression of both miR-155 (Figure 2) and miR-204 (Figure 2) was both epithelial and stromal; in the stroma it was localized both in fibroblast-like cells and lymphocytes. The abundance of the lymphocytic infiltrate varied from case to case, as shown in Figure 2 which depicts cases with poor (A,E), intermediate (C,F), and intense (B,D) lymphocytic infiltrate. Negative controls did not give any color signal (Figure 2). At 48 °C, scramble oligonucleotides nonspecifically bound to the tissue, and hence could not be used as negative control for miR-155 that hybridizes at 48 °C.

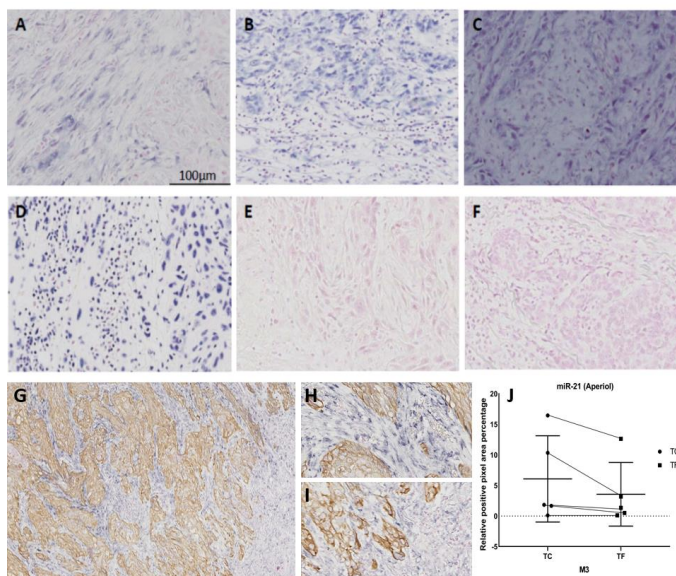


**Figure 2.** Representative images of ISH for various miRs: single ISH for miR-21 (A), miR-155 (B), and miR-204 (C); U6—positive control (D), scramble oligonucleotide with no target site—negative control (E), negative control without miR-binding probe (F), double ISH-IHC for miR-21 and pan-CK using method 3 (G) showing intense staining at tumor center (H) and weaker staining at tumor front (I) as quantified using Aperiol in (J). Original magnification: 10×; scale bar: 100 µm.

The epithelial marker pan-CK was specific to tumor cells in all double-stained tissue sections, as expected. No co-localization between pan-CK and miR-21 was observed, in line with previous studies that reported expression of miR21 exclusively in the tumor stroma of carcinomas, including OSCC [13]; however, both miR-155 (Figure 3) and miR-204 (Figure 4) colocalized with pan-CK in the epithelial islands. No nonspecific anti-DIG Fab binding or non-specific NBT-BCIP reaction to alkaline phosphatase was detected in negative controls run with scramble negative controls or without oligonucleotide probes.



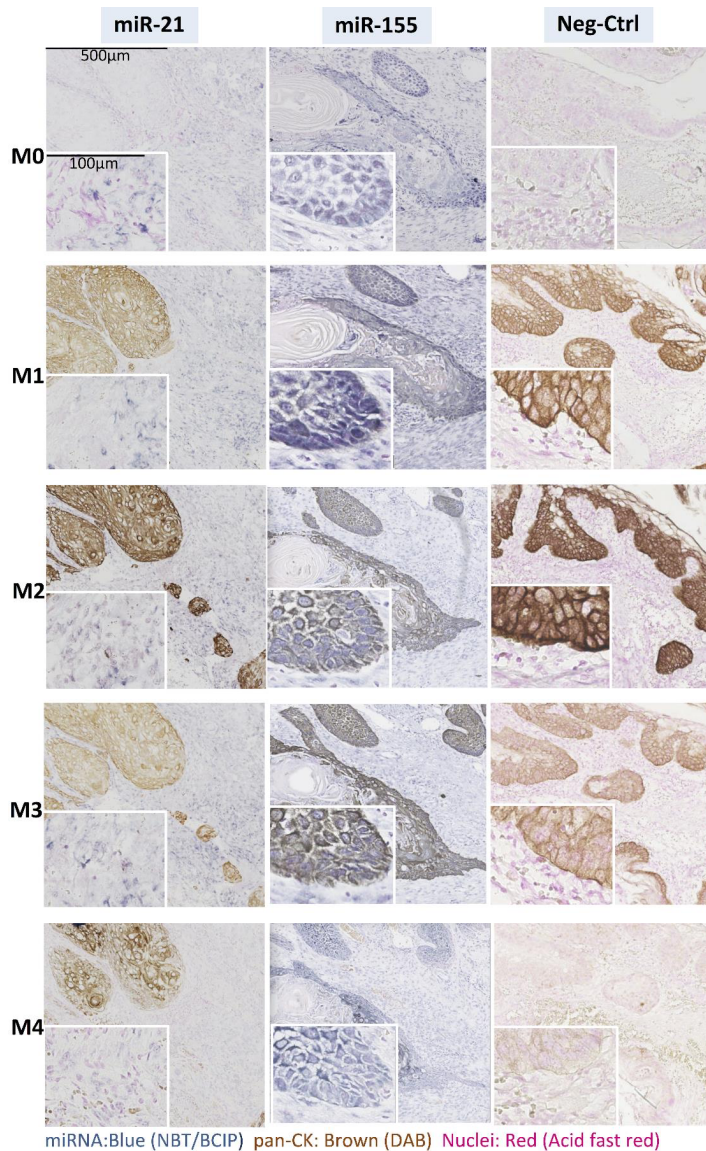


**Figure 3.** Representative images for combined miR ISH (miR-21 and miR-155) and IHC (pan-CK). Serial sections of the tissue were stained for miR alone (M0.ISH) or miRs ISH was combined with IHC of pan-CK (M1.ISH+IHC; M2.ISH-Fab+IHC+NBT-BCIP; M3.ISH-Fab+1oAb-2oAb+NBT-BCIP+DAB. M4. IHC+ISH). Scramble negative control or no probe control (Neg-Ctrl) was run for miR-21 and miR-155, respectively. Since no differences were observed, only scramble negative controls are presented. Original magnification: 5×; scale bar: 500 µm. Inset: original magnification: 20×; scale bar: 100 µm.

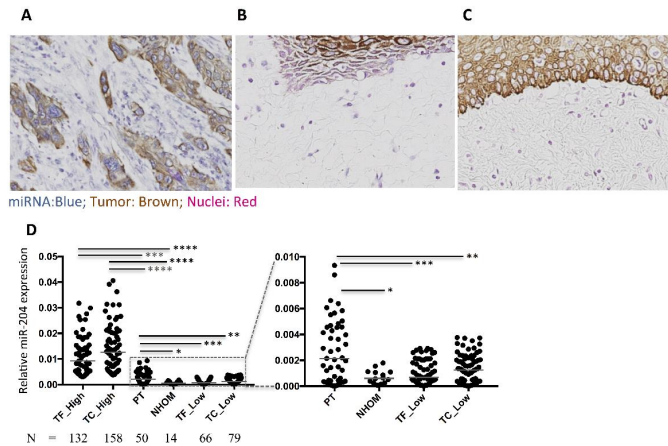


**Figure 4.** Representative images from a double stained section for miR-204 and pan-CK in tumor (A), peritumor (B), and normal mucosa (C) in OSCC. Original magnification: 20 $\times$ ; scale bar: 100  $\mu$ m. (D) Wilcoxon test for the paired variables (tumor front (TF), tumor centre (TC), and peritumor (PT)). Mann–Whitney U test for all other comparisons (independent). \*\*\*\*  $p < 0.0001$ ; \*\*\*  $p < 0.0005$ ; \*\*  $p < 0.001$ ; \*  $p < 0.05$ .

### 3.2. Effects of IHC on ISH and Vice Versa

Quantitative assessment of miR signals using color deconvolution (Figure 5) in both ImageJ and Aperio software did not show significant differences in positive pixel area percentage (PPAP) or integrated optical density (IOD) between the control and the dual staining methods (Figure 6). Irrespective of the order of procedures in the combined double staining methods, and whether there was co-localization or not, both pan-CK and miRs were accessible to either binding antibody or probes, respectively, after their preceding stain (Figure 3).

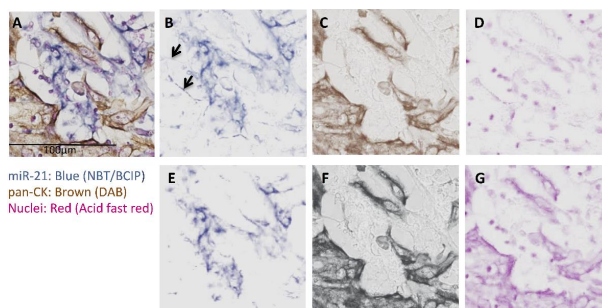


**Figure 5.** Color deconvolution of a representative image from a double stained section for miR-21 and pan-CK. (A) OSCC (oral squamous cell carcinoma) section stained for miR-21 (blue; NBT-BCIP), pan-CK (brown; DAB) and counter stained (red; acid fast red). Image A was color deconvoluted into individual color images: (B) (NBT-BCIP), (C) (DAB), and (D) (acid fast red). Color deconvolution using RGB vectors for black color instead for DAB (brown) for the same image took away non-NBT-BCIP signals ((E); indicated by arrows in (B)), while overexposing brown (F) and red (G). Original magnification: 20 $\times$ ; scale bar: 100  $\mu$ m. Vectors used: Nuclear fast red (NFR)-NBT-BCIP-DAB (NFR: R=0.350, G = 0.840, B = 0.408; NBT-BCIP: R = 0.677, G = 0.627, B = 0.384; DAB: R = 0.443, G = 0.598, B = 0.667), and NFR-NBT-BCIP-BLACK (NFR: R = 0.375, G = 0.827, B = 0.416; NBT-BCIP: R = 0.647, G = 0.649, B = 0.398; BLACK: R = 0.588, G = 0.578, B = 0.565).

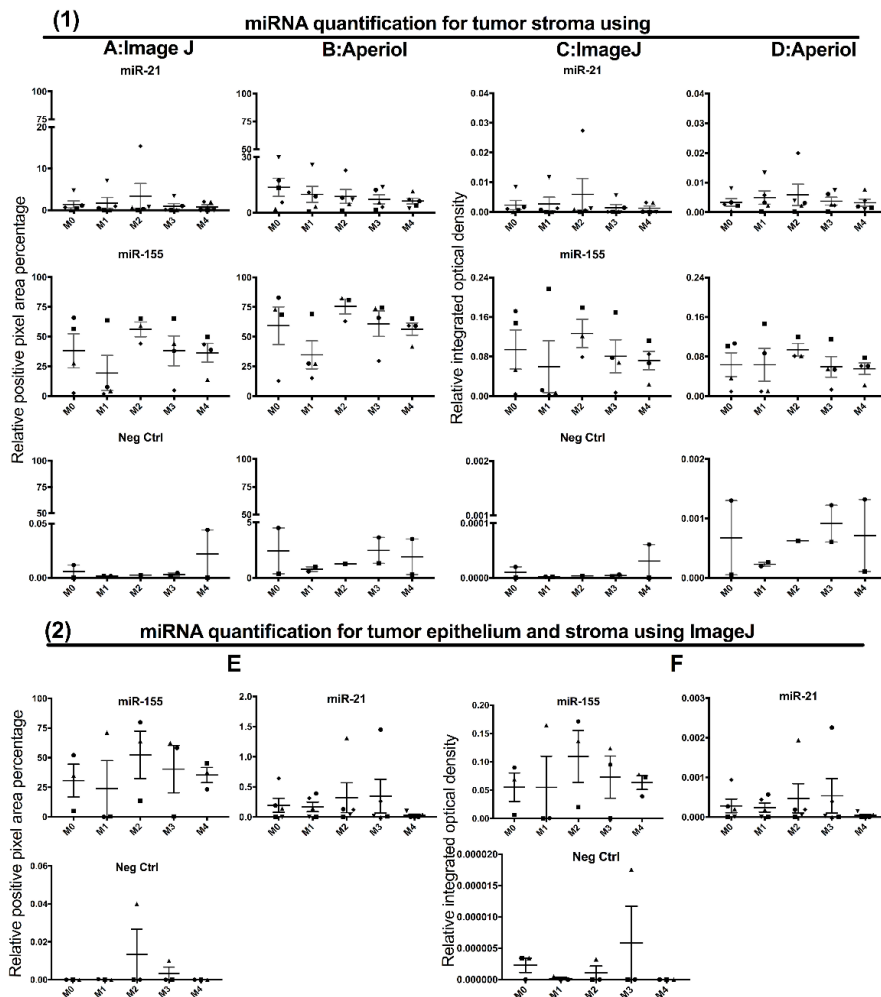


**Figure 6.** Graphs depicting quantification of miRs (miR-21 and miR-155) detected by different methods and using two different software. Means of positive pixel area percentage (PPAP, 1A and 1B) and integrated optical density (IOD, 1C and 1D) of miR signal in single ISH (control method: M0) and various combinations of double staining methods (M1-M4) were compared using paired Student’s t-test. No miR probe served as negative control tissue (Neg Ctrl). Two different types of image analysis software were used for the quantification: ImageJ (1A,1C,2E,2F) and Aperio (1B and 1D). In 2E and 2F, measurements include both tumor and stroma. Same symbols in the graphs indicate same tissue.

### 3.3. Contribution of Noise to miR Signal in the Double Staining Methods

Overall, higher PPAP and IOD for the miR stains were detected by Aperio compared to ImageJ. The contribution of noise in the PPAP and IOD measurements of miR signals were assessed against the negative controls. PPAPs of 0.044–0.22% and 0.29–4.49%, and IODs of  $0-0.2 \times 10^{-5}$  and  $1.3 \times 10^{-3}-5 \times 10^{-5}$  were observed for ImageJ and Aperio, respectively (Figure 6(1)), while they were nearly absent when the whole image (tumor epithelium and stroma) was analyzed (Figure 6(2)). Of note, the background contributing to true signals in general comes from the dark fibers present in the images (arrow Figure 5B). Color deconvolution using RGB vectors obtained for black color instead for brown (DAB) took away this unspecific signal from darkly stained tissues (DAB saturated) and dark fibers (Figure 5E), and therefore the latter was used in the successive color deconvolution of the images.

Since all methods gave comparable results, the least technically challenging and most straightforward method (M3) was chosen for miR-204 staining of the OSCC cohort. Aperio was chosen for the quantification of the staining for the cohort due to the more convenient use of the deconvolution plugin and the automated quantification steps.

### 3.4. Cohort Description and Prognostic Significance of Clinico-Pathological Parameters

Tests of associations in between clinicopathological parameters (Pearson's Chi-square: Phi and Cramer's V test) showed significant association of WPI type 4 ( $p = 0.042$ ), high tumor budding ( $p = 0.051$ ), and late tumor stage group (3 and 4) ( $p = 0.027$ ) with higher recurrence. Higher tumor budding ( $p = 0.019$ ) and late tumor stage ( $p = 0.000$ ) were associated with increased risk of lymph node metastasis. Localization of tumor in gingiva ( $p = 0.001$ ) compared to tongue, and poor histological degree of differentiation ( $p = 0.007$ ) were associated with late tumor stages. Tumor budding showed significant association with WPI ( $p = 0.001$ ) and histological degree of differentiation ( $p = 0.004$ ). Significant association between tumor stage and depth of invasion ( $p = 0.000$ ), alcohol and gender ( $p = 0.005$ ), smoking and gender ( $p = 0.001$ ), smoking and alcohol ( $p = 0.000$ ), age and gender ( $p = 0.001$ ), higher proportion of males were in the age group >65, age and tumor site ( $p = 0.031$ ), and age and smoking ( $p = 0.001$ ), lower proportion of smokers in age group >65 were also observed. KM survival analysis of the clinicopathological parameters demonstrated significantly lower OS for lymph node metastasis and late tumor stage groups (Figure 7). For age groups, age group greater than 65 showed poorer OS compared to the younger group. OS was poorer with poorer histological degree of differentiation and when the site of tumor was the gingiva (Figure 7). Subsequent univariate Cox regression of the clinicopathological variables showed significant increase in relative risk of death for age group >65 years, late stage tumor, and lymph node metastasis. Tumor site in gingiva and poor histological degree of differentiation also showed significant increase in OS risk (Table 1). Multivariate Cox regression of the significant parameters in the univariate model revealed age and tumor stage as the independent predictors of the OS (Table 2). Only tumor stage showed significant association with RFS in the univariate analysis (Table 1). Late tumor stages approximately doubled the risk of recurrence compared to early tumor stages (Table 2).

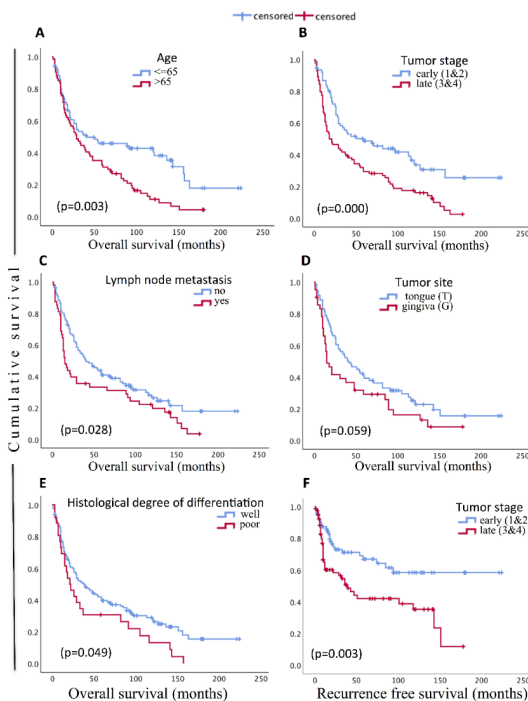


**Figure 7.** Kaplan–Meir plots of the survival functions (overall survival and recurrence-free survival) for sub-groups defined by different clinicopathological parameters and associated *p*-values (log-rank test). Only parameters with significant ( $p < 0.05$ ) or near significant survival differences are shown.

**Table 1.** Univariate estimates of the risks of the clinicopathological parameters by Cox regression.

Parameters	N (%)	Overall Survival		Recurrence Free Survival	
		<i>p</i> -Value	HR (95% CI)	<i>p</i> -Value	HR (95% CI)
miR-204_TF					
Low	67 (41.9)	0.04	1 0.657 (0.44–0.98)	0.036	1 0.56 (0.33–0.96)
High	65 (40.8)				
miR-204_TC					
Low	79 (49.4)	0.234	1 0.804 (0.56–1.15)	0.245	1 0.75 (0.46–1.22)
High	79 (49.4)				
Age (years)					
≤65	85 (53.1)	0.003	1 1.73 (1.20–2.48)	0.333	1 0.27 (0.78–2.08)
>65	74 (46.3)				
Gender					
Female	58 (36.3)	0.296	1 1.22 (0.84–1.8)	0.191	1 1.42 (0.84–2.38)
Male	102 (60.5)				
Alcohol					
Low-Normal	51 (31.9)	0.137	1 1.47 (0.89–2.43)	0.51	1 1.23 (0.63–2.55)
Moderate-High	35 (21.9)				
Smoking					
No	49 (30.6)	0.44	1 1.18 (0.78–1.79)	0.287	1 1.37 (0.77–2.46)
Yes	75 (46.9)				

Table 1. Cont.

Parameters	N (%)	Overall Survival		Recurrence Free Survival	
		p-Value	HR (95% CI)	p-Value	HR (95% CI)
Tumor site					
Tongue	71 (44.4)	0.063	1	0.591	1
Gingiva	42 (26.3)				
Stage					
Early (1&2)	76 (47.5)	0.001	1	0.004	1
Late (3&4)	84 (52.5)				
T stage		0.005		0.032	
T1			1		1
T2		0.002	1.90 (1.13–3.21)	0.107	1.82 (0.88–3.77)
T3		0.104	1.63 (0.90–2.929)	0.178	1.76 (0.77–4.02)
T4		0	2.47 (1.50–4.07)	0.003	2.86 (1.42–5.77)
Lymph node					
No metastasis	112 (87.0)	0.031	1	0.108	1
Metastasis	48 (30)				
Distant metastasis					
No	139 (86.9)	0.113	1	0.662	1
Yes	21 (13.1)				
Depth of invasion					
Superficial (<4mm)	41 (25.6)	0.21	1	0.261	1
Deep (≥4mm)	46 (28.7)				
Tumor budding score					
Low (<5 buds)	72 (45)	0.647	1	0.19	1
High (≥5 buds)	58 (36)				
Histological degree of differentiation					
Well diff	72 (45)	0.053	1	0.392	1
Poor diff	58 (36)				
Worst pattern of invasion					
Type 1–3	19 (11.9)	0.578	1	0.187	1
Type 4	111 (69.4)				

Table 2. Multivariate Cox regression for the significant parameters from the univariate model and miR expressions.

Parameters	N (%)	<sup>a</sup> Overall Survival		<sup>b</sup> Recurrence Free Survival	
		p-Value	HR (95% CI)	p-Value	HR (95% CI)
miR-204_TF					
Low	67 (41.9)	0.048	1	0.033	1
High	65 (40.8)				
miR-204_TC					
Low	79 (49.4)	0.26	1	0.193	1
High	79 (49.4)				
Age (years)					
≤65	85 (53.1)	0.004	1		
>65	74 (46.3)				
Stage					
Early (1&2)	76 (47.5)	0.005	1	0.004	1
Late (3&4)	84 (52.5)				
Lymph node					
No metastasis	112 (87.0)	0.108	1		
Metastasis	48 (30)				

<sup>a</sup> Adjusted for age and tumor stage; <sup>b</sup> Adjusted for tumor stage.

### 3.5. Expression of miR-204 in NHOM and OSCC

Expression of miR-204 was very low in the connective tissue subjacent to normal oral mucosa, followed by significantly higher expression in the peritumoral regions, stroma of tumor front, and tumor center, in ascending order (Figure 4). However, both intertumor and intratumor heterogeneity in stromal expression of miR-204 was observed in OSCC samples (Figure 4). A subset of OSCCs expressed stromal miR-204 at a comparative level to the connective tissue of NHOM. Another subset of OSCC tissues showed higher expression of stromal miR-204, with higher expression in the stroma of the tumor center compared to the stroma of the tumor front. Nevertheless, concurrent expression of miR-204 in the stroma in tumor center and stroma in the tumor front was observed, with Spearman's rho correlation revealing a very strong significant correlation ( $r_s = 0.903$ ;  $p = 0.000$ ). A concomitant expression of miR-204 in the stroma and tumor cells was also observed (Figure 4A). Since qRT-PCR is widely accepted as the gold standard for miR expression analyses, to further validate that the double ISH-IHC method is sensitive and specific enough for quantification of miR-204 in FFPE samples we performed qRT-PCR on 10% of the cohort samples (16 randomly selected tissue samples). The correlation analysis revealed a significant correlation (Pearson  $r = 0.60$ ;  $p = 0.01$ ) between the two methods (Figure S1).

### 3.6. Prognostic Significance of Stromal miR-204

A Pearson Chi-square test of miR-204 expression with the clinical variables showed significant association ( $p = 0.018$ ) of miR-204 expression in the stroma of the tumor center with histological degree of differentiation. Near significant association ( $p = 0.052$ ) with the same was observed for miR-204 expression in the stroma of the tumor front. For all other variables, no association was found. The test showed independence of age, gender, smoking, and alcohol with all the clinical variables, except for association of age with death ( $p < 0.001$ ). Further association tests by Spearman rho correlation between miR-204 expressions with the clinical variables showed significant positive association of stromal miR-204 in the tumor center with histological degree of differentiation ( $r = -0.189$ ;  $p < 0.05$ ), i.e., increased histological differentiation was linked to higher miR-204 expression.

KM analysis of survival difference of the miR-204 high and miR-204 low group in the stroma in the tumor front predicted significantly better OS and RFS for high miR-204 group. Though statistical significance was not obtained, similar survival distribution appeared for the stromal miR-204 groups in the tumor center (Figure 8). In line with KM analysis, univariate Cox regression showed significant reduction in the relative risk of dying by 34.3% and recurrence by 46% for the miR-204 high group. miR-204 expression predicted similar outcomes in the multivariate model after adjusting for the age and tumor stage for OS and adjusting for stage in RFS (Table 2).

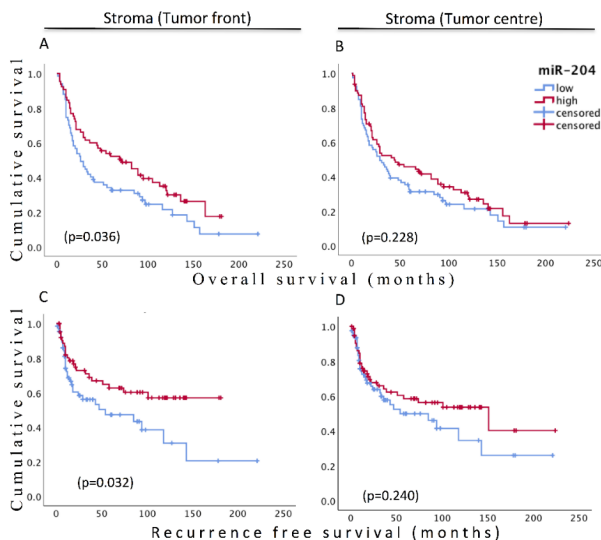


**Figure 8.** Kaplan–Meir survival plots (overall survival and recurrence-free survival) for low and high miR-204 expression groups in the stroma at the tumor front (A,C) and tumor center (B,D). *p* values are derived from log-rank test.

#### 4. Discussion

Information on spatial location and distribution of miR in cancer tissues that is obtainable through miRs staining is more informative than the PCR-based methods and provides details on the role of cell- or tissue compartment-specific miRs in cancer. In addition, while staining of miRs informs us about their presence/absence in comparison to the normal adjacent tissues and hence their involvement in carcinogenesis, concomitant IHC for proteins can provide better mechanistic insights into cancer progression by miRs. Thus, dual staining of miR and protein provides superior information that might be used for a more accurate stratification of patients compared to individual detection of biomarkers. In our study, the double staining allowed us to accurately identify tumor stroma. Methods employing dual staining of miR and protein in same tissue section have been achieved recently in some studies, mostly using fluorochromes [13,35–37] or chromogens Nuovo [38]. A major drawback with the established methods is that the information on the influence of IHC on staining of miR by ISH is lacking, with most of the established methods being limited to IHC performed only after miR ISH. This study adds in the flexibility to stain low expressed miR or proteins after the ones with higher expression.

Different alternatives of combining miR ISH and pan-CK IHC were tested (Figure 1) and the effect of the steps involved in the double staining methods on staining outcome of individual stains were also examined. All the combined methods tested in this study could reliably detect pan-CK and miRs in a single FFPE tissue section. The primary concern was if DAB-based IHC would affect the miR ISH stain. Single miRs ISH with counter nuclear staining (method M0) was taken as a control method, and all other methods were compared to it. Method 1, miR ISH and subsequent IHC, was chosen to see if IHC would diminish or overlay ISH staining, and to find out whether primary antibodies in the IHC method can still find the antigen epitopes. Methods 2 and 3 were chosen to see if miR probe bound to miR or Fab bound to the DIG-linked probe in the miR-binding probe would be affected by steps involved in IHC. DAB reaction was introduced before NBT-BCIP reaction in method 2 to test if the DAB product would affect Fab-AP accessibility to NBT-BCIP



reaction. DAB reaction was conducted at the final step in method 3, to see the similar effects of DAB reaction and/or product on miR stain as in method 1. Method 4 was chosen to see how IHC staining (DAB product) would affect miR accessibility, miR probe binding, and thus the final miR staining. On the other hand, the methods were also a guide as to how IHC staining is affected by steps involved in miR staining in the combined double staining methods.

All the protocols used showed absence of nonspecific miR signals by using different negative controls. One such negative control for the miR-specific probes is to use scramble oligonucleotide probes with no target-binding site. In this study a scramble oligonucleotide was tested at five different temperatures (48 °C, 50 °C, 51 °C, 53 °C, and 55 °C). The scramble oligonucleotide showed positive staining at 48 °C. Therefore, despite lacking any target-binding site, a scramble oligonucleotide may not be a universal control probe. A more suitable scramble control is the one with a melting temperature the same as that of miR specific probe. In ISH, melting temperature of a target oligonucleotide probe largely determines its specificity. The higher the hybridization temperature, the higher the specificity, but this may compromise the signal. On the contrary, a lower hybridization temperature may increase signal, but can result in cross-hybridization to a similar sequence, causing increases in unspecific binding or the noise. Having no miR target probe in a negative control in miR ISH is a test for antibody specificity, and a measure of efficient blocking. Failure in specific antibody binding, and insufficient blocking, both result in a false positive signal. Specific tissues can also be used as controls based upon established staining results, but the results can be the function of sensitivity of the methods used. Here we used miR-21 on OSCC samples; miR-21 is a well-established tumor stroma-specific miR in OSCC and it is not expressed in normal oral mucosa; however, it is also not expressed in a subgroup of oral cancers [13]. Therefore, inter-individual and intra-tissue heterogeneity that may result in heterogeneous staining outcomes should also be considered when evaluating the controls.

Noise and signal are completely unavoidable in any staining methods. Color deconvolution to blue from darkly stained DAB was observed previously in a pioneering color deconvolution study by Ruifrok and Johnston [39]. We have been able to remove a major part of the noise by demonstrating that vectors obtained for black color instead for brown (DAB) can take away signal from saturated stain and dark fibers. Another way to avoid noise would be to exclude such tissue compartments from annotation. In our observation, noise can also occur from inefficient blocking, low hybridization temperature, high antibody and substrate concentration, incubation and/or reaction temperature, and time. We also found a nonspecific binding of anti-DIG-Fab to stroma in normal oral mucosa. Perhaps this is inherent to some tissues or an outcome of harsh pre-treatments.

ImageJ is an open source program for image analysis. Free availability of ImageJ and its plugins is a major advantage over AperioI in image quantification. However, there are a few limitations. The first is related to annotation. Distance and area measurement require additional steps such as setting up the scale measurements and command for the measurements. In addition, annotations need to be permanently saved within the pictures if they are to be analyzed or revisited later. The annotation shortcomings of ImageJ can be compensated by annotation using freely available software such as NDP.view2 (Hamamatsu) or AperioI. Secondly, unless one can program ImageJ to record and install macros for the steps involved in quantification such as annotation selection, deconvolution, threshold setting, and quantification, for automated analysis and batch feeding, all the steps need to be carried out one at a time, and pictures fed individually, which takes a significant amount of time. All these steps are automated in AperioI and take less time, but the plugin required for the quantification requires paid licensing. In addition, introducing a new vector (color) in ImageJ color deconvolution plugin is technically challenging, while it is user friendly in AperioI once one has the plugin.

We further showed that the combined method gives comparable quantifiable results to the gold standard method of qRT-PCR, in addition to having the advantage of showing

cellular localization of the miR of interest. Although the aim of this study was not to investigate the expression of miR-21 and miR-155, and their staining was done on only a limited number of cases here, our results further confirm their pattern of expression in OSCC. MiR-21 was previously shown to be expressed exclusively in the tumor stroma of OSCC and to correlate with poor prognosis [13]. It was also shown to have a biological importance in development of tongue squamous cell carcinoma by inhibiting cancer cell apoptosis [40] and regulation of the expression of multiple target genes important for cancer progression such as phosphatase and tensin homolog (PTEN) and programmed cell death protein 4 (PDCD4) that regulate the radiosensitivity and sensitivity to cisplatin in OSCC [41]. MiR-155-5p has been previously shown to be expressed in both tumor cells and the associated stroma of OSCC, as confirmed by our staining pattern as well. However, the focus has been on its biological role in tumor cells and its expression was linked to EMT-associated OSCC progression [42].

A major limitation of our combined ISH and IHC double staining methods is that our methods are limited to antibodies that can be used with a proteinase K treatment for antigen retrieval in FFPE tissues. We have not tested antibodies that require other retrieval procedures. However, frozen tissues could be used for miR ISH and protein IHC without any pre-treatment [37]. In this study, the focus was on the quantification of the miR, while the visualization of protein (pan-CK) by IHC was used to differentiate between tumor and stromal compartments. In the context of a high degree of heterogeneity of both tumor cells and tumor stroma, the combinatorial detection of miR and one or more marker proteins at the same time will provide additional advantages for further cell identification and characterization. Although challenging, this methodological approach can also be further developed to determine co-expression of a miR and a potential target protein and to quantify the results of both ISH and IHC (including in addition to one miR, a second and/or a third protein) in the case of co-localization. The proteinase K digestion step used to improve tissue access in the protocols presented here may damage or remove some protein antigens, therefore the prehybridization digestion step must be particularly optimized and evaluated for a further, broader applicability.

After establishing a combined ISH-IHC method and digital quantification for the miRs, we tested the method in a clinically relevant biomarker quest on an OSCC cohort. Age, tumor stage, lymph node metastasis, and recurrence are the well-recognized prognostic indicators in OSCC. In this cohort we found tumor stage and age to be independent prognostic indicators of survival. Similarly, tumor stage was an independent prognostic indicator of recurrence. Lymph node metastasis and poor histological degree of tumor differentiation correlated with reduced survival in the univariate analysis. As reported in previous OSCC studies, we found that higher tumor stage correlated with reduced recurrence-free survival [13,34]. In this cohort the 5-year survival was 40%, which is comparable to some other previous reports [43,44]. Tumor site in the gingiva showed poorer survival compared to tumors in the tongue, probably due to its proximity to the bone leading to early bone invasion and the association with late tumor stages.

This study indicates a dynamic and complex regulation of miR-204 in the stroma of OSCC. Previous studies in different cancers including OSCC showed overall reduced expression of miR-204 [15–17]. Higher levels of miR-204 have been associated with better survival in several cancer types [16,17,20,22,23], including OSCC [25]. These findings are in line with our study, which shows association of higher expression of miR-204 with better survival, albeit the association is only for stromal expression, not whole tumor. Contrary to the previous study on whole tumor tissues, the present study finds an increased expression of miR-204 in the stroma in a subset of OSCC tissues when compared to NHOM. Nevertheless, previous studies on breast cancer [17] and OSCC [25] also exhibited a subset of tumors in which miR-204 expression was higher than a subset of the normal counterpart tissues. Meanwhile, cell context-based tumor suppressive and oncogenic dual function of miR-204 in pancreatic cancer cells lines [45], and miR-204 expression-dependent metastasis of cancer cells in vivo in mice, have been shown earlier [17].

Moreover, compared to NHOM, we also found a relatively higher expression of miR-204 in the matched peritumoral connective tissue of the high miR-204-expressing OSCC, often subjacent to epithelial dysplastic changes. This may indicate that alterations of miR-204 occur early in carcinogenesis and evolve concomitant to cancer progression, at least in a subset of OSCC. These findings might point towards increased miR-204 expression as a protective mechanism that the stroma develops as a reaction to the progressive changes in the epithelium. This is the first study to show that, similar to the antitumor effect when expressed in tumor cells, high expression of miR-204 in stromal cells is also detrimental to tumor progression. Hence, this study on patient material, together with previous studies, suggests a prognostic benefit of higher expression of miR-204 in cancers including OSCC.

## 5. Conclusions

The approach of using pan-CK to exclude epithelium, especially difficult when identifying single cells or poorly differentiated cancer cells, is important in studying tumor stroma in tumors of epithelial origin. The double staining and the quantification methods demonstrated in this study can be used in integrative biomarker studies based on the same tissue sections that can provide superior information to single biomarkers. We have applied the method in studying stromal miR-204 in OSCC and found miR-204 as a prognostic indicator of survival and recurrence-free survival in OSCC.

**Supplementary Materials:** The following are available online at <https://www.mdpi.com/2072-6694/13/6/1307/s1>, Figure S1: QQ correlation plot between the levels of miR-204 detected by qRT-PCR (y-axis) and by dual ISH-IHC (method 3—x-axis) in 16 FFPE tissue sections, Table S1: Clinical and pathological characteristics of the OSCC cohort.

**Author Contributions:** Conceptualization, S.R. and D.E.C.; methodology, S.R., H.D., H.P., A.M., E.S.N., A.K., S.L., D.S., D.E.C.; software, S.R. and H.D.; formal analysis, S.R., H.D., D.S.; investigation, S.R., H.D., H.P., A.M., E.S.N., A.K., S.L., D.S., D.E.C.; writing—original draft preparation, S.R.; writing—review and editing, S.R., H.D., H.P., A.M., E.S.N., A.K., S.L., D.S., A.C.J. and D.E.C.; visualization, S.R., H.D., A.M., D.S.; supervision, D.S., A.C.J. and D.E.C.; project administration, D.S., A.C.J. and D.E.C.; funding acquisition, A.C.J. and D.E.C. All authors have read and agreed to the published version of the manuscript.

**Funding:** This research was funded by research Council of Norway through its Centers of Excellence funding scheme (Grant No. 22325), The Western Norway Regional Health Authority (Helse Vest project nr. 912260/2019), and The Norwegian Centre for International Cooperation in Education (project number CPEA-LT-2016/10106).

**Institutional Review Board Statement:** The study was conducted according to the guidelines of the Declaration of Helsinki and approved by The Ethical Committee of West Norway (REK Vest 3.2006.2620 REKVest 3.2006.1341).

**Informed Consent Statement:** Informed consent was obtained from all subjects involved in the study that were alive at the beginning of the study. Patient consent was waived for the patients who were dead at the beginning of the study.

**Data Availability Statement:** Data supporting reported results will be made publicly available if the manuscript is accepted for publication.

**Conflicts of Interest:** The authors declare no conflict of interest.

## References

1. Kalluri, R. The biology and function of fibroblasts in cancer. *Nat. Rev. Cancer* **2016**, *16*, 582–598. [[CrossRef](#)] [[PubMed](#)]
2. Kalluri, R.; Zeisberg, M. Fibroblasts in cancer. *Nat. Rev. Cancer* **2006**, *6*, 392–401. [[CrossRef](#)] [[PubMed](#)]
3. Ronnov-Jessen, L.; Petersen, O.W.; Bissell, M.J. Cellular changes involved in conversion of normal to malignant breast: Importance of the stromal reaction. *Physiol. Rev.* **1996**, *76*, 69–125. [[CrossRef](#)]
4. Hayes, J.; Peruzzi, P.P.; Lawler, S. MicroRNAs in cancer: Biomarkers, functions and therapy. *Trends Mol. Med.* **2014**, *20*, 460–469. [[CrossRef](#)] [[PubMed](#)]
5. Shenouda, S.K.; Alahari, S.K. MicroRNA function in cancer: Oncogene or a tumor suppressor? *Cancer Metastasis Rev.* **2009**, *28*, 369–378. [[CrossRef](#)]

6. Zhang, B.; Pan, X.; Cobb, G.P.; Anderson, T.A. microRNAs as oncogenes and tumor suppressors. *Dev. Biol.* **2007**, *302*, 1–12. [[CrossRef](#)]
7. Min, A.; Zhu, C.; Peng, S.; Rajthala, S.; Costea, D.E.; Sapkota, D. MicroRNAs as Important Players and Biomarkers in Oral Carcinogenesis. *BioMed Res. Int.* **2015**, *2015*, 1–10. [[CrossRef](#)]
8. Chen, L.; Jin, H. MicroRNAs as novel biomarkers in the diagnosis of non-small cell lung cancer: A meta-analysis based on 20 studies. *Tumor Biol.* **2014**, *35*, 9119–9129. [[CrossRef](#)] [[PubMed](#)]
9. Ye, Y.; Wang, Y.; Roth, J.; Wu, X. Abstract 298: Serum MicroRNAs as biomarkers in early stage non-small cell lung cancer. *Epidemiology* **2014**, *74*, 298. [[CrossRef](#)]
10. Zahran, F.; Ghalwash, D.; Shaker, O.; Al-Johani, K.; Scully, C. Salivary microRNAs in oral cancer. *Oral Dis.* **2015**, *21*, 739–747. [[CrossRef](#)] [[PubMed](#)]
11. Mlcochova, H.; Hezova, R.; Stanik, M.; Slaby, O. Urine microRNAs as potential noninvasive biomarkers in urologic cancers. *Urol. Oncol. Semin. Orig. Investig.* **2014**, *32*, 41.e1–41.e9. [[CrossRef](#)]
12. Yang, J.-Y.; Sun, Y.-W.; Liu, D.-J.; Zhang, J.F.; Li, J.; Hua, R. MicroRNAs in stool samples as potential screening biomarkers for pancreatic ductal adenocarcinoma cancer. *Am. J. Cancer Res.* **2014**, *4*, 663–673.
13. Hedbäck, N.; Jensen, D.H.; Specht, L.; Fiehn, A.-M.K.; Therkildsen, M.H.; Friis-Hansen, L.; Dabelsteen, E.; Von Buchwald, C. MiR-21 Expression in the Tumor Stroma of Oral Squamous Cell Carcinoma: An Independent Biomarker of Disease Free Survival. *PLoS ONE* **2014**, *9*, e95193. [[CrossRef](#)]
14. Bartel, D.P. MicroRNAs: Genomics, biogenesis, mechanism, and function. *Cell* **2004**, *116*, 281–297. [[CrossRef](#)]
15. Xia, Y.; Zhu, Y.; Ma, T.; Pan, C.; Wang, J.; He, Z.; Li, Z.; Qi, X.; Chen, Y. miR-204 functions as a tumor suppressor by regulating SIX1 in NSCLC. *FEBS Lett.* **2014**, *588*, 3703–3712. [[CrossRef](#)]
16. Sacconi, A.; Biagioni, F.; Canu, V.; Mori, F.; Di Benedetto, A.; Lorenzon, L.; Ercolani, C.; Cambria, A.; Germoni, S.; et al. miR-204 targets Bcl-2 expression and enhances responsiveness of gastric cancer. *Cell Death Dis.* **2012**, *3*, e423. [[CrossRef](#)]
17. Hong, B.S.; Ryu, H.S.; Kim, N.; Kim, J.; Lee, E.; Moon, H.; Kim, K.H.; Jin, M.-S.; Kwon, N.H.; Kim, S.; et al. Tumor Suppressor miRNA-204-5p Regulates Growth, Metastasis, and Immune Microenvironment Remodeling in Breast Cancer. *Cancer Res.* **2019**, *79*, 1520–1534. [[PubMed](#)]
18. Flores-Pérez, A.; Marchat, L.A.; Rodríguez-Cuevas, S.; Bautista-Piña, V.; Hidalgo-Miranda, A.; Ocampo, E.A.; Martínez, M.S.; Palma-Flores, C.; Fonseca-Sánchez, M.A.; La Vega, H.A.-D.; et al. Dual targeting of ANGPT1 and TGFBR2 genes by miR-204 controls angiogenesis in breast cancer. *Sci. Rep.* **2016**, *6*, 34504. [[CrossRef](#)] [[PubMed](#)]
19. Bao, W.; Wang, H.-H.; Tian, F.-J.; He, X.-Y.; Qiu, M.-T.; Wang, J.-Y.; Zhang, H.-J.; Wang, L.H.; Wan, X.-P. A TrkB-STAT3-miR-204-5p regulatory circuitry controls proliferation and invasion of endometrial carcinoma cells. *Mol. Cancer* **2013**, *12*, 155. [[CrossRef](#)] [[PubMed](#)]
20. Barambe, H.S.; Paul, R.; Panwalkar, P.; Jalali, R.; Sridhar, E.; Gupta, T.; Moiyadi, A.; Shetty, P.; Kazi, S.; Deogharkar, A.; et al. Downregulation of miR-204 expression defines a highly aggressive subset of Group 3/Group 4 medulloblastomas. *Acta Neuropathol. Commun.* **2019**, *7*, 52. [[CrossRef](#)] [[PubMed](#)]
21. Imam, J.S.; Plyler, J.R.; Bansal, H.; Prajapati, S.; Bansal, S.; Rebeles, J.; Chen, H.-I.H.; Chang, Y.F.; Panneerodoss, S.; Zoghi, B.; et al. Genomic Loss of Tumor Suppressor miRNA-204 Promotes Cancer Cell Migration and Invasion by Activating AKT/mTOR/Rac1 Signaling and Actin Reorganization. *PLoS ONE* **2012**, *7*, e52397. [[CrossRef](#)]
22. Butrym, A.; Rybka, J.; Baczynska, D.; Tukiendorf, A.; Kuliczowski, K.; Mazur, G. Low expression of microRNA-204 (miR-204) is associated with poor clinical outcome of acute myeloid leukemia (AML) patients. *J. Exp. Clin. Cancer Res.* **2015**, *34*, 1–5. [[CrossRef](#)]
23. Ryan, J.; Tivnan, A.; Fay, J.; Bryan, K.; Meehan, M.; Creevey, L.; Lynch, J.; Bray, I.M.; O'Meara, A.; Tracey, L.; et al. MicroRNA-204 increases sensitivity of neuroblastoma cells to cisplatin and is associated with a favourable clinical outcome. *Br. J. Cancer* **2012**, *107*, 967–976. [[CrossRef](#)]
24. Tsai, S.-C.; Huang, S.-F.; Chiang, J.-H.; Chen, Y.-F.; Huang, C.-C.; Tsai, M.-H.; Tsai, F.-J.; Kao, M.-C.; Yang, J.-S. The differential regulation of microRNAs is associated with oral cancer. *Oncol. Rep.* **2017**, *38*, 1613–1620. [[CrossRef](#)]
25. Chattopadhyay, E.; Singh, R.; Ray, A.; Roy, R.; De Sarkar, N.; Paul, R.R.; Pal, M.; Aich, R.; Roy, B. Expression deregulation of mir31 and CXCL12 in two types of oral precancers and cancer: Importance in progression of precancer and cancer. *Sci. Rep.* **2016**, *6*, 32735. [[CrossRef](#)] [[PubMed](#)]
26. Lee, Y.; Yang, X.; Huang, Y.; Fan, H.; Zhang, Q.; Wu, Y.; Li, J.; Hasina, R.; Cheng, C.; Lingen, M.W.; et al. Network Modeling Identifies Molecular Functions Targeted by miR-204 to Suppress Head and Neck Tumor Metastasis. *PLoS Comput. Biol.* **2010**, *6*, e1000730. [[CrossRef](#)] [[PubMed](#)]
27. Yu, C.-C.; Chen, P.-N.; Peng, C.-Y.; Yu, C.-H.; Chou, M.Y. Suppression of miR-204 enables oral squamous cell carcinomas to promote cancer stemness, EMT traits, and lymph node metastasis. *Oncotarget* **2016**, *7*, 20180–20192. [[CrossRef](#)]
28. Shi, L.-J.; Zhang, C.-Y.; Zhou, Z.-T.; Ma, J.-Y.; Liu, Y.; Bao, Z.-X.; Jiang, W.-W. MicroRNA-155 in oral squamous cell carcinoma: Overexpression, localization, and prognostic potential. *Head Neck* **2014**, *37*, 970–976. [[CrossRef](#)] [[PubMed](#)]
29. Ni, Y.-H.; Huang, X.-F.; Wang, Z.-Y.; Han, W.; Deng, R.-Z.; Mou, Y.-B.; Ding, L.; Hou, Y.-Y.; Hu, Q.-G. Upregulation of a potential prognostic biomarker, miR-155, enhances cell proliferation in patients with oral squamous cell carcinoma. *Oral Surg. Oral Med. Oral Pathol. Oral Radiol.* **2014**, *117*, 227–233. [[CrossRef](#)]
30. Concato, J.; Peduzzi, P.; Holford, T.R.; Feinstein, A.R. The Importance of Events Per Independent Variable in Proportional Hazards and Other Multivariable Analyses. I. Background, goals, and general strategy. *J. Clin. Epidemiol.* **1995**, *48*, 1495–1501. [[CrossRef](#)]

31. Altman, D.G.; McShane, L.M.; Sauerbrei, W.; Taube, S.E. Reporting Recommendations for Tumor Marker Prognostic Studies (REMARK): Explanation and elaboration. *PLoS Med.* **2012**, *9*, e1001216. [[CrossRef](#)]
32. Woolgar, J.A.; Scott, J. Prediction of cervical lymph node metastasis in squamous cell carcinoma of the tongue/floor of mouth. *Head Neck* **1995**, *17*, 463–472. [[CrossRef](#)]
33. Almangush, A.; Bello, I.O.; Keski-Säntti, H.; Mäkinen, L.K.; Kauppila, J.H.; Pukkila, M.; Hagström, J.; Laranne, J.; Tommola, S.; Nieminen, O.; et al. Depth of invasion, tumor budding, and worst pattern of invasion: Prognostic indicators in early-stage oral tongue cancer. *Head Neck* **2013**, *36*, 811–818. [[CrossRef](#)]
34. Brandwein-Gensler, A.; Teixeira, M.S.; Lewis, C.M.; Lee, B.; Rolnitzky, L.; Hille, J.J.; Genden, E.; Urken, M.L.; Wang, B.Y. Oral squamous cell carcinoma—Histologic risk assessment, but not margin status, is strongly predictive of local disease-free and overall survival. *Am. J. Surg. Pathol.* **2005**, *29*, 167–178. [[CrossRef](#)] [[PubMed](#)]
35. Sempere, L.F.; Preis, M.; Yezefski, T.; Ouyang, H.; Suriawinata, A.A.; Silahatoglu, A.; Conejo-Garcia, J.R.; Kauppinen, S.; Wells, W.; Korc, M. Fluorescence-Based Codetection with Protein Markers Reveals Distinct Cellular Compartments for Altered MicroRNA Expression in Solid Tumors. *Clin. Cancer Res.* **2010**, *16*, 4246–4255. [[CrossRef](#)]
36. Chaudhuri, A.D.; Yelamanchili, S.V.; Fox, H.S. Combined fluorescent in situ hybridization for detection of microRNAs and immunofluorescent labeling for cell-type markers. *Front. Cell. Neurosci.* **2013**, *7*, 160. [[CrossRef](#)] [[PubMed](#)]
37. Nielsen, B.S.; Holmström, K. Combined MicroRNA In Situ Hybridization and Immunohistochemical Detection of Protein Markers. *Methods Mol. Biol.* **2013**, *986*, 353–365. [[CrossRef](#)]
38. Nuovo, G.J. In situ detection of microRNAs in paraffin embedded, formalin fixed tissues and the co-localization of their putative targets. *Methods* **2010**, *52*, 307–315. [[CrossRef](#)]
39. Ruifrok, A.C.; Johnston, D.A. Quantification of histochemical staining by color deconvolution. *Anal. Quant. Cytol. Histol.* **2001**, *23*, 291–299. [[PubMed](#)]
40. Li, J.; Huang, H.; Sun, L.; Yang, M.; Pan, C.; Chen, W.; Wu, D.; Lin, Z.; Zeng, C.; Yao, Y.; et al. MiR-21 Indicates Poor Prognosis in Tongue Squamous Cell Carcinomas as an Apoptosis Inhibitor. *Clin. Cancer Res.* **2009**, *15*, 3998–4008. [[CrossRef](#)] [[PubMed](#)]
41. Irimie-Aghiorghiesei, A.I.; Pop-Bica, C.; Pintea, S.; Braicu, C.; Cojocneanu, R.; Zimța, A.-A.; Gulei, D.; Slabý, O.; Berindan-Neagoe, I. Prognostic Value of MiR-21: An Updated Meta-Analysis in Head and Neck Squamous Cell Carcinoma (HNSCC). *J. Clin. Med.* **2019**, *8*, 2041. [[CrossRef](#)] [[PubMed](#)]
42. Kim, H.; Yang, J.M.; Ahn, S.-H.; Jeong, W.-J.; Chung, J.-H.; Paik, J.H. Potential Oncogenic Role and Prognostic Implication of MicroRNA-155-5p in Oral Squamous Cell Carcinoma. *Anticancer. Res.* **2018**, *38*, 5193–5200. [[CrossRef](#)]
43. Parkin, D.M.; Pisani, P.; Ferlay, J. Global cancer statistics. *CA A Cancer J. Clin.* **1999**, *49*, 33–64. [[CrossRef](#)]
44. Lo, W.-L.; Kao, S.-Y.; Chi, L.-Y.; Wong, Y.-K.; Chang, R.C.-S. Outcomes of oral squamous cell carcinoma in Taiwan after surgical therapy: Factors affecting survival. *J. Oral Maxillofac. Surg.* **2003**, *61*, 751–758. [[CrossRef](#)]
45. Ding, M.; Lin, B.; Li, T.; Liu, Y.; Li, Y.; Zhou, X.; Miao, M.; Gu, J.; Pan, H.; Yang, F.; et al. A dual yet opposite growth-regulating function of miR-204 and its target XRN1 in prostate adenocarcinoma cells and neuroendocrine-like prostate cancer cells. *Oncotarget* **2015**, *6*, 7686–7700. [[CrossRef](#)]

Article

# Combined in situ Hybridization and Immunohistochemistry on Archival Tissues Reveals Stromal microRNA-204 as Prognostic Biomarker for Oral Squamous Cell Carcinoma

Saroj Rajthala, Harsh Dongre, Himalaya Parajuli, Anjie Min, Elisabeth Sivy Nginamau, Arild Kvalheim, Stein Lybak, Dipak Sapkota, Anne Christine Johannessen and Daniela Elena Costea

## Supplementary Materials:

**Table S1.** Clinical and pathological characteristics of the OSCC cohort.

Parameters	N (%)	Parameters	N (%)
Gender		Histological degree of differentiation	
Female	58 (36.3) (median range 74)	Well diff	72 (45)
Male	102 (60.5) (median range 62)	Poor diff	58 (36)
Alcohol		Recurrence	
Low-Normal	51 (31.9)	No	95 (59.4)
Moderate-High	35 (21.9)	Yes	65 (40.6)
Unkown	36 (22.5)		
Smoking		Depth of invasion	
No	49 (30.6)	Superficial(<4 mm)	41 (25.6)
Yes	75 (46.9)	Deep(≥4 mm)	46 (28.7)
Unkown	36 (22.5)	Unquantifiable	73 (45.6)
Tumor Site		Tumor budding score	
Tongue	71 (44.4)	Low (<5 buds)	72 (45)
Gingvia	43 (26.9)	High (≥5 buds)	58 (36)
Buccal	20 (12.5)	Unquantifiable	30 (18.8)
Floor of mouth	18 (11.3)		
Overlapping	8 (5)		
T stage		Worst pattern of invasion	
T1	43 (26.9)	Type 1	2 (1.3)
T2	47 (29.3)	Type 2	3 (1.9)
T3	26 (16.3)	Type 3	14 (8.8)
T4	44 (27.5)	Type 4	111 (69.4)
		Unquantifiable	30 (18.8)
N stage		Distant metastatic progression	
N0	112 (70)	No	
N1	22 (13.7)	Yes	139 (86.9)
N2	26 (16.3)	Lung	21 (13.1)
N3	0	Skin	9 (5.6)
M stage		Other	5 (3.1)
M0	156 (97.5)	(bone, brain, adrenals)	7 (4.4)
M1	4 (2.5)		
Stage			
Stage I	43 (26.9)		
Stage II	37 (23.1)		
Stage III	25 (15.6)		

---

Stage IV	57 (35.6)	
		†

---

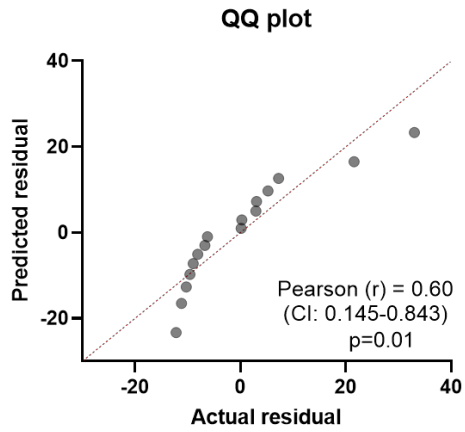


Figure S1. QQ correlation plot between the levels of miR-204 detected by qRT-PCR (y-axis) and by dual ISH-IHC (method 3—x-axis) in 16 FFPE tissue sections.



# MicroRNA-138 Abates Fibroblast Motility With Effect on Invasion of Adjacent Cancer Cells

Saroj Rajthala<sup>1,2</sup>, Himalaya Parajuli<sup>1,2</sup>, Harsh Nitin Dongre<sup>1,2</sup>, Borghild Ljøkel<sup>3</sup>, Kristin Marie Hoven<sup>3</sup>, Arild Kvalheim<sup>4</sup>, Stein Lybak<sup>3</sup>, Evelyn Neppelberg<sup>3,5</sup>, Dipak Sapkota<sup>6</sup>, Anne Christine Johannessen<sup>1,7</sup> and Daniela-Elena Costea<sup>1,2,7\*</sup>

<sup>1</sup> The Gade Laboratory for Pathology, Department of Clinical Medicine, Faculty of Medicine, University of Bergen, Bergen, Norway, <sup>2</sup> Centre for Cancer Biomarkers (CCBIO), Faculty of Medicine, University of Bergen, Bergen, Norway, <sup>3</sup> Head and Neck Clinic, Haukeland University Hospital, Bergen, Norway, <sup>4</sup> Tannteam Private Dental Practice, Bergen, Norway, <sup>5</sup> Department of Oral Surgery, Institute of Clinical Dentistry, University of Bergen, Bergen, Norway, <sup>6</sup> Department of Oral Biology, University of Oslo, Oslo, Norway, <sup>7</sup> Department of Pathology, Haukeland University Hospital, Bergen, Norway

## OPEN ACCESS

### Edited by:

Ondrej Slaby,  
Central European Institute of  
Technology (CEITEC), Czechia

### Reviewed by:

Eduardo López-Urrutia,  
National Autonomous University of  
Mexico, Mexico

Luis E. Arias-Romero,  
National Autonomous University of  
Mexico, Mexico

### \*Correspondence:

Daniela-Elena Costea  
Daniela.costea@uib.no

### Specialty section:

This article was submitted to  
Cancer Genetics,  
a section of the journal  
Frontiers in Oncology

Received: 11 December 2021

Accepted: 08 February 2022

Published: 17 March 2022

### Citation:

Rajthala S, Parajuli H, Dongre HN, Ljøkel B, Hoven KM, Kvalheim A, Lybak S, Neppelberg E, Sapkota D, Johannessen AC and Costea D-E (2022) MicroRNA-138 Abates Fibroblast Motility With Effect on Invasion of Adjacent Cancer Cells. *Front. Oncol.* 12:833582. doi: 10.3389/fonc.2022.833582

**Background:** Recent studies have shown aberrant expression of micro-RNAs in cancer-associated fibroblasts (CAFs). This study aimed to investigate miR-138 dysregulation in CAFs in oral squamous cell carcinoma (OSCC) and its effects on their phenotype and invasion of adjacent OSCC cells.

**Methods:** Expression of miR-138 was first investigated in OSCC lesions ( $n = 53$ ) and OSCC-derived CAFs ( $n = 15$ ). MiR-138 mimics and inhibitors were used to functionally investigate the role of miR-138 on CAF phenotype and the resulting change in their ability to support OSCC invasion.

**Results:** Expression of miR-138 showed marked heterogeneity in both OSCC tissues and cultured fibroblasts. Ectopic miR-138 expression reduced fibroblasts' motility and collagen contraction ability and suppressed invasion of suprajacent OSCC cells, while its inhibition resulted in the opposite outcome. Transcript and protein examination after modulation of miR-138 expression showed changes in CAF phenotype-specific molecules, focal adhesion kinase axis, and TGF $\beta$ 1 signaling pathway.

**Conclusions:** Despite its heterogeneous expression, miR-138 in OSCC-derived CAFs exhibits a tumor-suppressive function.

**Keywords:** cancer-associated fibroblasts, oral cancer, heterogeneity, motility, invasion

## INTRODUCTION

Carcinogenesis is a multistep process that is not only dependent on the intrinsic properties of cancer cells, but also determined by the host stroma or the surrounding tumor microenvironment (1–3). Fibroblasts are one of the major cell types in the stroma that can modulate the behavior of cancer cells at all stages of carcinogenesis, including metastasis (3, 4). In oral squamous cell carcinoma (OSCC), the role of cancer-associated fibroblasts (CAFs) for tumor progression has been demonstrated in *in vitro* cell culture studies (5–7) and *in vivo* animal studies (5). In clinical



studies involving patient biopsies, CAFs have been associated to lymph node metastasis (8, 9) and poor prognosis in OSCC (8–12).

Apart from genetic alterations, epigenetic changes in cancer cells, including dysregulation of micro-RNAs (miRNAs) (13, 14) have also been widely recognized to have critical roles in cancer (15, 16). Dysfunction of miRNAs in stromal cells has been as well proven and shown to support further progression of transformed epithelial cells (17). Previous studies have shown miRNA deregulation in OSCC, their role in tumor progression, and their possible use as diagnostic and prognostic biomarkers, as well as therapeutical targets (18–20). However, few studies investigated consequences of alterations of miRNAs in tumor stroma for tumor progression in general, and for OSCC in particular.

In a recent study that involved miRNA profiling of primary cultures of OSCC-derived CAFs and normal oral fibroblasts (NOFs), we found altered expression of twelve miRNAs in CAFs (21). When coupled with the results of our previous transcriptomic study on the same strains of OSCC-derived CAFs and NOFs that found integrin  $\alpha 11$  upregulated in CAFs of OSCC (5), miR-204 and miR-138 were identified by *in silico* prediction tools as possible upstream regulators of integrin  $\alpha 11$ . We further showed that indeed integrin  $\alpha 11$  is a direct target of miR-204 and that miR-204 plays an anti-invasive role in OSCC (21), but we did not investigate miR-138 for its role in OSCC.

MiR-138 has been found to be downregulated in many cancer types, including OSCC, and it was therefore coined as a tumor suppressor (22). On the other hand, it has been linked to tumor progression and recurrence in glioblastoma (23). In a previous study on OSCC (42 cases), miR-138 was shown to have a decreased expression in OSCC compared to adjacent normal mucosa (24). In another study ( $n = 35$ ), its expression was relatively higher in about half of OSCC when compared to normal oral mucosa (25). *In vitro* studies showed anti-proliferative and anti-invasive role for miR-138 when expressed in OSCC cells (26), and it was suggested to have a role in suppressing cancer stemness (27).

While the above-mentioned studies illustrate the role of miR-138 in several cancers when dysregulated in either whole tumor tissue or only in the epithelial compartment, studies on the consequences of altered miR-138 expression in stromal fibroblasts for tumor progression are, to our best knowledge, non-existent. This study aimed to investigate the role of miR-138 dysregulation in CAFs on OSCC progression.

## MATERIALS AND METHODS

### Patient Material

For miRNA *in situ* hybridization, formalin-fixed paraffin-embedded (FFPE) tissue blocks from OSCC lesions ( $n = 53$ ) were used from the diagnostic archive of the Department of Pathology of Haukeland University Hospital. Clinical data were obtained from the Electronic patient journal ( $n = 38$ , **Supplementary Table S1**). Clinical-pathological correlations of

the cohort were in line with a previous finding from larger cohorts of OSCC, indicating that the cohort could be used for preliminary biomarker analysis. Multi-variate Cox regression found tumor stage, age, and gender as independent predictors of survival with increased death risk for late tumor stage HR: 2.22 (1.03–4.76), age group above 65 HR: 2.28 (1.04–5.00), and male group HR: 4.29 (1.44–12.79), respectively (**Supplementary Figure S1**). Similarly, tumor stage was as independent predictor of recurrence-free survival, with increased risk for recurrence for the late stage group HR: 3.662 (1.18–11.31). Controlled for tumor stage, tumor site predicted higher risk of recurrence for OSCC lesions involving gingiva compared to tongue HR: 3.19 (1.985–10.322).

For isolation of paired cancer-associated and normal fibroblasts, fresh tissues from the tumor and healthy mucosa (more than 1 cm away from the OSCC lesion) from OSCC patients ( $n = 6$ ) were collected at the time of the surgical excision. Non-matched CAFs were also isolated from additional primary OSCC lesions ( $n = 9$ ) and normal oral fibroblasts (NOFs) from oral mucosa of non-cancer individuals ( $n = 10$ ). Only HPV negative primary tumors without any prior therapies were included in the study. Informed consent was obtained in all cases. Ethical approval for the study was obtained from the regional ethical committee (REK Vest 2010/481).

### *In Situ* Hybridization and miRNA Semi-Quantification

ISH of OSCC tissues was performed as described earlier (28). In brief, 3- $\mu$ m sections of formalin-fixed and paraffin-embedded tissues were deparaffinized in xylene, rehydrated in series of 99%, 96%, and 70% alcohol concentration, and epitope retrieved with 15  $\mu$ g/ml Proteinase K (90000; Exiqon, Denmark) solution at 37°C for 10 min. At 53°C, sections were pre-hybridized with ISH buffer (90000; Exiqon; Denmark) for 30 min, and then incubated for an hour with digoxigenin (DIG) labeled miR-138-5p specific oligonucleotides (612107-360; Exiqon, Denmark). Thereafter, tissues were washed with decreasing concentrations of saline-sodium citrate buffer (S66391L; Sigma, USA), and then blocked with 2% sheep serum (013-000-121; Jackson ImmunoResearch, USA) in 1% bovine serum albumin. Subsequently, tissues were incubated with alkaline phosphatase (ALP)-linked anti-DIG Fc fragments (1:400; 11093274910; Roche, Germany) overnight at room temperature. The tissues were thoroughly washed and then incubated with ALP substrate-Nitro blue tetrazolium chloride/5-Bromo-4-chloro-3-indolyl phosphate (NBT-BCIP) (11681451001; Roche, Germany) at 30°C for 2 h. Levamisole (X3021; Dako, USA) was mixed with the substrate to block endogenous ALP activity. Finally, tissues were counterstained with nuclear fast red. A scramble oligonucleotide without target and small nuclear RNA-U6 were used as negative and positive controls, respectively.

miR-138 staining in OSCC sections were scored negative (0) or 1–4 according to increasing stain intensity by experienced pathologists.

### TCGA Data Analysis

TCGA miR-138 expressions from TCGA miRNA sequence data ( $n = 488$ ) and clinical data for head and neck squamous cell

carcinoma cohort ( $n = 528$ ) were accessed from the Firebrowse database version 2016\_01\_28 (<http://www.firebrowse.org>). The same cohort contained miR-138 data for normal human oral mucosa (NHOM). After exclusion of HPV-positive, non-oral cancers cases and cases with history of neoadjuvant treatment, 277 oral cancer cases (alveolar ridge: 13; base of tongue: 11; buccal mucosa: 30; floor of mouth: 56; hard palate: 5; lip: 3; unspecified region in oral cavity: 62; tongue: 112; oropharynx: 7) with miR-138 data remained. Using the same exclusion criteria, out of 45 cases, only 25 NHOM cases remained. Of the 25 NHOM cases, 24 were matched to OSCC lesions (from the same patient).

## Cell Culture

Isolated CAFs and NOFs from OSCC patients and healthy donors were cultured in Dulbecco's Modified Eagle's Medium (DMEM; D6429, SIGMA) supplemented with 10% heat-inactivated newborn calf serum (NBCS; 31765068, GIBCO). OSCC cell lines UK1 (29) and Luc4 (30) were grown in DMEM/Nutrient Mixture F-12 Ham medium (D8437, Sigma) supplemented with 10% NBCS, 1× Insulin-Transferrin-Selenium (41400-04, ThermoFisher Scientific), 0.4 µg/ml hydrocortisone (H0888, Sigma), 50 µg/ml L-ascorbic acid (A7631, Sigma), and 10 ng/ml epidermal growth factor (E9644, Sigma). All cell lines were propagated in humidity incubator at 5% CO<sub>2</sub> and 37°C temperature and regularly tested for mycoplasma contamination.

## miRNA Modulation in Fibroblasts and Proliferation Assay

Each of the  $1 \times 10^6$  NOFs and CAFs was reverse transfected with mimics and inhibitors of miR-138-5p (C/IH-300605; Dharmacon), and the respective controls (mimic: CN-0010000-01; inhibitor: IN-001005-05; Dharmacon) at 50 nM concentration using Lipofectamine™ 3000 Transfection Reagent (L3000015; Invitrogen, USA) following the manufacturer's protocol. Forty-eight hours after the transfection, the cells were either harvested for molecular profiling or subjected to further functional studies. In order to see the effect of miR-138 on fibroblast proliferation,  $1 \times 10^4$  NOFs or CAFs were reverse transfected with mimics and inhibitors of miR-138-5p and the respective controls in quadruplicates in 24-well plates. After 48 h, the cells were Trypsin EDTA detached and counted using Trypan blue in Invitrogen Countess automated cell counter.

## RNA and miRNA Isolation

Total RNA was isolated using mirVana miRNA isolation kit (AM1560, mirVana). In brief, sub-confluent CAFs and NOFs in monolayer cultures were washed with phosphate buffered saline (PBS), lysed with Lysis/Binding buffer and Phenol : Chloroform extracted. Subsequently, RNA was captured in glass fiber filter column and eluted in elution solution. The purity and quantity of the RNA was measured using NanoDrop® ND-1000 Spectrophotometer (Nanodrop Technologies; USA). Total RNA and enriched small RNAs were stored at -80°C until use.

## Reverse Transcription

Total RNAs were reverse transcribed to cDNAs using miRNAs specific primers using TaqMan MicroRNA Reverse

Transcriptase kit (4366596, Applied Biosystem). In brief, 10 ng of total RNA was mixed with dNTPs, reverse transcription buffer, RNase inhibitor, and miRNA specific primer and reverse transcribed to a final reaction mixture of 15 µl. Thereafter, the reaction mixture was subjected to thermal cycle at 16°C for 30 min, 42°C for 30 min, and 85°C for 5 min. For mRNA quantification, total RNA was reverse transcribed using the Taqman Reverse Transcription kit (N8080234, Applied Biosystems). In brief, 100 ng of total RNA was mixed with reverse transcription buffer, MgCl<sub>2</sub>, dNTPs, random hexamer, RNase inhibitor, and reverse transcriptase to a final volume of 25 µl with RNase-free water. cDNA synthesis was performed at 20°C for 10 min, 48°C for 30 min, and 90°C for 5 min.

## Quantitative Real-Time Polymerase Chain Reaction

The expression of miRNAs and gene transcripts were quantified using Taqman assays in ABI Prism 7900 HT sequence detector system (Applied Biosystems). The PCR reaction volume was set to 10 µl for each well in 384-well plates. The PCR was then run at 50°C for 2 min, 95°C for 10 min, and for 40 cycles at 95°C for 15 s and 60°C for 1 min. Each sample was run in triplicate. mRNA expression was normalized to the housekeeping gene GAPDH, and miRNA expression was normalized to the expression of RNU48. Taqman assays used are listed in **Supplementary Table S2**.

## Western Blot

Semi-quantitative assessment of proteins of interest was performed using Western blot technique. In brief, protein lysates of fibroblast culture, 48 h post transfection of miR-138 mimics, inhibitors, and controls, were resolved in NuPAGE Novex 10% Bis-Tris Protein Gel (NP0303, Invitrogen) in NuPAGE MOPS SDS Running Buffer (NP0001, Invitrogen) at 160 V for 90 min and were transferred to PVDF membrane (10600069, GE Healthcare) in NuPAGE transfer buffer (NP0006, Invitrogen) at 40 V for an hour. Thereafter, PVDF membrane was blocked with 5% non-fat dry milk or 3% BSA in TBS-tween buffer for half an hour and incubated with primary antibody overnight at 4°C. The following day, PVDF membrane was thoroughly washed with TBS-tween, incubated at room temperature with secondary antibody tagged with horseradish peroxidase and thoroughly washed again. Finally, bands of proteins were visualized using SuperSignal West Pico Chemiluminescent Substrate (34080, ThermoFisher) using Image Reagent LAS 1000 (Fujifilm), and protein band intensity in the captured images was quantified using ImageJ using Gel commands. GAPDH was used as loading control. Antibodies used in this study are listed in **Supplementary Table S3**.

## miRNA Dual Luciferase Target Reporter Assay

3'UTR sequence of ITGA11 (NM\_001004439.1) was retrieved from the UCSC genome browser (<http://genome.ucsc.edu>) (31). A plasmid vector with luciferase upstream of 3'UTR and renilla as a control reporter was designed and purchased from Vector Builder. Position 1-1355 of ITGA11 3'UTR length harboring

miR-138 binding site (724–730: CACCAGC)→ was inserted into the vector. For a control vector, non-complimentary mutant sequence GTGGTCG was introduced to miR-138 binding site. Transfection mix of plasmid DNA (250 ng per well in 24-well plates) and miR-204 mimic (calculated at 50 nM concentration in cell culture medium) was prepared using Lipofectamine™ 3000 Transfection Reagent. Required volume of transfection mix and  $5 \times 10^5$  CAFs were mixed in each well, and the cells were maintained in the culture chamber for 48 h. Thereafter, the cells were harvested, and luciferase activity was measured using Dual luciferase detection system (E1910, Promega) following the manufacturer's protocol using a Tecan Infinite M200PRO luminometer.

### Fibroblast Migration in Collagen Gel Assay

On the first day of the experiment,  $1 \times 10^5$  UK1 cells were plated in 24-well plates. The next day, collagen type I matrices were prepared by mixing collagen type I (354236, Corning), DMEM, NBCS and reconstitution buffer (2.2 g  $\text{NaHCO}_3$  + 0.6 g NaOH + 4.766 g HEPES 100 ml water) at a volume ratio of 7:1:1:1 on ice. The collagen matrix (250  $\mu\text{l}$  per well) was pipetted into 0.4- $\mu\text{m}$  24-well Corning transwell inserts (CLS3413, Sigma) and allowed to gel at 37°C in an incubation chamber. Two hours later, the gels were layered on the top with 250  $\mu\text{l}$  of  $5 \times 10^5/\text{ml}$  fibroblasts modulated with miR-138. The co-culture system was maintained at 37°C for 5 days.

### Collagen Contraction Assay

Ninety-six-well plates were blocked with 2% BSA overnight at 37°C in an incubation chamber. Forty-eight hours post miRNA modulations, fibroblasts were suspended in collagen type I matrix prepared as described above at a density of  $5 \times 10^5$  cells/ml. Subsequently, 100  $\mu\text{l}$  of fibroblast-collagen matrix was dispensed into each well and allowed to gel for 90 min. The gels were then gently dislodged from the surface of culture plate using 100  $\mu\text{l}$  of DMEM medium. The gels were maintained at an incubation chamber and the change in gel dimension was measured at different time points.

### Fibroblast-OSCC Cell 3D Organotypic Co-Culture

3D co-culture models mimicking local invasion of OSCC cells into subjacent connective tissue were constructed by layering OSCC cells on top of a fibroblast-embedded collagen I matrix. In brief, either CAFs or NOFs at a density of  $2.5 \times 10^5$  cells/ml were suspended in the matrix of collagen type I prepared as above, on ice. Seven hundred microliters of the CAF- or NOF-populated collagen suspensions was pipetted into each well in 24-well plates and allowed to polymerize in a humidified incubator at 37°C. After 2 h, each well was gently added with 1 ml of complete DMEM medium to allow the cells to grow until the next day. The next day,  $5 \times 10^5$  cells of UK1 or Luc4 were added on the top of the fibroblast gel. A day after, the gels were transferred to a metal grid layered with a filter paper and grown on air-medium interface in DMEM : Ham's F12 Nutrient mixture (31765068, ThermoFisher) supplemented with insulin-transferrin-selenium, hydrocortisone, and L-ascorbic acid as above, but NBCS was replaced with 0.1% bovine albumin fraction (V15260-037,

ThermoFisher). The gels were cultured for the next 10 days. Medium was changed at each alternative day.

### Quantification of Invasion of OSCC Cells in 3D-Organotypic Models

FFPE-embedded organotypic tissues were cut into 5- $\mu\text{m}$  sections and stained with hematoxylin and eosin. Images of the stained tissues were captured at 20 $\times$  objective using a slide scanner (Hamamatsu NaNoZoomer-XR, Shizuoka, Japan) and the invasion depth of OSCC cells was measured using NDP.view2 (Hamamatsu, Japan). Depth of invasion was defined as the vertical distance from the reconstructed basement membrane (horizontal line along the non-invading cells) to the deepest invaded OSCC cells in the respective point. Twenty measurements of invasion at 50- $\mu\text{m}$  distance along the tissue were taken and averaged. The non-uniform thick or tapered 100- $\mu\text{m}$  ends of the 3D organotypic tissues were excluded from measurements.

### Statistical Analysis

Student's unpaired or paired *t*-test or one-way ANOVA was used to examine significant differences in means in between two or more than two groups, respectively. Where data did not show a normal distribution (D'Agostino & Pearson test;  $p > 0.05$ ), non-parametric comparisons (Wilcoxon for paired comparison and Mann-Whitney for unpaired comparison between two, and Kruskal-Wallis for unpaired comparison among groups) were carried out to determine significant difference in median expression. All analysis was performed using GraphPad Prism Version 7. For statistical analysis, the OSCC cohort was categorized into a negative or a positive miR-138 staining group or a low-no (0–1) and a high (2–4) miR-138 staining group. Overall survival (OS) and recurrence-free survival (RFS) analysis for clinicopathological parameters and miR-138 expression (positive and negative staining group) was carried out using log-rank test (Mantel-Cox). Clinicopathological parameters were further tested with multivariate Cox's proportional regression to identify independent predictors of OS and RFS. Pearson's chi-square test was carried out to determine the association of miR-138 status [positive ( $n = 31$ ) versus negative ( $n = 7$ ); low-no miR-138 ( $n = 33$ ) versus high miR-138 ( $n = 4$ )] with clinicopathological parameters. Survival and association tests were carried out using IBM SPSS Statistics Version 25.

## RESULTS

### miR-138 Was Expressed in a Subset of OSCC Lesions Only and Showed a Marked Heterogeneity in Both Epithelial and Stromal Compartments

Epithelial expression of miR-138 was observed in 17% ( $n = 9$ ) of OSCC cases while stromal expression was detected in 9.4% ( $n = 5$ ) of the cases. In 7.5% ( $n = 4$ ) of the cases, miR-138 was expressed in both tumor and stromal compartments (Figure 1A). Pearson chi-square test showed that miR-138 staining

positivity associated with lower depth of invasion: <4 mm ( $p = 0.05$ ) and relatively higher miR-138 expression (epithelial and stromal) associated with lower OSCC recurrence ( $p = 0.03$ ). Expression of miR-138 did not associate to any other clinical or pathological parameters, including tumor stages. Epithelium of NHOM controls showed miR-138 expression in 50% of cases ( $n = 3$ ) while no expression was observed in subjacent normal stroma. Compared to histologically normal peritumoral

epithelium, miR-138 expression in tumor epithelium was increased in 16.1% ( $n = 5$ ) and decreased in 3.2% ( $n = 1$ ) cases. Stromal miR-138 expression was increased in tumor stroma compared to respective stroma in normal/peritumor regions in 9.7% ( $n = 3$ ) cases, while no difference was observed for the rest (**Figure 1B**). When expressed in tumor stroma, miR-138 was localized in cells with fibroblast morphology and in a sub-population of lymphocytes (**Figures 1C, D**).

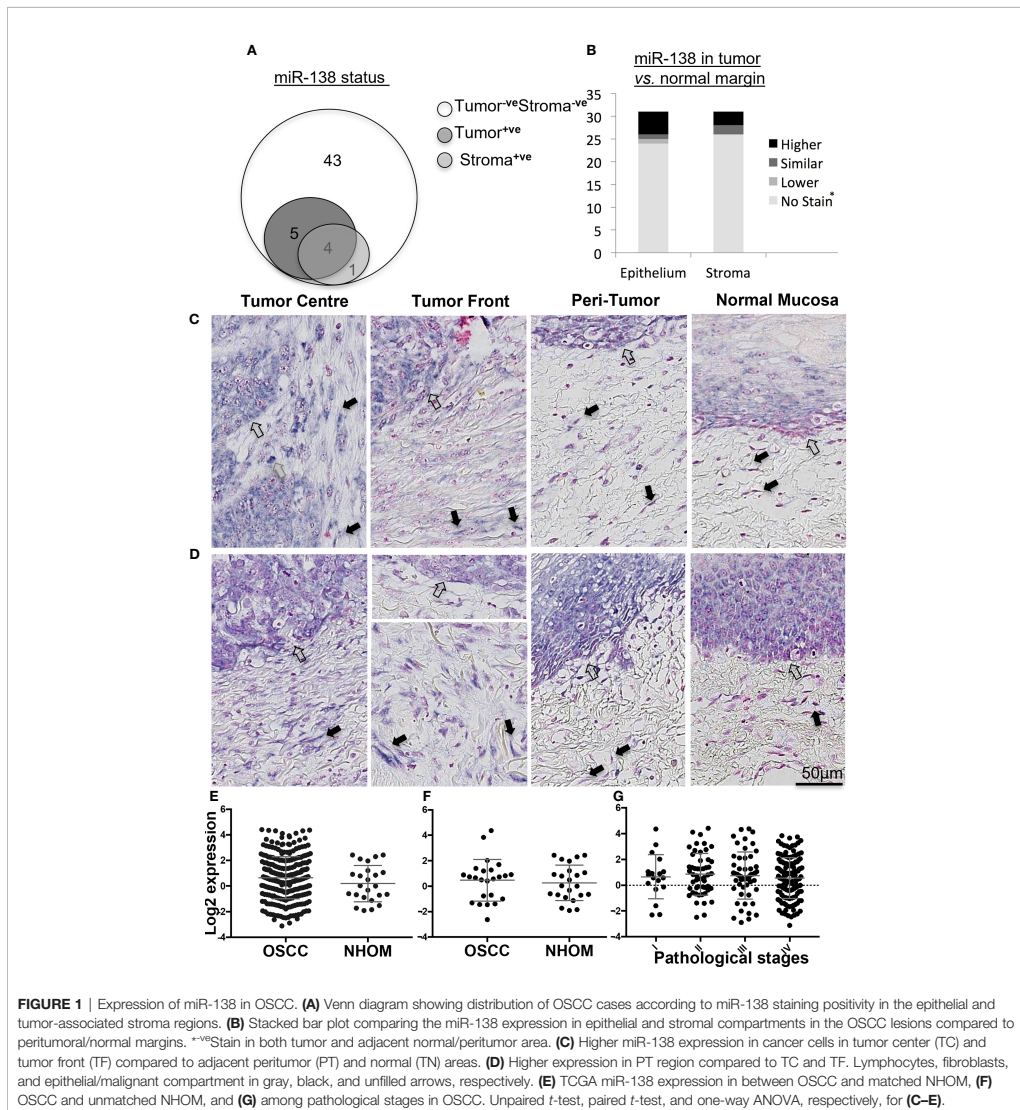


**FIGURE 1 |** Expression of miR-138 in OSCC. **(A)** Venn diagram showing distribution of OSCC cases according to miR-138 staining positivity in the epithelial and tumor-associated stroma regions. **(B)** Stacked bar plot comparing the miR-138 expression in epithelial and stromal compartments in the OSCC lesions compared to peritumoral/normal margins. <sup>\*\*ve</sup>Stain in both tumor and adjacent normal/peritumor area. **(C)** Higher miR-138 expression in cancer cells in tumor center (TC) and tumor front (TF) compared to adjacent peritumor (PT) and normal (TN) areas. **(D)** Higher expression in PT region compared to TC and TF. Lymphocytes, fibroblasts, and epithelial/malignant compartment in gray, black, and unfilled arrows, respectively. **(E)** TCGA miR-138 expression in between OSCC and matched NHOM. **(F)** OSCC and unmatched NHOM, and **(G)** among pathological stages in OSCC. Unpaired *t*-test, paired *t*-test, and one-way ANOVA, respectively, for **(C-E)**.

Analysis of the TCGA data showed no significant difference in miR-138 expression between whole OSCC lesions compared to NHOM (Figure 1E). A difference in miR-138 expression was still not observed when the subset of OSCC cases was compared to their matched NHOM (Figure 1F). No significant difference in miR-138 expression among overall pathological tumor stages (I–IV) was found (Figure 1G).

### Fibroblasts From OSCC Lesions Displayed a Heterogeneous Expression of miR-138

Positive and negative miR-138-stained fibroblasts were observed to co-exist nearby the stroma of a subset of OSCC lesions (Figures 2A, B). qRT-PCR profiling of miR-138 expression in CAFs isolated from OSCC lesions and NOFs isolated from oral mucosa of non-related healthy, non-cancer individuals showed significantly higher expression in CAFs by 4.52-fold (Figure 2C). However, profiling of miR-138 in matched CAFs and NOFs showed a marked heterogeneity; out of the six matched pairs, miR-138 expression was higher in CAFs, then in NOF only in one matched pair, similar in two pairs, and lower in three pairs (Figure 2D).

### Ectopic Expression of miR-138 Decreased Fibroblast Proliferation and Expression of Several CAF-Related Markers, but Not of ITGA11

Ectopic expression of miR-138 (modulation of miR-138 expression in fibroblasts by use of mimics and inhibitors is presented in Supplementary Figure S2) resulted in significantly reduced proliferation of both CAFs and NOFs compared to mimic controls in monolayer culture (Figures 3A, B). Reduced proliferation of fibroblasts was accompanied by significant reduction in expression of CCND1 transcript (Figure 3C). However, despite upregulation of CCND1 following inhibition of miR-138, a change in fibroblast proliferation was not observed between the target and control group. Modulation of miR-138 expression also induced significant changes in expression of several CAF-related molecules (TGFB2, TGFβ1, and FAP) and EGFR (Figures 3D–K).

qRT-PCR profiling of miR-138 and ITGA11 transcripts in cultured fibroblasts showed an inverse correlation between their expression (Figure 4A). However, modulation of miR-138 expression did not result in alterations of ITGA11 expression at mRNA or protein levels (Figures 4B–D). Gene reporter assay showed no difference in expression of ITGA11 or mutant transcripts (Figure 4E), indicating that miR-138 does not target ITGA11.

### Ectopic Expression of miR-138-5p Induced a Change in Fibroblasts' Morphology and Decreased Their Motility and Collagen Contraction Ability

Increasing miR-138 expression in fibroblasts (both CAFs and NOFs) changed their cellular morphology from an elongated, slender shape (Figures 5G–H, L) to a flattened, stellar shape and bigger size, compared to mimic controls (Figures 5E, F, K). Fibroblasts' motility in 3D collagen I gels towards OSCC cell line UK1 was significantly impaired following transfection with miR-138 mimics; the number of fibroblasts that migrated inside the collagen gels and the distance crossed were significantly reduced in fibroblasts transfected with mimics, compared to controls (Figures 5M, N). Additionally, mimicking increased miR-138 in CAFs and NOFs and significantly reduced collagen contraction ability by both CAFs and NOFs, and reversing miR-138 expression by using inhibitors resulted in the opposite effect (Figures 5A–D and 6).

### miR-138 Expression in Fibroblasts Decreased Invasion of Suprajacent OSCC Cells

In order to study the role of miR-138 expression in CAFs on tumor invasion or progression, miR-138 expression was altered in CAFs and NOFs prior to their co-culture with the established OSCC cell lines UK1 and Luc4 in 3D-organotypic models. Inhibition of miR-138 in both CAFs and NOFs increased invasion by OSCC cell lines UK1 and Luc4, while transfection of both fibroblasts with mimics of miR-138 significantly decreased or almost completely neutralized invasion of both UK1 and Luc4 (Figure 7).

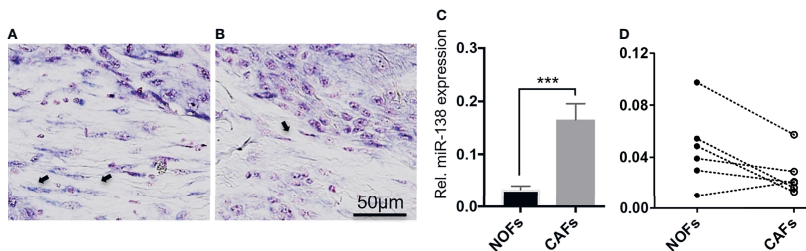


**FIGURE 2 |** Heterogeneous expression of miR-138 in cultured fibroblasts from OSCC lesions and normal mucosa. **(A, B)** Differential miR-138 expression in CAFs from different regions of tumor center. Fibroblasts are marked with arrows. **(C)** miR-138 expression in non-matched CAFs and NOFs. **(D)** miR-138 expression in matched NOFs and CAFs. Each pair is connected by dotted lines. \*\*\* $p < 0.001$ .

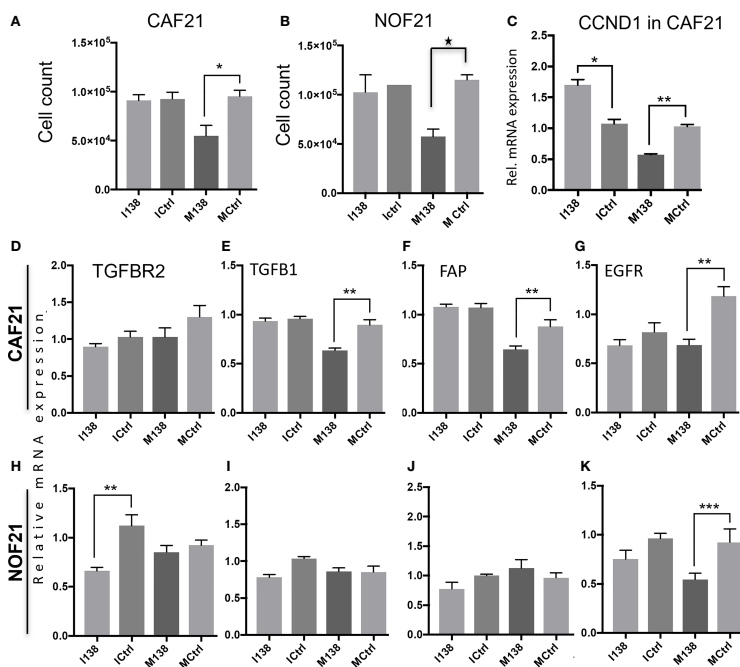


**FIGURE 3 |** Fibroblasts' proliferation and expression of CAF markers in monolayer culture following miR-138 modulation. Proliferation of (A) CAFs and (B) NOFs, (C) regulation of CCND1 transcript in CAFs, and (D–K) other transcripts related to the CAF-phenotype (TGFB1, TGFB2, and FAP) and EGFR in CAFs and NOFs 48 h post miR-138 modulation. \* Significant; unpaired *t*-test  $p < 0.05$ . I138: inhibition of endogenous miR-138. M138: mimicking of miR-138 expression. Ictrl and MCtrl: respective controls for inhibitors and mimics. \*\* $p < 0.01$ , \*\*\* $p < 0.001$ .

### Pathway Focus Analysis of Molecules Targeted by miR-138 Indicates Alterations in the Focal Adhesion Pathway

Pathway analysis of genes targeted by miR-138 using miRTarBase database release 7 (32) identified several miR-138 targeted pathways, including focal adhesion and TGF- $\beta$ 1 pathways (Supplementary Table S4 and Figure S3). Since FAK, AKT, ROCK, and CCND1 have been previously proven by luciferase gene reporter assays to be direct targets of miR-138, we decided to focus on these molecules in the focal adhesion pathway. An effect on FAK (PTK2) mRNA was observed when the cells were transfected with mimics. At the FAK, protein level seemed to be altered by both mimics and inhibitors of miR-138, in opposite directions (Figure 8).

## DISCUSSION

This study shows that expression of miR-138 displays a marked heterogeneity, and it is detectable in a subset of OSCC

lesions only. Although performed on a limited number of cases, insufficient for a definitive conclusion, this study points towards a trend for decreased miR-138 expression in tumor tissue when compared to normal oral epithelium. The absence of miR-138 staining in a relatively higher percentage (83%) of tumor samples compared to NHOM (50%) might be an indication for a tumor-suppressive role of miR-138. Inconsistent with this might be the finding that when present, in few cases, the expression of miR138 was increased in both tumor cells and CAFs compared to normal/peritumor regions. Nevertheless, increased expression was associated with lower recurrence and less depth of invasion, indicative again for a tumor-suppressive role. Of note, in our cohort, there was also no specific pattern of association of miR-138 expression with tumor stage, lymph node involvement, or later distant metastasis. This might be due to the relatively low number of cases we have studied, but analysis of the TCGA data set, which comprises many more cases, did not show either any specific association of miR-138 to clinical parameters in OSCC. Taken together, these data do not support a biomarker role for miR-138 in OSCC. However, there are indications for a tumor-suppressive function

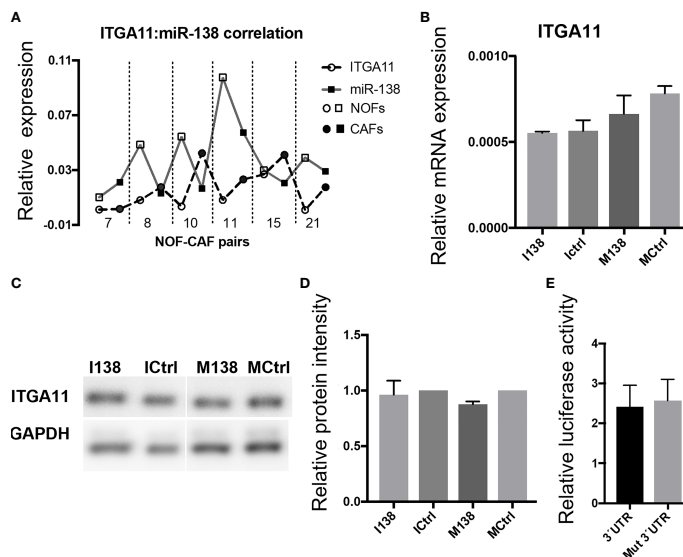


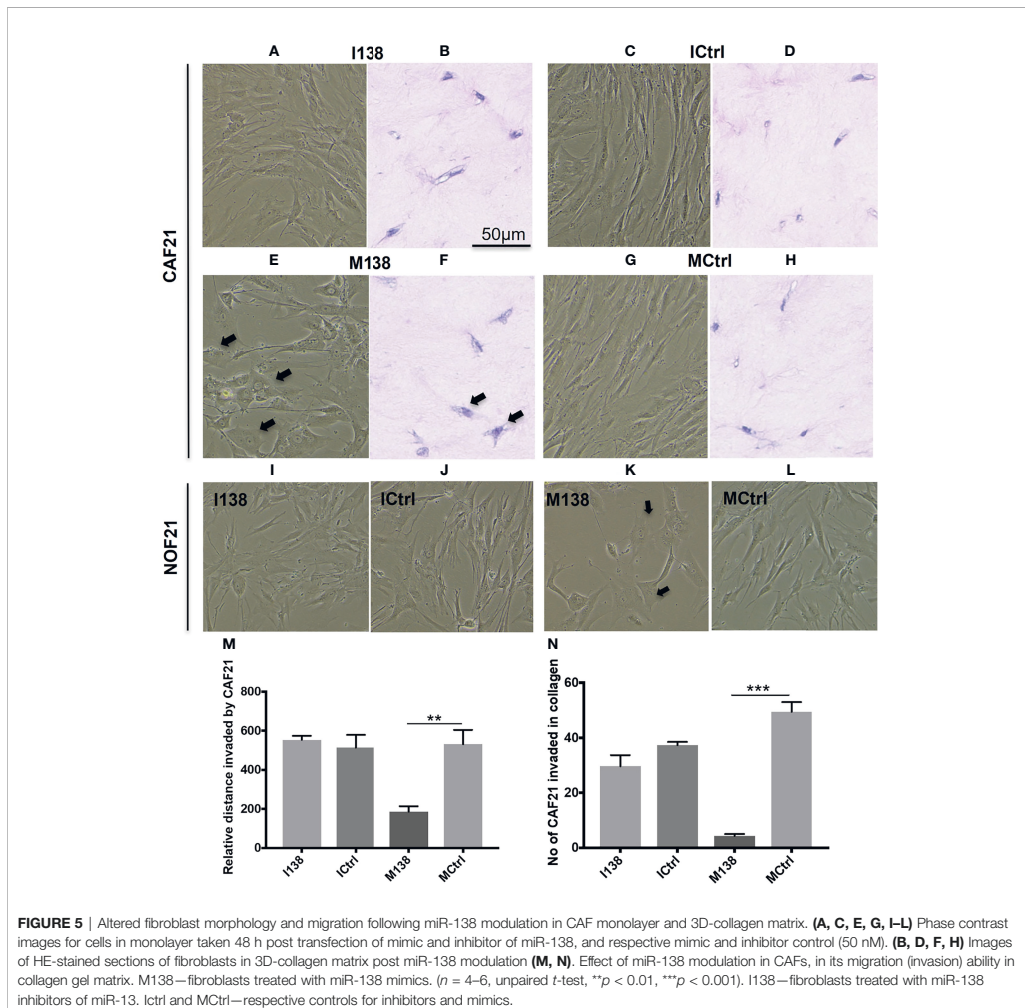
**FIGURE 4** | miR-138 does not target ITGA11. **(A)** Graph showing an inverse correlation between miR-138 and ITGA11 levels in the fibroblasts. **(B)** Modulation of miR-138 expression did not result in alterations of ITGA11 expression at mRNA or **(C, D)** protein levels in CAF. **(E)**: Gene reporter assay showing no difference in the expression of ITGA11 or mutant transcripts.

for miR-138 from both previous and current studies, and thus miR-138 might be of biological importance for a subset of OSCCs.

The heterogeneity of miR-138 expression observed in stroma of OSCC tissues was paralleled by a marked heterogeneity detected in cultured fibroblasts, which might have been even more increased due to selection of different sub-populations of fibroblasts during isolation in culture. We could not identify, however, indications for selective isolation of a certain sub-population over the other. Of importance, despite its heterogenous regulation in fibroblasts, with no clear trend between CAFs and NOFs, increased expression of miR-138 using miR-138 mimics in both CAFs and NOFs had a remarkable effect on their ability to migrate in 3D, to contract collagen gels, and to induce OSCC invasion. Therefore, this study shows that regardless of type of fibroblasts used (CAF or NOF), ectopic expression of miR-138 in the fibroblasts results in a consistent inhibition of migration of fibroblasts themselves and of invasion of the adjacent OSCC cells. These findings are in line with the literature suggesting a tumor-suppressive function for miR-138, but while the previous studies addressed the role of miR-138 expressed in tumor cells (26, 27), here we show for the first time a tumor-suppressive effect for miR-138 expression in stromal fibroblasts. In an attempt to understand the mechanism by which alteration in miR-138 expression in the fibroblasts modulates the invasion capabilities by OSCC cells, a couple of

functional assays were performed. A crucial effect of increased miR-138 expression in fibroblasts was the morphological transition from spindle-shaped CAFs and NOFs into a stellar morphology, accompanied by a decrease in their motility. The effect on motility might be the underlying mechanism by which decreased miR-138 expression in CAF decreased invasion of adjacent OSCC cells, since CAFs have been shown previously to “lead” the invasion of adjacent OSCC cells (6), and changes in their motility were reflected directly into the invasion ability of adjacent OSCC cells (5).

Similar morphological and motility changes have been previously reported to be associated to loss of FAK function, which regulates focal adhesion assembly and disassembly required for cell motility (33, 34). Our study indicates that FAK was regulated in OSCC-derived CAFs by miR-138, suggesting therefore that the changes in fibroblast morphology and motility observed to occur with increased miR-138 expression might be mediated, among other molecules, *via* FAK. However, these results need to be further confirmed by phenotype rescue experiments to prove that the motility effects we observed after modulation of miR-138 expression are mediated *via* focal adhesion kinase axis. The changes in fibroblasts’ morphology and motility were accompanied by other changes in their molecular profile; ectopic expression of miR-138 significantly decreased several CAF-related markers, particularly those on the TGF- $\beta$ 1 pathway. A link between



TGF $\beta$ 1 pathway and fibroblasts' motility is well established (35). Moreover, cyclin D1 (CCND1), well known to control proliferation of cells, has also been found to be decreased by ectopic expression of miR-138, and it was linked to cell motility. CCND1-deficient mouse embryonic fibroblasts were previously shown to exhibit increased cellular adhesion and decreased motility compared to the wild type (36). CCND1 deficiency was also associated with reduced migration and increased adhesion or focal adhesion substrate by mice bone marrow-derived macrophages (37). This is in line with the changes in fibroblast morphology and motility we observed in our experiments.

FAK (32, 38, 39), ROCK2 (32, 40), and CCND1 (32, 41) have all been previously shown to be direct targets of miR-138; therefore, it is not surprising that we found their expression changed in the fibroblasts that had an altered miR-138 expression. Taken together, our findings suggest that they act in cohort to control fibroblast migration, and that their expression is regulated by miR-138. ITGA11 has been previously associated with the CAF phenotype (42). Our own qRT-PCR data also showed an inverse correlation between the expression levels of miR-138 and ITGA11, which would indicate that ITGA11 is a direct target of miR-138. However, both the inhibitor/mimic experiments and the gene reporter assay could not confirm this hypothesis.



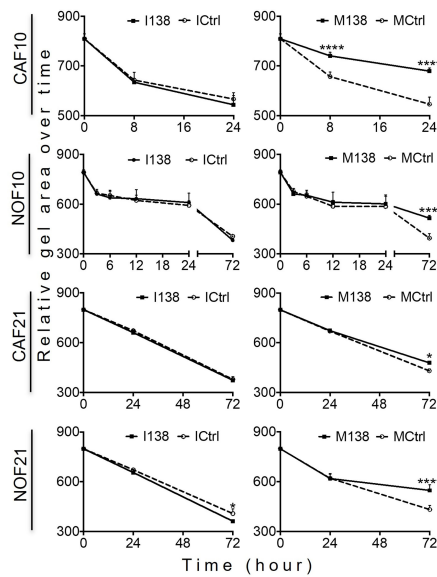


**FIGURE 6 |** Altered miR-138 expression modulates the ability of fibroblasts to contract collagen gels: Collagen I contraction by CAFs and NOFs over time. *n* = 4–6; one-way ANOVA; mean ± SD; \**p* < 0.05, \*\*\*\**p* < 0.0001.

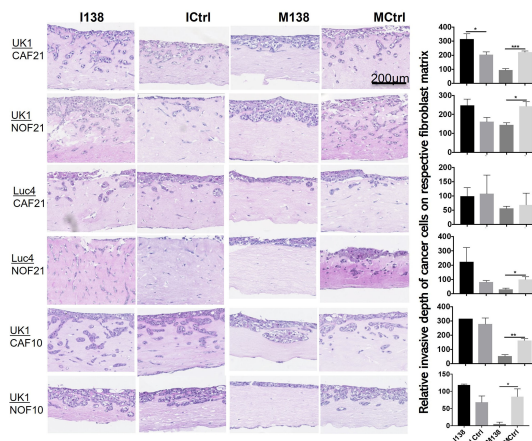


**FIGURE 7 |** Altered miR-138 expression in fibroblasts modulates invasion of adjacent OSCC cells. HE images of 3D organotypic co-culture depicting invasion of OSCC cells in fibroblast-collagen matrix. Measurement of corresponding invasion distance by OSCC cells on the right. \**p* < 0.05, \*\**p* < 0.01, \*\*\**p* < 0.001.

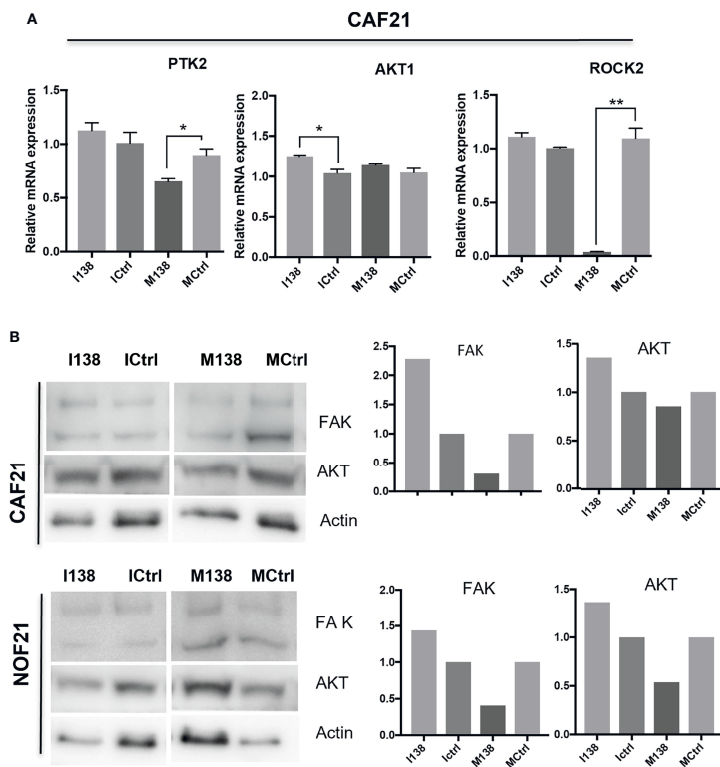


**FIGURE 8** | miR-138 expression and investigation of focal adhesion kinase (FAK) axis in CAFs. Alterations in **(A)** mRNA and **(B)** protein expression of several molecules of the FAK axis following miR-204 modulation in CAFs and NOFs. **(B)** Western blot images and the semi-quantification of protein blots with ImageJ. \* $p < 0.05$ , \*\* $p < 0.01$ .

In conclusion, this study supports a tumor-suppressive role for miR-138 in OSCC while expressed in stromal fibroblasts, despite its heterogeneous expression.

## DATA AVAILABILITY STATEMENT

The raw data supporting the conclusions of this article will be made available by the authors, without undue reservation.

## ETHICS STATEMENT

Ethical approval was obtained from the regional ethical committee in Norway (West Norway; REK Vest 3.2006.2620,

REK Vest 3.2006.1341). The patients/participants provided their written informed consent to participate in this study.

## AUTHOR CONTRIBUTIONS

Conceptualization: SR, AJ, DS, and D-EC. Data curation: SR, HP, and HD. Formal analysis: SR and DS. Funding acquisition: D-EC. Investigation: SR, HP, HD, BL, KH, AK, SL, and EN. Methodology: SR, HD, HP, and DS. Project administration: AJ, DS, and D-EC. Supervision: AJ, DS, and D-EC. Validation: SR. Visualization: SR. Writing—original draft: SR. Writing—review and editing: SR, HP, HD, BL, KH, AK, SL, EN, AJ, DS, and D-EC. All authors contributed to the article and approved the submitted version.

## FUNDING

This work was supported by the Research Council of Norway through its Centers of Excellence funding scheme (Grant No. 22325), the Western Norway Regional Health Authority (Helse Vest Grant Nos. 911902/2013 and 912260/2019), and the Norwegian Centre for International Cooperation in Education (project number CPEA-LT-2016/10106).

## SUPPLEMENTARY MATERIAL

The Supplementary Material for this article can be found online at: <https://www.frontiersin.org/articles/10.3389/fonc.2022.833582/full#supplementary-material>

**Supplementary Figure S1** | Diagram showing *in silico* Kaplan-Meier plot for the survival functions of the clinicopathological characteristics using Log-Rank or \* Breslow test. Only significant parameters ( $p < 0.05$ ) are shown. Stage I and II: early stage. Stage III and V: late stage.

## REFERENCES

- Fidler IJ. Timeline - The Pathogenesis of Cancer Metastasis: The 'Seed and Soil' Hypothesis Revisited. *Nat Rev Cancer* (2003) 3(6):453–8. doi: 10.1038/nrc1098
- Hanahan D, Weinberg RA. Hallmarks of Cancer: The Next Generation. *Cell* (2011) 144(5):646–74. doi: 10.1016/j.cell.2011.02.013
- Junttila MR, de Sauvage FJ. Influence of Tumour Micro-Environment Heterogeneity on Therapeutic Response. *Nature* (2013) 501(7467):346–54. doi: 10.1038/nature12626
- Kalluri R. The Biology and Function of Fibroblasts in Cancer. *Nat Rev Cancer* (2016) 16(9):582–98. doi: 10.1038/nrc.2016.73
- Costea DE, Hills A, Osman AH, Thurlow J, Kalna G, Huang X, et al. Identification of Two Distinct Carcinoma-Associated Fibroblast Subtypes With Differential Tumor-Promoting Abilities in Oral Squamous Cell Carcinoma. *Cancer Res* (2013) 73(13):3888–901. doi: 10.1158/0008-5472.CAN-12-4150
- Gaggioli C, Hooper S, Hidalgo-Carcedo C, Grosse R, Marshall JF, Harrington K, et al. Fibroblast-Led Collective Invasion of Carcinoma Cells With Differing Roles for RhoGTPases in Leading and Following Cells. *Nat Cell Biol* (2007) 9(12):1392–400. doi: 10.1038/ncb1658
- Daly AJ, McIlreavey L, Irwin CR. Regulation of HGF and SDF-1 Expression by Oral Fibroblasts - Implications for Invasion of Oral Cancer. *Oral Oncol* (2008) 44(7):646–51. doi: 10.1016/j.oraloncology.2007.08.012
- Kawashiri S, Tanaka A, Noguchi N, Hase T, Nakaya H, Ohara T, et al. Significance of Stromal Desmoplasia and Myofibroblast Appearance at the Invasive Front in Squamous Cell Carcinoma of the Oral Cavity. *Head Neck-J Sci Special Head Neck* (2009) 31(10):1346–53. doi: 10.1002/hed.21097
- Kellermann MG, Sobral LM, da Silva SD, Zecchin KG, Graner E, Lopes MA, et al. Myofibroblasts in the Stroma of Oral Squamous Cell Carcinoma Are Associated With Poor Prognosis. *Histopathology* (2007) 51(6):849–53. doi: 10.1111/j.1365-2559.2007.02873.x
- Parajuli H, Teh MT, Abrahamson S, Christoffersen I, Neppelberg E, Lybak S, et al. Integrin Alpha11 Is Overexpressed by Tumour Stroma of Head and Neck Squamous Cell Carcinoma and Correlates Positively With Alpha Smooth Muscle Actin Expression. *J Oral Pathol Med* (2017) 46(4):267–75. doi: 10.1111/jop.12493
- Fujii N, Shomori K, Shiomi T, Nakabayashi M, Takeda C, Ryoike K, et al. Cancer-Associated Fibroblasts and CD163-Positive Macrophages in Oral Squamous Cell Carcinoma: Their Clinicopathological and Prognostic Significance. *J Oral Pathol Med* (2012) 41(6):444–51. doi: 10.1111/j.1600-0714.2012.01127.x
- Marsh D, Suchak K, Moutasim KA, Vallath S, Hopper C, Jerjes W, et al. Stromal Features Are Predictive of Disease Mortality in Oral Cancer Patients. *J Pathol* (2011) 223(4):470–81. doi: 10.1002/path.2830
- Bartel DP. MicroRNAs: Genomics, Biogenesis, Mechanism, and Function. *Cell* (2004) 116(2):281–97. doi: 10.1016/S0092-8674(04)00045-5
- He L, Hannon GJ. MicroRNAs: Small RNAs With a Big Role in Gene Regulation. *Nat Rev Genet* (2004) 5(7):522–31. doi: 10.1038/nrg1379
- Esquela-Kerscher A, Slack FJ. Oncomirs - microRNAs With a Role in Cancer. *Nat Rev Cancer* (2006) 6(4):259–69. doi: 10.1038/nrc1840
- Calin GA, Croce CM. MicroRNA Signatures in Human Cancers. *Nat Rev Cancer* (2006) 6(11):857–66. doi: 10.1038/nrc1997
- Suzuki HI, Katsura A, Matsuyama H, Miyazono K. MicroRNA Regulons in Tumor Microenvironment. *Oncogene* (2015) 34(24):3085–94. doi: 10.1038/onc.2014.254
- Tran N, O'Brien CJ, Clark J, Rose B. Potential Role of Micro-Rnas in Head and Neck Tumorigenesis. *Head Neck-J Sci Special Head Neck* (2010) 32(8):1099–111. doi: 10.1002/hed.21356
- Min AJ, Zhu C, Peng SP, Rajthala S, Costea DE, Sapkota D. MicroRNAs as Important Players and Biomarkers in Oral Carcinogenesis. *BioMed Res Int* (2015) 2015:186904. doi: 10.1155/2015/186904
- Sethi N, Wright A, Wood H, Rabbitts P. MicroRNAs and Head and Neck Cancer: Reviewing the First Decade of Research. *Eur J Cancer* (2014) 50(15):2619–35. doi: 10.1016/j.ejca.2014.07.012
- Rajthala S, Min A, Parajuli H, Debnath KC, Ljokjel B, Hoven KM, et al. Profiling and Functional Analysis of microRNA Deregulation in Cancer-Associated Fibroblasts in Oral Squamous Cell Carcinoma Depicts an Anti-Invasive Role of microRNA-204 via Regulation of Their Motility. *Int J Mol Sci* (2021) 22(21). doi: 10.3390/ijms222111960
- Yeh M, Oh CS, Yoo JY, Kaur B, Lee TJ. Pivotal Role of microRNA-138 in Human Cancers. *Am J Cancer Res* (2019) 9(6):1118–26.
- Chan XHD, Nama S, Gopal F, Rizk P, Ramasamy S, Sundaram G, et al. Targeting Glioma Stem Cells by Functional Inhibition of a Prosurvival OncomiR-138 in Malignant Gliomas. *Cell Rep* (2012) 2(3):591–602. doi: 10.1016/j.celrep.2012.07.012
- Manikandan M, Rao AKDM, Rajkumar KS, Rajaraman R, Munirajan AK. Altered Levels of miR-21, miR-125b-2\*, miR-138, miR-155, miR-184, and miR-205 in Oral Squamous Cell Carcinoma and Association With Clinicopathological Characteristics. *J Oral Pathol Med* (2015) 44(10):792–800. doi: 10.1111/jop.12300
- Brito BD, Lourenco SV, Damascena AS, Kowalski LP, Soares FA, Coutinho-Camillo CM. Expression of Stem Cell-Regulating miRNAs in Oral Cavity and Oropharynx Squamous Cell Carcinoma. *J Oral Pathol Med* (2016) 45(9):647–54. doi: 10.1111/jop.12424

26. Liu X, Jiang L, Wang A, Yu J, Shi F, Zhou X. MicroRNA-138 Suppresses Invasion and Promotes Apoptosis in Head and Neck Squamous Cell Carcinoma Cell Lines. *Cancer Lett* (2009) 286(2):217–22. doi: 10.1016/j.canlet.2009.05.030
27. Zhuang Z, Xie N, Hu J, Yu P, Wang C, Hu X, et al. Interplay Between DeltaNp63 and miR-138-5p Regulates Growth, Metastasis and Stemness of Oral Squamous Cell Carcinoma. *Oncotarget* (2017) 8(13):21954–73. doi: 10.18632/oncotarget.15752
28. Rajthala S, Dongre H, Parajuli H, Min A, Nginamau ES, Kvalheim A, et al. Combined *In Situ* Hybridization and Immunohistochemistry on Archival Tissues Reveals Stromal microRNA-204 as Prognostic Biomarker for Oral Squamous Cell Carcinoma. *Cancers (Basel)* (2021) 13(6). doi: 10.3390/cancers13061307
29. Locke M, Heywood M, Fawell S, Mackenzie IC. Retention of Intrinsic Stem Cell Hierarchies in Carcinoma-Derived Cell Lines. *Cancer Res* (2005) 65(19):8944–50. doi: 10.1158/0008-5472.CAN-05-0931
30. Biddle A, Liang X, Gammon L, Fazil B, Harper LJ, Emich H, et al. Cancer Stem Cells in Squamous Cell Carcinoma Switch Between Two Distinct Phenotypes That Are Preferentially Migratory or Proliferative. *Cancer Res* (2011) 71(15):5317–26. doi: 10.1158/0008-5472.CAN-11-1059
31. Kent WJ, Sugnet CW, Furey TS, Roskin KM, Pringle TH, Zahler AM, et al. The Human Genome Browser at UCSC. *Genome Res* (2002) 12(6):996–1006. doi: 10.1101/gr.229102
32. Chou CH, Shrestha S, Yang CD, Chang NW, Lin YL, Liao KW, et al. Mirtarbase Update 2018: A Resource for Experimentally Validated microRNA-Target Interactions. *Nucleic Acids Res* (2018) 46(D1):D296–302. doi: 10.1093/nar/gkx1067
33. Mierke CT, Fischer T, Puder S, Kunschmann T, Soetje B, Ziegler WH. Focal Adhesion Kinase Activity is Required for Actomyosin Contractility-Based Invasion of Cells Into Dense 3D Matrices. *Sci Rep* (2017) 7:42780. doi: 10.1038/srep42780
34. Parsons JT, Martin KH, Slack JK, Taylor JM, Weed SA. Focal Adhesion Kinase: A Regulator of Focal Adhesion Dynamics and Cell Movement. *Oncogene* (2000) 19(49):5606–13. doi: 10.1038/sj.onc.1203877
35. Sahai E, Astsaturov I, Cukierman E, DeNardo DG, Egeblad M, Evans RM, et al. A Framework for Advancing Our Understanding of Cancer-Associated Fibroblasts. *Nat Rev Cancer* (2020) 20(3):174–86. doi: 10.1038/s41568-019-0238-1
36. Li Z, Wang C, Jiao X, Lu Y, Fu M, Quong AA, et al. Cyclin D1 Regulates Cellular Migration Through the Inhibition of Thrombospondin 1 and ROCK Signaling. *Mol Cell Biol* (2006) 26(11):4240–56. doi: 10.1128/MCB.02124-05
37. Neumeister P, Pixley FJ, Xiong Y, Xie HF, Wu KM, Ashton A, et al. Cyclin D1 Governs Adhesion and Motility of Macrophages. *Mol Biol Cell* (2003) 14(5):2005–15. doi: 10.1091/mbc.02-07-0102
38. Kawamoto M, Yamaji T, Saito K, Shirasago Y, Satomura K, Endo T, et al. Identification of Characteristic Genomic Markers in Human Hepatoma HuH-7 and Huh7.5.1-8 Cell Lines. *Front Genet* (2020) 11:546106. doi: 10.3389/fgene.2020.546106
39. Golubovskaya VM, Sumbler B, Ho B, Yemima M, Cance WG. MiR-138 and MiR-135 Directly Target Focal Adhesion Kinase, Inhibit Cell Invasion, and Increase Sensitivity to Chemotherapy in Cancer Cells. *Anticancer Agents Med Chem* (2014) 14(1):18–28. doi: 10.2174/187152061401140108113435
40. Jiang L, Liu XQ, Kolokythas A, Yu JS, Wang AX, Heidbreder CE, et al. Downregulation of the Rho GTPase Signaling Pathway is Involved in the microRNA-138-Mediated Inhibition of Cell Migration and Invasion in Tongue Squamous Cell Carcinoma. *Int J Cancer* (2010) 127(3):505–12. doi: 10.1002/ijc.25320
41. Liu X, Lv XB, Wang XP, Sang Y, Xu SB, Hu KS, et al. MiR-138 Suppressed Nasopharyngeal Carcinoma Growth and Tumorigenesis by Targeting the CCND1 Oncogene. *Cell Cycle* (2012) 11(13):2495–506. doi: 10.4161/cc.20898
42. Zeltz C, Alam J, Liu H, Erusappan PM, Hoschuetzky H, Molven A, et al. Alpha11beta1 Integrin is Induced in a Subset of Cancer-Associated Fibroblasts in Desmoplastic Tumor Stroma and Mediates *In Vitro* Cell Migration. *Cancers (Basel)* (2019) 11(6). doi: 10.3390/cancers11060765

**Conflict of Interest:** The authors declare that the research was conducted in the absence of any commercial or financial relationships that could be construed as a potential conflict of interest.

**Publisher's Note:** All claims expressed in this article are solely those of the authors and do not necessarily represent those of their affiliated organizations, or those of the publisher, the editors and the reviewers. Any product that may be evaluated in this article, or claim that may be made by its manufacturer, is not guaranteed or endorsed by the publisher.

Copyright © 2022 Rajthala, Parajuli, Dongre, Ljokjel, Hoven, Kvalheim, Lybak, Neppelberg, Sapkota, Johannessen and Costea. This is an open-access article distributed under the terms of the Creative Commons Attribution License (CC BY). The use, distribution or reproduction in other forums is permitted, provided the original author(s) and the copyright owner(s) are credited and that the original publication in this journal is cited, in accordance with accepted academic practice. No use, distribution or reproduction is permitted which does not comply with these terms.

Supplementary Material

1 Supplementary Figures and Tables

1.1 Supplementary Figures

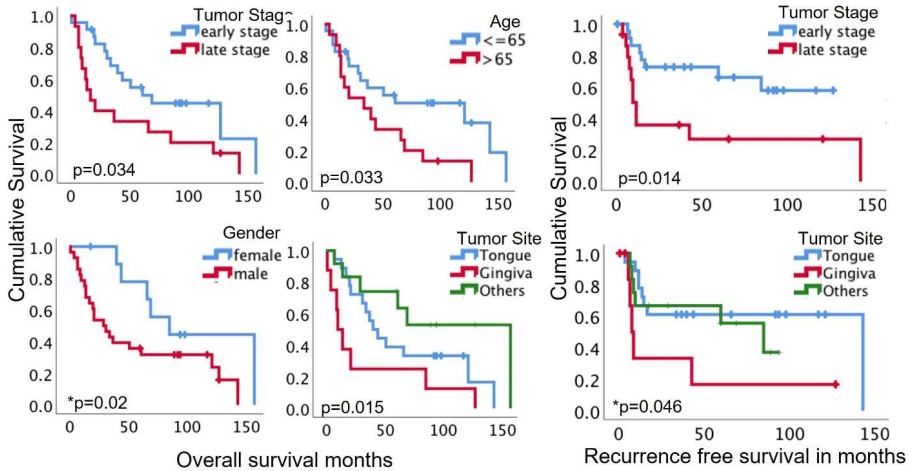


**Fig S1.** Kaplan-Meier plot for the survival functions of the clinicopathological characteristics using Log-Rank or \* Breslow test. Only significant parameters ( $p < 0.05$ ) are shown. Stage I&II: early stage. Stage II&IV: late stage.

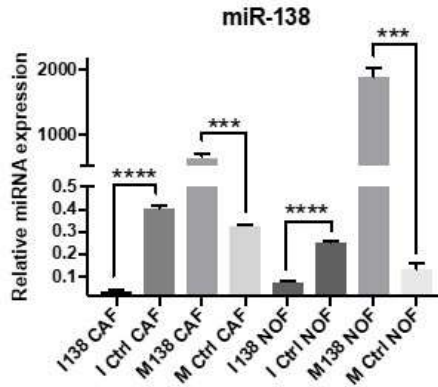


**Fig S2.** miR-138 expression in CAF and NOF 48 hours post transfection of respective mimics and inhibitors of miRNAs, and mimics and inhibitor controls (50nM).

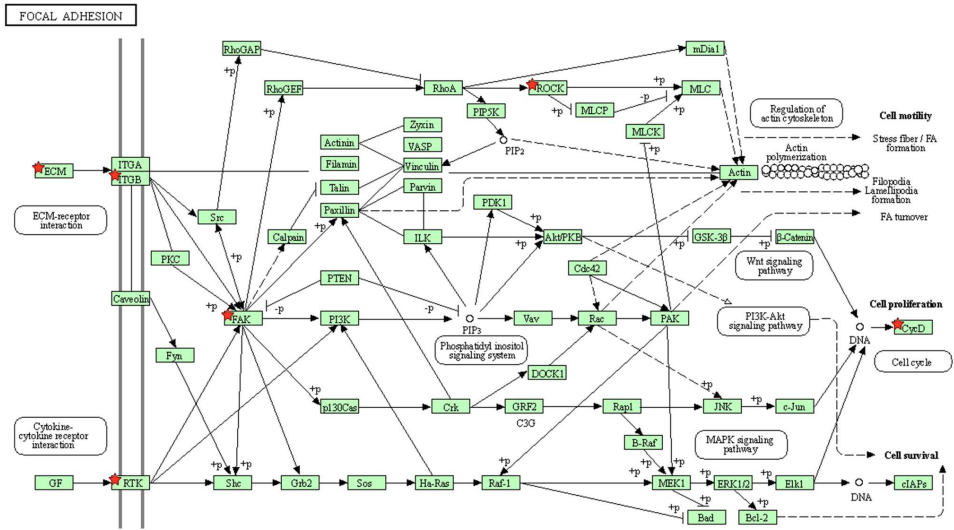


**Fig S3.** In silico interrogation of miR-138 targets using miRTarBase database indicating focal adhesion as a significantly affected pathway. Targeted pathways related to cell motility were selected. Pathways relevant to cancer cells were not selected. All 202 miR-138 – target genes interaction registered in miRTarBase were included in the analysis.

## 1.2. Supplementary Tables

**Table S1:** Patient history and tumour characteristics of OSCC cohort

Patient population: N=38, Median age: 62, Age range: 34-86			
Parameters	N (%)	Parameters	N (%)
<b>Gender</b>			
Female: 10 (26.3)		Male: 28 (73.7)	
Median age: 70		Median age: 62	
<b>Smoking</b>		<b>Alcohol</b>	
No	9 (23.7)	No- low	10 (26.3)
Yes	18 (47.4)	Moderate- High	12 (31.6)
Unknown	11 (28.9)	Unknown	16 (42.1)
<b>Tumor site</b>		<b>TNM Stage</b>	
Tongue	18 (47.4)	I	11 (28.9)
Gingiva	8 (21.1)	II	12 (31.6)
Buccal	5 (13.2)	III	5 (13.2)
Floor of mouth	5 (13.2)	IV	10 (26.3)
Overlapping	2 (5.2)		
<b>Depth of Invasion</b>		<b>T Stage</b>	
Superficial (< 4mm)	9 (23.7)	T1	11 (28.9)
Deep (≥ 4mm)	9 (23.7)	T2	12 (31.6)
Unquantifiable	20 (52.6)	T3	6 (15.8)
		T4	9 (23.7)
<b>Tumor budding score</b>		<b>N Stage</b>	
Low (< 5 buds)	18 (47.4)	N0	30 (78.9)
High (≥ 5 buds)	11 (38.9)	N1	5 (13.2)
Unquantifiable	9 (23.7)	N2	3 (7.9)
		N3	0 (0)
<b>Histological degree of differentiation</b>		<b>M Stage</b>	
Well	32 (84.2)	M0	38 (100)
Poor	5 (13.2)	M1	0 (0)
<b>Worst pattern of invasion</b>		<b>Recurrence</b>	
Type I&II	9 (23.6)	Yes	19 (50.0)
Type III	6 (15.8)	No	19 (50.0)
Type IV	23 (60.5)		
<b>Distant metastatic progression</b>			
Yes	5 (13.2)		
No	32 (84.2)		

**Table S2** List of Taqman Assays (ThermoFisher, USA)

<b>Genes</b>	<b>Taqman Assay ID</b>
hsa-miR-138-5p	002284
ITGA11	Hs00201927 m1
PTK2	Hs01056457 m1
EGFR	Hs01076090 m1
GAPDH	Hs99999905 m1
FAP	Hs00990806 m1
TGFB1	Hs00998130 m1
AKT1	Hs00178289 m1
ROCK2	Hs00178154 m1
18s	Hs99999901 s1
TGFBR2	Hs00559660 m1
RPL13A	Hs04194366 g1

**Table S3** List of antibodies used in western blot

<b>1<sup>o</sup> Antibodies</b>	<b>Cat No</b>	<b>Dilution</b>	<b>Protein block</b>
Integrin $\alpha$ 11 (1)	-	1:2000	5% Dry milk
FAK (D2R2E)	#13009, Cell Signalling	1:1000	3%BSA
AKT (pan) (C67E7)	#4691, Cell Signalling	1:1000	3%BSA
Beta-Actin	AB8226, Abcam	1:10000	5% Dry milk

**Table S4** KEGG Pathways target for miR-138 with miRTarBase

<b>S.N</b>	<b>KEGG Pathway Term</b>	<b>Gene Count</b>	<b>P Value</b>
1	Pathways in cancer	11	2.1E-4
2	Transcriptional misregulation in cancer	7	7.8E-4
3	p53 signaling pathway	5	9.8E-4
4	Proteoglycans in cancer	7	2.0E-3
5	MicroRNAs in cancer	8	2.6E-3
6	Acute myeloid leukemia	4	6.1E-3
7	AMPK signaling pathway	5	8.9E-3



8	<b>Focal adhesion</b>	6	1.2E-2
9	Thyroid cancer	3	1.6E-2
10	Hippo signaling pathway	5	1.8E-2
11	HIF-1 signaling pathway	4	2.6E-2
12	Viral carcinogenesis	5	4.7E-2
13	Axon guidance	4	5.3E-2
14	Wnt signaling pathway	4	6.4E-2
15	PPAR signaling pathway	3	7.4E-2
16	PI3K-Akt signaling pathway	6	7.9E-2
17	Adherens junction	3	8.1E-2
18	Melanoma	3	8.1E-2

Errata for  
**Functional and Prognostic Role of MicroRNAs in  
Cancer Associated Fibroblasts and Stroma in  
Oral Squamous Cell Carcinoma**

**Saroj Rajthala**



Thesis for the degree philosophiae doctor (PhD)  
at the University of Bergen

01.11.2023

\_\_\_\_\_  
(date and sign. of candidate)

03.11.23

(date and sign. of faculty)

## Errata

Page 5 Misspelling: “differentiatlly ” – corrected to “differentially”

Page 5 Preposition change: “Transcript and protein examination showed that the anti-tumour effect of miR-138 in CAFs was associated to changes of CAF phenotype-specific molecules” – corrected to “Transcript and protein examination showed that the anti-tumour effect of miR-138 in CAFs was associated to changes in CAF phenotype-specific molecules”

Page 5 Grammar correction: “Taken together, results of this thesis demonstrate significant **alterations of miRNA** ” – corrected to “ Taken together, results of this thesis demonstrate significant alteration of miRNAs”

Page 7 Extra word removal: “that which permits use” – corrected to “that permits use”

Page 7 Misspelling: “Attributuín ” – corrected to “ Attribution ”

Page 14 Missing signs in Figure 1 : “ ” – corrected to “ ≥ ”

Page 15 Misspelling: “ethiology” – corrected to “etiology ”

Page 15 Misspelling: “evolutionarry ” – corrected to “evolutionary ”

Page 17 Figure 2 legend Misspelling: “ Attributuín” – corrected to “Attribution ”

Page 19 Repetition of word the “Irrespective of the the anatomical ” – corrected to “Irrespective of the anatomical ”

Page 21 Figure 4 legend Misspelling: “Attributuín ” – corrected to “Attribution ”

Page 23 Correcting preposition “to be able to classify tumors **in** low- and high-risk cases” – corrected to “to be able to classify tumors into low- and high-risk cases”

Page 24 Misspelling: “metastatic/reccurent HNSCC patients” – corrected to “metastatic/recurrent HNSCC patients”

Page 25 Misspelling: “malignat ” – corrected to “ malignant”

Page 26 Figure 5 legend Misspelling: “Attributuín ” – corrected to “Attribution ”

Page 26 Conjunction correction: “HNSCC and OSCC” – corrected to “HNSCC, including OSCC”

Page 29 Figure 7 legend Misspelling: “Attributuín” – corrected to “Attribution”

Page 30 Missing comma : “minor subset was depleted of markers for myofibroblasts and CAFs and was interpreted as ” – corrected to “minor subset was depleted of markers for myofibroblasts and CAFs, and was interpreted as ”

Page 31 Figure 8 legend Misspelling: “Attributuín” – corrected to “Attribution”

---

Page 36 Section 3.1 Misspelling: “Colaborators ” – corrected to “Collaborators ”

Page 36 Section 3.2 Misspelling: “reccurrence” – corrected to “recurrence”

Page 37 Section 3.3 Missing comma: “The purity of each strain of primary cells, NOFs or CAFs, was confirmed by flow cytometry which”- corrected to “The purity of each strain of primary cells, NOFs or CAFs, was confirmed by flow cytometry, which”

Page 37 Section 3.3 Missing space: “99.4%of” corrected to “99.4% of”

Page 37 Section 3.5 Missing verb: “The gels were then placed on a metal grid layered with a lens paper with OSCC cells facing the top and the gels grown” corrected to “The gels were then placed on a metal grid layered with a lens paper with OSCC cells facing the top and the gels were grown”

Page 37 Section 3.5 Figure 9 legend Missing word: “from primary fibroblasts isolated from” corrected to “ from primary fibroblasts and cancer cells isolated from”

Page 37 Section 3.6 Missing word: “miRNA overexpression mimicked” corrected to “miRNA overexpression was mimicked”

Page 40 Section 3.8 Misspelling: “ benmark” – corrected to “benchmark ”

“ Thermifisher” – corrected to “Thermofisher ”

Page 41 Section 3.10 Misspelling: “ intergrin  $\alpha 11$  ” – corrected to “integrin  $\alpha 11$  ”

Page 41 Section3.10 Missing space: “ miRDB(” corrected to “miRDB ”

Page 42 Section3.11 Missing verb: “two primary protein coding transcripts of ITGA11 used for target reporter assay.” corrected to “two primary protein coding transcripts of ITGA11 were used for target reporter assay. ”

Page 42 Section3.11 Misspelling: “Non-complimentary” corrected to “Non-complimentary”

Page 42 Section3.11 Misspelling: “targetting” corrected to “targeting ”

Page 42 Section3.11 Missing word: “(Promega)” corrected to “E1910, Promega”

Page 45 Table 4 Missing superscript: “miRCURY LNATM; 5`-DIG and 3`-DIG labeled.” corrected to “miRCURY LNA<sup>TM</sup>; 5`-DIG and 3`-DIG labeled)”

Page 46 Section3.13 Incorrect preposition: “miRNA staining in double stained OSCC tissues were digitally quantified using scanned images of stained tissue sections **using** Hamamatsu NanoZoomer-XR, Japan. ” corrected to “miRNA staining in double stained OSCC tissues were digitally quantified using scanned images of stained tissue sections by Hamamatsu NanoZoomer-XR, Japan. ”

Page 46 Section3.13 Misspelling: “individual stainings” corrected to “ individual staining”

Page 46 Section 3.13 Missing superscript: “PPAP and IOD were quantified in the tissue regions of approximately 0.4-0.8 mm<sup>2</sup>. ” corrected to “PPAP and IOD were quantified in the tissue regions of approximately 0.4-0.8 mm<sup>2</sup> ”

Page 46 Section 3.14 Misspelling: “ tissues” corrected to “ tissues”

Page 46 Section 3.15 Misspelling: “ upaired T-test” corrected to “ unpaired T-test”

Page 46 Section 3.15 Misspelling: “ goups” corrected to “ groups”

Page 47 Section 3.15 Misspelling: “ ploted” corrected to “ plotted”

Page 48 Section 4.1.2 Misspelling: “response” corrected to “response”

Page 49 Section 4.1.3 Incorrect word: “An increase in these molecules was observed when the **CAFs** were treated with miR-204 mimics. ” corrected to “ However, increase in some of these molecules was observed when NOFs were treated with miR-204 inhibitors ”

Page 40 Section 4.2.2 Misspelling: “tumour stoma” corrected to “tumour stroma”

Page 51 Section 4.3.1 Misspelling: “Inhibition of miR-138-5p” corrected to “Inhibition of miR-138 ”

Page 52 Section 4.3.2 Misspelling: “NOM ” corrected to “NHOM ”

Page 53 Section 5 Misspelling: “challage” corrected to “challenge”

Page 54 Section 5 Misspelling: “reporte” corrected to “reported”

Page 55 Section 5 Preposition correction: “Increasing miR-204 expression **by** miR-204 mimics” corrected to “Increasing miR-204 expression with miR-204 mimics”

Page 57 Section 5 Misspelling: “clinical ” corrected to “clinical ”

Page 58 Misspelling: “normal/peritumouuur” corrected to “normal/peritumour”

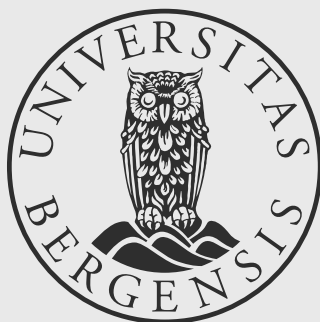
Page 58 Misspelling: “fibroblats ” corrected to “fibroblasts ”

Page 59 Misspelling: “thorough ” corrected to “through ”

Page 62 Misspelling: “concominant ” corrected to “concomitant ”

Page 63 Misspelling: “intergrative” corrected to “integrative ”

Page 61 Extra word: “other potential differentially regulated” corrected to “other differentially regulated”



[uib.no](http://uib.no)

ISBN: 9788230861844 (print)  
9788230855911 (PDF)